ADDIS ABABA UNIVERSITY

ADDIS ABABA INSTITUTE OF TECHNOLOGY

SCHOOL OF CIVIL & ENVIRONMENTAL ENGINEERING

Developing Superpave Bitumen Performance Grade Mapping for Ethiopia: Adapting to Historical and Future Climate Condition

by

Birhanu Demissie

A Thesis Submitted to School of Graduate Studies in
Partial Fulfillment of the Requirement for Degree of
Master of Science
In
Road and Transport Engineering

Advisor.

Dr.Robeam Solomon

June, 2023

Addis Ababa, Ethiopia

ADDIS ABABA UNIVERSITY

ADDIS ABABA INSTITUTE OF TECHNOLOGY

SCHOOL OF CIVIL & ENVIRONMENTAL ENGINEERING

The undersigned have examined the thesis entitled 'Developing Superpave Bitumen Performance Grade Mapping for Ethiopia: Adapting to Historical and Future Climate Condition' presented by Birhanu Demissie, a candidate for the degree of Master of Science in Road and Transport Engineering and hereby certify that it is worthy of acceptance.

Robeam Solomon (Ph.D)		27/10/2015
Advisor	Signature	Date
Yonas Minalu (Ph.D)		27/10/2015
Internal Examiner	Signature	Date
Mr.Tewodros Nigatu		05/07/2023
External Examiner	Signature	Date
	Abrham Gebre (Dr.) Dean, School of Civil & Environmental Engineering	
Chair person	Signature	Date

Addis Ababa Institute of Technology Director of Postgraduate Program

Declaration

I certify that research work titled "*Developing Superpave Bitumen Performance Grade Mapping for Ethiopia: Adapting to Historical and Future Climate Condition*" is my own work. The work has not been presented elsewhere for assessment. Where material has been used from other sources it has been properly acknowledged / referred.

Name **Birhanu Demissie**

Signature 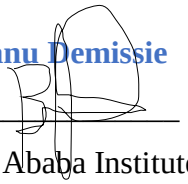

Place Addis Ababa Institute of Technology (**AAiT**)

Addis Ababa University,

Addis Ababa.

Date June, 2023

Table of Contents

List of Tables

List of Figures

LIST OF ACRONYMS

America petroleum Index	**API-**
Assessment Report	**AR**
American Association of State Highway and Transport Officials	**AASHTO**
Coupled Model Intercomparing Project Phase 6	**CMIP6**
Dynamic Shear Rheometer	**DSR**
Ethiopia National Metrological Agency	**ENMA**
Intergovernmental Panel on Climate Change	**IPCC**
Global climate model	**GCM**
Greenhouse Gas	**GHG**
Long term pavement performances	**LTPP**
Network Common Data form	**NetCDF**
National Metrology Agency	**NMA**
Strategic highway research program	**SHRP**
Shared Socioeconomic Pathway	**SSP**
Superior performance Asphalt pavement	**Superpave**
Performanc**e** Grade.	**PG**
World Meteorological Organization.	**WMO**
Working Group on Coupled Modelling.	**WGCM**

ACKNOWLEDGMENTS

I would like to express my deepest gratitude to Dr. Robeam Solomon for his invaluable guidance, unwavering support, and exceptional mentorship throughout the course of my research. His expertise, enthusiasm, and dedication have been instrumental in shaping the direction and success of this research.

Dr. Robeam Solomon's insightful feedback and constructive criticism have challenged me to think critically and push the boundaries of my research. His ability to provide clarity and direction, even during the most complex situations, has been truly remarkable.

I am incredibly fortunate to have had the opportunity to work under Dr. Robeam Solomon's mentorship. His patience, accessibility, and willingness to engage in fruitful discussions have greatly enhanced my understanding of the subject matter and have fueled my passion for scientific inquiry.

Finally, I would like to extend my gratitude to my classmates and my family members, Abey (My mother) and Selam (my sister), for their unwavering support and encouragement throughout this research journey. Their belief in my abilities and their constant encouragement have been a source of inspiration.

ABSTRACT

The study aims to adapting a Superpave bitumen specification performance grading system for Ethiopia, considering historical and future climate conditions. By conducting statistical analysis and examines the performance characteristics of different bitumen grades across varying temperatures. Historical climate data from 1990 to 2020, obtained from the Ethiopia National Metrology Agency, establish the baseline climate conditions. Future climate projections from 2020 to 2100, based on two global climate models (CMIP6) and climate change scenarios (SSP 2(4.5) and SSP 5(8.5)), are used to assess future conditions and prediction pavement temperature using SHRP and LTPP models. The findings indicate that, for different reliability level, PG58-10 and PG64-10 are predominantly required in historical contexts, yet future projections indicate a notable transition towards PG64-10 and PG70-10, encompassing a larger expanse of the country. Furthermore, the Afar region and western Ethiopia are projected to necessitate PG76-10 in the future. A considerable number of locations in Ethiopia mandate one grade increment due to climate change, exhibiting average percentage increases of 20%, 23%, and 27% for the moderate climate change scenario SSP2 (4.5), and 44%, 27%, and 35% for hottest climate change scenario SSP5 (8.5) of the study area during 2020-2040, 2040-2070, and 2070-2100, respectively.

Climate change significantly impacts road pavement performance in Ethiopia, resulting in an overall elevation of grade changes as observed. Specifically, under the SSP5 (8.5) scenario, Adigrat and Sekota locations experience a two-grade increase. Additionally, t-test is employed to compare two pavement temperature prediction models, revealing a statistically significant difference in Superpave bitumen specifications due to the characteristic nature of the models. However, both models demonstrate effectiveness in predicting pavement performance grade (PG) and evaluate performance of currently used asphalt grade using DSR-machine with the SHRP PG determination criteria of penetration-grade fail temperature for pet-grade 40/50(69.29^{o}c unaged and 71.66 ^{o}c for Aged Sample),60/70((68.03^{o}c unaged and 64.52 ^{o}c for Aged Sample),80/100((59.13^{o}c unaged and 59.66 ^{o}c for Aged Sample) &85/100(62.35 ^{o}c unaged and 61.35 ^{o}c)then the recommended PG Grade are PG64,PG64,PG58&PG58 Respectively.

Finally, the study proposes a new performance grading system for Ethiopian roads, considering future climate conditions. The findings provide valuable insights for policymakers and road construction companies in Ethiopia.

Keyword: Superior performance Asphalt pavement (Superpave), Long term pavement performances (**LTPP**), Strategic highway research program (**SHRP)**, performance grade (**PG**), Coupled Model Intercomparing Project Phase 6 (**CMIP6**), Shared Socioeconomic Pathway (**SSP**)

CHAPTER -ONE

1 Introduction

Asphalt pavement is vital for transportation infrastructure worldwide, enabling efficient movement of people and goods and contributing to economic development. However, climate change poses challenges to the quality and longevity of asphalt pavement. In Ethiopia, road transport is the dominant mode, supporting the majority of inter-urban freight and passenger movements (Shiferaw et al., 2012). The Road Sector Development Program (RSDP) has improved the road network significantly, but concerns remain about its quality, prompting the government to recognize the need for better bitumen quality in asphalt pavement (Alder et al., 2022).

The performance of flexible pavements in Ethiopia is greatly influenced by the quality of asphalt concrete. Despite highways being designed and constructed for a minimum of 20 years(ERA Manual, 2013), they often exhibit premature distresses like cracking, rutting, and potholes. Factors such as high traffic intensity, overloaded trucks, and significant temperature variations contribute to these issues. Various asphalt mix design methods and bitumen specifications are practiced globally, but in Ethiopia, the penetration/viscosity grading systems are commonly used. However, these empirical methods do not accurately simulate field conditions, making it difficult to predict real-world performance(Harman, 2002).

The Superpave was developed to address these shortcomings, with the Strategic Highway Research Program (SHRP) conducting research to overcome the limitations of empirical systems(Kennedy, 1994). Climate change, a global phenomenon, brings about changes in temperature, precipitation, and other environmental factors that impact asphalt pavement performance. Higher temperatures lead to softening and deformation of asphalt, causing rutting, while changes in precipitation patterns weaken the pavement structure and result in cracking and damage (Delgadillo et al., 2020). The quality of asphalt pavement heavily relies on the quality of the bitumen used as a binder. Bitumen, a complex mixture of hydrocarbons, possesses critical properties such as viscosity, stiffness, and durability, which directly affect asphalt pavement performance(Sabita., 2012).

This research focuses on Superpave bitumen specifications for Ethiopia using temperature data from meteorological agency stations for baseline PG from 1990-2020. The study also assesses the impact of different climate change using different scenarios, such as SSP2(4.5) and SSP5(8.5), on the performance of asphalt pavement in Ethiopia from 2020 to 2100.

1.1 Statement of Problem

Ethiopia currently uses the conventional methods (penetration and viscosity Bitumen Grading Systems) for different road projects. The penetration and viscosity bitumen grading systems were developed based on past experiences and empirical methods, which can be applicable as long as the past conditions still exist. However, Current traffic and climatic conditions are highly different from those that prevailed when these systems were developed, making past experiences have some limitation to establish binder grading. This Conventional method are conducted at a unique test temperature, which means that they do not provide information about low-temperature and high-temperature performance. But Bitumen is a viscoelastic material where temperature and rate of load application have a great influence on its behavior.

In addition, climate change has become a major global concern, and its impact on asphalt pavement performance with the changing climate, the asphalt pavement's thermal properties are expected to be affected, which in turn affects its performance. There is a need to evaluate the impact of climate change on asphalt pavement performance in Ethiopia Furthermore, although one research has been done in Ethiopia on the '**Mapping of temperature zones for binder performance grading system**", the study used only the minimum required temperature data for the past 20 years for 27 station and relied solely on the SHRP model(Mahlet Gashaw, 2018). Therefore, there is a need for further research to explore the impact of climate change on asphalt has not been extensively studied, particularly in the context of Ethiopia.

This research addressed such problem to shift binder grading system and to investigate the impact of climate change on asphalt binder in Ethiopia.

1.2 Objective

1.2.1 General Objective

The General objective of the study adapt Superpave pavement bitumen specifications for Ethiopia based on climate conditions. It analyzes temperature data to determine the baseline performance grade (PG) of asphalt pavement. Additionally, develops customized specifications for future climate conditions.

1.2.2 Specific Objective.

- Determine Performance grade (PG xx-yy) of representative area for Ethiopia using SHRP and LTPP Model with different reliability percentage and compare two model.
- Assess the climate change impact on performance grade of asphalt.
- Determining rise of future asphalt binder grade.
- Mapping temperature zoning for each representative area for both baseline and future.
- Determine Performance grade of currently used in Penetration grade Binder using DSR.

1.3 Research Question.

- How to predict pavement temperature of asphalt binder?
- What is impact of climate change on Performance Grade (PG) of bitumen?
- What is the importance of determining future asphalt binder grade?
- Why we map the PG-temperature zoning?

1.4 Significant of The Study.

This study is to suggest essential information and guidelines for various stakeholders involved in the industry, including contractors, consultants, and clients such as government entities and other organizations. By providing this valuable knowledge, the study aims to assist these stakeholders in making informed decisions and implementing effective strategies related to their respective roles and responsibilities. The guidelines derived from this research will serve as a practical reference, enabling contractors to enhance their construction practices, consultants to improve their design and advisory services, and clients to make well-informed decisions regarding infrastructure

development and maintenance. Moreover, the findings obtained from this study will contribute to the body of knowledge in the field and can serve as a valuable resource for future studies and initiatives, promoting further advancements and improvements in the industry as a whole.

1.5 Limitation of the Study

The studies limited by the lack of data recording of Metrology agency, constraints in available data, limited generalizability to other regions, a lack of long-term data, technological limitations specific to the country, cost implications, factors beyond climate that influence pavement performance, assumptions and simplifications made during the analysis, implementation challenges, a limited focus on temperature in the analysis, and external factors outside the scope of the research and Lack of Laboratory instrument(PAV-Pressure Air Vessel, Compaction Gyration) to do Long term aging of Binder , LAS(Linear Amplitude Sweep Test) and To compare super pave and marshal mix design.

1.6 Paper organization

The paper is structured into six main sections. **The first section** is the introduction, **the second section** is the literature review, which provides an overview of asphalt pavement and Superpave specifications. It also discusses climate change and its potential impact on asphalt pavement, as well as previous studies on Superpave pavement specifications in other countries. **The third section** is the methodology, which outlines the data collection and analysis methods used in the research. It also explains the establishment of the baseline performance grade of asphalt pavement in Ethiopia, the assessment of the potential impact of climate change on asphalt pavement, and the development of Superpave pavement specifications for each administrative zone. **The fourth section** is the results and discussion, which presents the analysis of National Meteorological data and maximum and minimum temperature data. It also includes the baseline performance grade of asphalt pavement in Ethiopia, the potential impact of climate change on asphalt pavement, and the Superpave pavement specifications for each station and method of Experimental plan. **The fifth section** is the conclusion and recommendations, which summarizes the research findings and provides recommendations for future research and implementation Finally, the **sixth section** is the reference.

CHAPTER TWO

2 Literature Review.

2.1 Bitumen Binder.

The term 'bitumen' is to describe refined crude oil, a hydrocarbon product produced by removing the lighter fractions (such as liquid petroleum gas, petrol and diesel) from crude oil during the refining process. In North America, bitumen is commonly known as asphalt binder or asphalt. (Robert N Hunter, 2015)

Bitumen is the most commonly used binding and water-resisting material for highway pavement construction, as it serves as a fundamental component of the upper layers. It possesses the ability to withstand deformation and withstand variations in temperature. By binding the aggregates together, bitumen prevents the loss of material from the pavement surface and effectively inhibits the penetration of water into the pavement structure. There are two primary types of bituminous binder that exist. The first is **tar**, which is derived from the production of coal gas or the manufacturing of coke. However, due to reduced availability, tar is no longer widely used. The second type is **bitumen**, which is obtained from the process of refining crude oil. Bitumen has become the predominant choice for binding and providing water resistance in highway pavement construction.(Rogers, 2003)

The vast majority of asphalt binders used throughout the world today are obtained from crude oil (petroleum) refining. At room temperature (25°C) asphalt binder is a highly viscous, black material whose primary purpose is to bind the aggregates in the production of asphalt mixtures for pavement **(**Robeam.2020**)** With its adhesive properties, water resistance, thermoplastic, durability, modifiability, and recyclability, bitumen has emerged as an ideal construction and engineering material.

The production of asphalt binder can be divided into two primary phases: refining the asphalt base stock and formulating it into a final asphalt binder. The introduction of new Superpave specifications has led to the need for enhanced logistical control and heightened emphasis on quality in both phases of production. Additionally, there has been a growing focus on the environmental, health, and safety aspects of asphalt. This increased emphasis on environmental,

health, and safety characteristics has generated a demand for asphalt binders with improved properties, specifically lower volatility. The volatility of asphalt can be influenced by both the refining and formulation stages of production. Efforts are being made to develop asphalt binders with reduced volatility to address concerns related to emissions and potential health hazards. These advancements aim to enhance the overall performance and sustainability of asphalt materials.(Anderson, n.d.)

It is produced to meet a variety of specifications based upon physical properties for specific end uses.85% of all the bitumen is used as the binder in various kinds of asphalt pavements: pavements for roads, airports, parking lots, etc. About 10% of the bitumen is estimated to be used for roofing: shingles, hot applied built up roofing, cold applied roll on roofing. The remaining part (approximately 5% of the total), is used for a variety of applications each small in volume: (Asphalt Institute & European Bitumen, 2015**)**

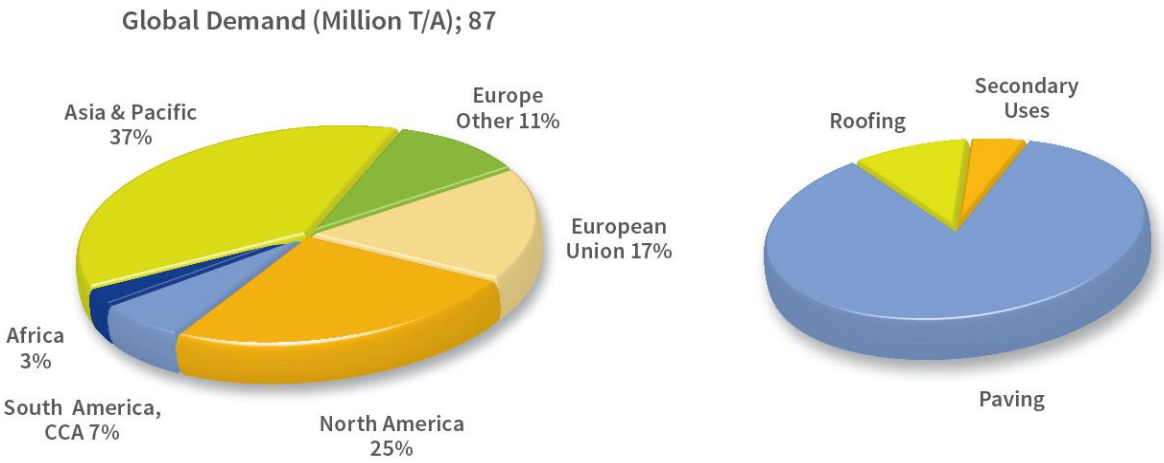

Figure 2-1: Global bitumen use (Source: Asphalt Institute & Euro bitumen)

Bitumen has a long history of usage, dating back to our ancestors, and in the late 19th century, it became a popular choice for constructing roads and pavements. The discovery of oil and the subsequent production of residual bitumen opened up vast possibilities for its utilization. However, not all crude oils contain a sufficient number of heavy components to economically yield bitumen. For instance, crude oils from Indonesia and Nigeria, referred to as light crudes, have limited suitable heavy residue for bitumen production. On the other hand, heavy crude oils sourced from

the Middle East and South America often possess a substantial amount of heavy residue suitable for bitumen production.(Member of RAHA Group, 2022) Bitumen is derived through the refining process of petroleum crude oil, but it can also be naturally found as a deposit. (Sabita., 2012) **.**

2.1.1 Composition of bitumen binder

Bitumen is a complex mixture of hydrocarbons that contains small amounts of sulfur, oxygen, nitrogen, and trace metals such as vanadium, nickel, iron, magnesium, and calcium. Crude oils typically contain a small quantity of polycyclic aromatic hydrocarbons (PAHs), some of which are present in bitumen. The composition of most bitumen, which is produced from various crude oils, consists of approximately 82-88% carbon, 8-11% hydrogen, 0-6% sulfur, 0-1.5% oxygen, and 0-1% nitrogen.**(**Sabita., 2012**)**

2.1.2 Refining Method of Bitumen

The quality of asphalt binder specifications is strongly influenced by both the specific crude oil used and the refining processes employed. Crudes can be classified based on their API gravity, with lower gravity crudes typically containing a higher percentage of bitumen in their distillable overhead fractions. On the other hand, higher gravity crudes have a higher proportion of overhead fractions with a lower bitumen content. Crudes with low API gravity are often referred to as heavy or sour crudes if they have a high sulfur content. In contrast, if high API gravity crudes have a low sulfur content, they are commonly referred to as light crudes or sweet crudes. The fractional composition of a crude oil is a crucial factor for refiners as they need to strike a balance between product yield and market demand. Crude oils are identified by their name or source in conjunction with their API gravity for reference purposes.(Corbett, 1984)

The API (American petroleum institute) gravity is a scale expressing the gravity or density of a crude oil or crude oil products and is calculated by the empirical equation:

API gravity = (141.5/SG at 60 deg F) – 131.5…… Equation 2-1

where SG is the specific gravity of the fluid. (Puzinauskas et al., 1990)

Asphalt is produced in two types of petroleum refineries: **1. Integrated refineries** are operated primarily to produce transportation and heating fuels in large volumes, as well as petrochemical feedstocks; **2**. **Asphalt refineries** at which asphalt is the major or the primary product, and which

produce relatively small volumes of blending components for transportation and heating fuels and petrochemical feedstocks.(Puzinauskas et al., 1990)

In the 1920s, fractional distillation was developed. In this method, petroleum is heated then piped into a distillation column or fractionation tower. Inside the tower or column are perforated trays, which catch liquid petroleum products at various levels and drain the separated components off to storage or further processing.(pavement interactive, 2023)

2.1.3 Refining Process

- Desalting: -Once crude oil enters the refinery, water and salts are removed to make processing easier and less expensive. Sand, rust, minerals, salts, and other contaminants would foul a distilling column.
- Distillation: - The charge pump pumps crude from storage or the desalting tanks into the system. After desalting, crude oil passes through a series of heat exchangers to raise its temperature.

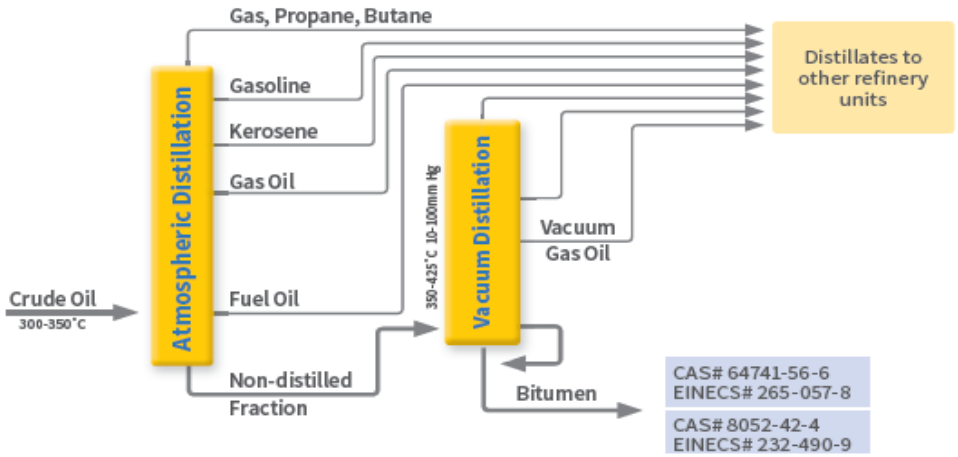

Figure 2-2: Refining process of bitumen

This process can occur in one or several towers, and the towers may be at atmospheric pressure or can be pressurized, depending on the product and refinery.

- Vacuum Flashing or Vacuum Distillation: - Above 900 degrees Fahrenheit, cracking occurs. Cracking is when high temperatures cause the large hydrocarbon molecules to crack into smaller ones.
- Refining Vacuum Flasher**:** - This distillation tower produces a bottom residual, which tests as a **PG 64-22**. It also produces flasher tops, or light vacuum gas oil, and flasher bottoms, or heavy vacuum gas oil, which are sent to a catalytic cracker offsite. From this tower, the asphalt is moved to storage tanks.

2.1.4 Property of bitumen Binder

2.1.4.1 Chemical property:

Generally believed that performance-based specifications for binders will be mainly physical property tests. Chemical studies of asphalt are important to note that many chemical properties will not correlate with performance. The measurable chemical properties that are believed to relate to the mechanical or structural strength of a pavement are several**.**(Robertson, 1991)

- asphalt or asphalt binder, exhibits several chemical properties that contribute to its characteristics and behavior. Some key chemical properties of bitumen include: Composition, Oxidation, Volatility, Chemical, Reactivity, Compatibility and Waterproofing.

2.1.4.2 Physical property

Bitumen is a type of material that exhibits unique characteristics depending on temperature. At room temperature, it is either a solid or semi-solid substance, which becomes softer as the temperature rises and harder as it decreases. However, when heated, bitumen transforms into a Newtonian liquid, meaning its viscosity decreases with higher temperatures. Consequently, bitumen needs to be heated before it can be effectively handled and applied in various applications. Another important aspect of bitumen is its Visco-elastic nature. It behaves like an elastic solid when subjected to short loading times, but acts like a viscous liquid when subjected to longer loading times. This property enables bitumen to respond to different types of stresses and strains. Since bitumen is primarily used in engineering applications, the specifications for this material

focus more on defining its physical properties rather than its chemical composition.(Asphalt Institute & European Bitumen, 2015).

Some key physical properties of bitumen include-Viscosity and Penetration, Density, Softening Point, Ductility and Solubility and Adhesion

2.1.4.3 Rheological (Visco-elastic) properties asphalt binder.

Binder rheology involves the study of the flow and deformation of binders to predict their performance in pavements. The three key performance measures for asphalt binders are rutting, fatigue cracking, and low-temperature cracking. These measures assess the binder's behavior under different conditions and help evaluate its resistance to permanent deformation, repetitive loading-induced cracking, and cracking at low temperatures.(Robeam, 2020)

Viscoelasticity is a time-dependent material behavior, typical of materials showing both elastic and viscous characteristics when experiencing deformation.(Salvatore Magnifico, 2014)and Visco-elastic behavior of a material can be quantified using a dimensionless number known as the Deborah number (De). This number, proposed by Marcus Reiner, a professor at the Israel Institute of Technology, is used to measure the extent of a material's Visco-elasticity.(Robert N Hunter, 2015)(Poole, 2012)

$$De = {}^{\lambda}/_{t_0} \quad \text{..... Equation 2-2}$$

where $\boldsymbol{\lambda}$ is the relaxation time and $\boldsymbol{t_0}$ is the observation time?

In transient (steady) flow, the Weissenberg number (Wi) which applies to dynamic flows is used to determine the nature of the Visco-elastic response. If the relaxation time is long and the rate of deformation high, then a material will display non-linear Visco-elastic behavior. (Poole, 2012)

$$w_i = \lambda\ddot{\gamma} \quad \text{.....Equation 2-3}$$

where $\boldsymbol{\lambda}$ is the **relaxation time** and $\ddot{\gamma}$ is the **Shear rate**

Bitumen or asphalt binders in road pavement undergo different types of chemical and mechanical stresses, such as stress, tension, bending, impact, and their combined effects. Understanding the resistance of bitumen to these stresses is crucial, including the rate and

conditions under which it can withstand them. In the medium to high temperature range, bitumen binders exhibit a viscoelastic behavior, meaning they possess characteristics of both viscosity and elasticity.(Remišová et al., 2016) It also a thermoplastic liquid that behaves as a viscoelastic material depending on temperature and time of loading. At low temperatures elastic properties dominate. At high temperatures, the bitumen behaves like a liquid, usually with Newtonian viscous flow properties. At normal pavement temperatures, the bitumen has properties that are in the viscoelastic region.(Izzi & Yusoff, 2012)

The descriptions given of elastic, viscous and viscoelastic response are for a linear response; that is the deformation at any time and temperature is directly proportional to the applied load. Non-linear response, especially for viscoelastic materials, is extremely difficult to characterize in the laboratory or to model in practical engineering applications.(Gordon da airey, 1997) The principal viscoelastic parameters that are obtained from the **DSR** are the magnitude of the complex shear modulus (|G*|) and the phase angle (δ). |G*| contains elastic and viscous components which are designated as the storage modulus (G') and loss modulus (G'') respectively. (Airey & Collop, 2002)

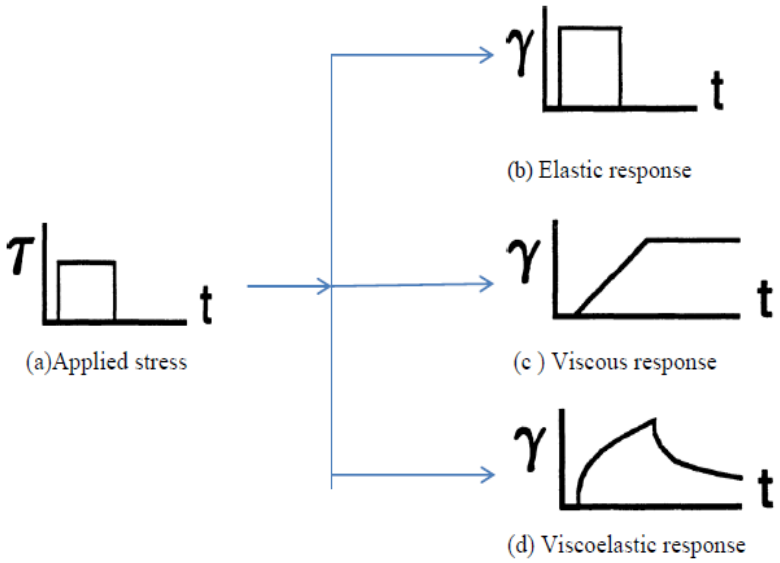

Figure 2-3 : Response of Elastic, Viscous and Viscoelastic materials

Source: (Mahlet Gashaw, 2018)

Determining of viscos elastic property of Asphalt

There are two different modes of strain or stress application during tests to determine viscos-elastic properties of materials:

- **Transient flow** on this mode there are two different method

Creep test: **Creep** is a physical phenomenon that causes non-reversible deformation of a material exposed to constant stress over a given length of time. The behavior of a viscos-elastic material in creep tests varies with time and consists of three regions.(Robert N Hunter, 2015).

- an instantaneous elastic response
- a delayed elastic response
- a steady state viscous response

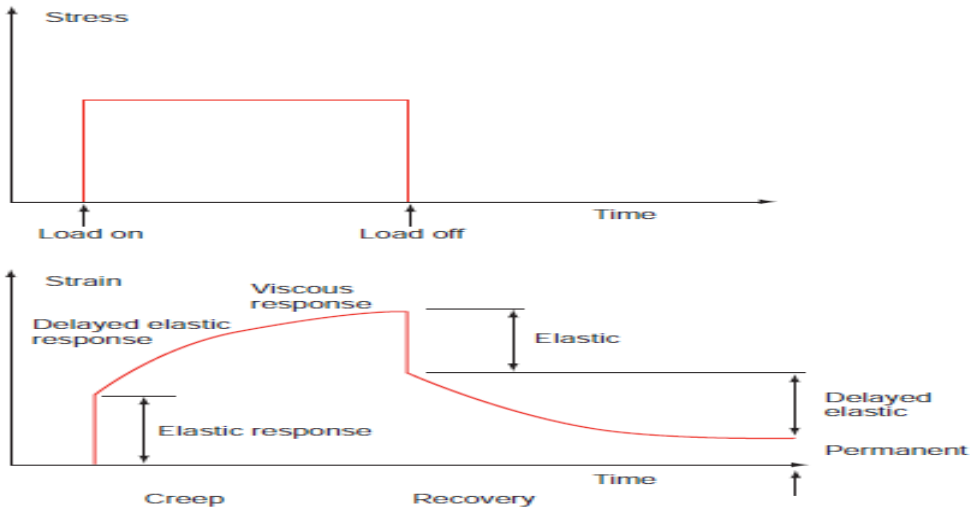

Figure 2-4 : Creep test of viscos elastic material.

source:(Robert N Hunter, 2015)

- **Dynamic Mechanical Analysis (DMA)**

Dynamic mechanical analysis (DMA) is a commonly employed technique for assessing the properties of materials, considering factors such as temperature, time, frequency, stress, atmosphere, or a combination of these parameters. In the case of bituminous binders, different

forms of DMA, typically utilizing oscillatory-type Dynamic Shear Rheometer (DSR) testing, are used to measure their rheological properties. These tests help characterize the behavior of bitumen under varying conditions and provide valuable insights into its viscoelastic properties.(Izzi & Yusoff, 2012).

2.2 Bitumen Binder specification.

2.2.1 Penetration and viscosity specification

The development of binder testing at 1888, when H. C. Bowen invented the Bowen Penetration Machine, after several modifications of penetration equipment, by 1910 the penetration equipment became the standard for establishing the consistency of asphalt at 25 ^{o}c. The penetration grading system for asphalt was introduced by the Bureau of Public Road in the United States in 1918. Subsequently, in 1931, the American Association of State Highway and Transportation Officials (AASHTO) published a standard specification to establish the grading of asphalt based on penetration. The next major change in asphalt grading specification came with the introduction of viscosity grading system in early 1960s. Both ASTM and AASHTO adopted the viscosity grading system and provided grading specification by measuring the viscosity at 60 ^{o}c when these systems were developed, making past experiences have some limitation of this Conventional method are conducted at a unique test temperature, which means that they do not provide information about low-temperature and high-temperature performance. But Bitumen is a viscoelastic material where temperature and rate of load application have a great influence on its behavior.(Pak.j. Engg &Appl.Sci, 2021)

2.2.2 Superior Performing Asphalt Pavements (Superpave) Specification.

The Strategic Highway Research Program (SHRP) in the United States conducted a project from 1987 to 1993 to address the limitations of existing penetration and viscosity-based grading systems for asphalt. As a result of this project, a performance-based binder specification known as SUPERPAVE (Superior Performing Asphalt Pavements) was developed.

This binder specification includes a new set of tests and is applicable to both modified and unmodified asphalt binders, including those with dispersed, dissolved, or reacted modifiers. The performance-based asphalt binder specification relies on evaluating the rigidity of the binder after it has undergone either short term and long-term aging, considering particular traffic loading and

environmental circumstances. This allows for the selection of a single binder grade based on the anticipated pavement temperatures for a given design, considering high and low temperature performance. The high-temperature performance is associated with a vehicle speed of 100 km/hr and a traffic volume of less than 10 million equivalent single axle loads (ESALs).(Kennedy, 1994).

On this specification, the physical characteristics of the asphalt binder remain consistent across all grades. However, the specific temperature requirements at which these properties must be met vary depending on the climate conditions in which the binder will be utilized. For example, a PG 58-40 grade is designed to be used in an environment where the average seven day maximum pavement temperature is 58 ^{O}C and a minimum pavement design temperature of 40 ^{O}C.(john read, 2003)

An asphalt binder graded as PG 58-40 would comply with the specification for a maximum high 7-day pavement temperature below 58°C and a minimum low annual pavement temperature above -40°C. However, it's important to note that due to the intermediate temperature requirements primarily related to fatigue, an asphalt binder graded as PG 64-28 may not meet the criteria for a lower high-temperature grade, such as PG 52-28.(Kennedy, 1994)

To determine the required PG of asphalt binder, the weather data covering at least 20 years should be used(Kennedy, 1994). For each year and weather station, the hottest consecutive seven-day period is identified and the average temperature of these seven days is calculated. Similarly, the lowest one-day air temperature is determined for each year. The mean and standard deviation of the average seven-day maximum air temperatures and minimum air temperatures of all years are computed for each location. The air temperatures, along with other factors, are utilized to estimate the high and low temperatures experienced by the pavement. These temperature predictions are crucial in determining the appropriate Performance Grade (PG) binder grades required for each specific location. Superpave defines the high pavement design temperature at a 20-mm depth below the pavement surface, and the low pavement temperature at the pavement surface(Abo-Hashema et al., 2016);(Kennedy, 1994)

2.2.3 History of Pavement Temperature prediction model development.

Pavement temperature prediction has been extensively investigated by many researchers all over the world(Arangi & Jain, 2015), They adopted three primary methods: **numerical and**

finite elements, **theoretical and analytical**, and **statistical and probabilities techniques**(Adwan et al., 2021) The Enhanced Integrated Climatic Model (EICM) (NCHRP 1 -37A is used in the mechanistic empirical pavement design guide (MEPDG) for pavement temperature prediction. Several empirical models based on linear regression analysis have been developed to predict maximum and minimum temperatures in the pavement(Arangi & Jain, 2015). In united states of America 2002 Mechanistic Empirical Pavement Design Guide was developed by ERES Consultants (A division of Applied Research Associates, Inc.) through a contract from the AASHTO Joint Task Force on Pavements (JTFP), under the National Cooperative Highway Research Program (NCHRP Project I-37 A) which is administrated by the Transportation Research Board of the National Research Council.(Quintero, 2007)

Barber, one of the early researchers, focused on calculating maximum pavement temperatures using weather reports. Through observations in Hybla Valley, Virginia, USA, he noticed that changes in pavement temperature roughly followed a sine curve pattern with a daily cycle. His analyses indicated that by incorporating solar radiation and air temperature, the sine approximation offered reasonable estimates of surface temperatures. However, his model utilized a total daily radiation factor instead of a more precise measure like hourly radiation. Additionally, he proposed a correlation model that related pavement surface temperatures and temperatures at a depth of 3.5 inches with information from weather stations. (Quintero, 2007)

Until the inception of the Long-Term Pavement Performance (LTPP) program, there was limited published activity in the general literature regarding the topic. However, in 1969, Rumney and Jimenez created nomographs to predict surface and 50 mm depth pavement temperatures based on collected data that included pavement temperature and hourly solar radiation. Subsequently, in 1970, Dempsey developed a simulation model based on the principles of heat transfer and energy balance at the pavement surface.(Al-Qadi et al., 2006).

As (H. F. Hassan, A. S. Al-Nuaimi, R. Taha, and T. M. A. Jafar) said that in was Developed models in 2005 to predict high and low asphalt pavement temperatures in Oman. To monitor air temperatures, pavement temperatures, and solar radiation, a pavement monitoring station was set up at the campus of Sultan Qaboos University (SQU). Data was collected for 445 days. Daily minimum and maximum temperatures were recorded. A regression analysis was used to develop the low pavement temperature model. To develop high temperature models, a stepwise regression

approach was employed, utilizing air temperature, solar radiation, and the duration of solar radiation as independent variables. The instrumentation used is described and collected data are presented. The developed models were compared with the SHRP and LTPP models(Hassan et al., 2005). the Strategic Highway Research Program (SHRP) was launched in both Canada and the United States in 1987. This comprehensive study spanned a period of 20 years and aimed to enhance the characterization of pavement performance in real-world conditions. Apart from this, the study introduced a new bitumen classification system called Performance Grading (PG)(Adwan et al., 2021)

The Urban Heat Island (UHI) effect refers to a phenomenon where noticeable temperature variations occur between urban areas and their adjacent rural surroundings, or even within different parts of a city itself. It manifests as higher temperatures in urban regions compared to their non-urban counterparts.(O'Malley et al., 2014).

Current models for predicting the asphalt pavement's temperature consider environmental factors' impact on the asphalt pavement. However, these models do not consider the reverse impact that occurs from the heated pavement and thus contributing to heat accumulation in the surrounding environment, such as that found in urban heat island (UHI) effects. To summarize, these models cannot fully reflect the two-way interactions that become apparent between the pavement and the environment, thus making them incapable of evaluating the effect of pavement on UHI effects.(Adwan et al., 2021).

2.2.4 Pavement Temperatures prediction Model

Table 2-1: Pavement temperature prediction Model develop in different country.

Model and year of develop	Location	Influencing Factors	Summary and Findings
Barber (1957)	USA	• Pavement temperature • Wind • Precipitation • Air temperature • Solar radiation • Coefficient of thermal properties	• The model was applied to asphalt pavements with a thickness of 6.35 cm. • The actual temperature was compared with the obtained results; the expected maximum temperature error is about 3 ^{0}C and occasionally exceeds 5 ^{0}C. • The model calculated the maximum temperature and was able to predict the minimum temperature
Solaimanian and Kennedy (1993)	USA	• Maximum air temperature • Hourly solar radiation	• The model did not consider winter conditions since this study investigated maximum temperature
Highter and Wall (1984)	USA	• Thermal conduction of asphalt • pavement temperature at a different specific density	• A typical recycling process where an external heat source applied to asphalt pavements. A significant difference was observed in the surface limestone course's thermal conduction spread and base limestone course, which is apparently due to the gradient and total size of aggregates.
Liang and Niu 1998)	USA	• Ambient air temperature • Pavement surface temperature	• The main findings showed that the temperature distribution within depth could be non-linear, especially when considering the daily temperature change. • The analytical solution to the temperature distribution was in a three-layer system using a simplified boundary condition that involved only heat transfer between the pavement surface and ambient air.
Liu and Yuan (2000)	USA	• Ambient air temperature • Pavement surface temperature • Depth • Time	• The analytical solution can be expanded to understand or predict temperature • distribution within the asphalt pavement over weeks or months

SHRP (1987)	USA	$1331\alpha\tau a\frac{1}{\cos Z}.\cos Z + \varepsilon\sigma T_a^4 - hc(Ts - Ta) - 164k - \varepsilon\sigma Ts^4 = 0$ where α is absorptivity of pavement surface, τa is heat conduct coefficient for air, Z is 20 degrees latitude, ε is pavement surface emissivity, σ is the Stefan-Boltzman constant (5.7×10^{-8} W/m^2), hc is surface coefficient of heat transfer (W/m^2 °C), k is heat conduction coefficient (W/m^2 °C), Ta is air temperature (K), and Ts is surface temperature (K).	• The model based on the assumption of a balance of energy during the highest temperatures, which is an erroneous assumption • The energy balance was not achieved despite the stability of solar radiation, wind speed and atmospheric circumstances
Abdul Al-Wahhab et al. (2001)	Saudi Arabia	T(d) = 3.714 + 1.006T(a) - 0.146d where T(d) is pavement temperature at depth d (^{O}C), T(a) is air temperature (^{O}C), and d is depth below pavement surface (cm).	• The model could predict maximum and minimum temperatures that play an essential role in asphalt pavement. • Saudi Arabia is located in a desert region where ambient temperature fluctuation is minimal throughout the year.
Park et al. (2001)	USA	Td = Ts + (-0.3451d -0.0432d2 + 0.00196d3) *sin (0.325C+ 5.0967) where Td is the temperature of pavement (^{O}C), Ts is the surface temperature (^{O}C), d is depth (mm), C is the coefficient associated with time.	• This model was verified for a surface temperature range of between -28.4 to 53.7 ^{O}C and a depth ranging from 14 to 27.7 cm.
Diefenderfer et al. (2003)	USA	Tpmax = 3.2935 + 0.6356Tmax + 0.1061Y - 27.7975Pd Tpmin = 1.6472 + 0.6504Tmin + 0.0861Y + 7.2385db where Tpmax is predicted maximum temperature (^{O}C), Tmax is the maximum daily temperature (), Tpmin is predicted minimum temperature (^{O}C), Tmin is the minimum daily temperature (^{O}C), Y is one day of the year (1 to 365), and db is depth below the surface (m).	• This model can be used for the four seasons and across different climate zones after confirming the equation using the data from SMP sites in the United states
Hassan et al. (2004)	Oman	Tsurf = -1.437 + 1.121 Tair T20mm = 3.160 + 1.319 Tairx where Tsurf is minimum temperature of pavement (^{O}C), Tair is minimum temperature of air (^{O}C), T20mm is pavement temperature at 20 mm in ^{O}C, and Tairx is maximum air temperature in ^{O}C.	• The experimental application of these formulae is used to predict the temperature at a particular pavement depth.

Jia et al. (2008)	China	Tp = P1 + (P2 Ta5 + P3 (Q5)2) + H (P4 Ta + P5 Q) + (P6 H + P7 H2 + P8 H3) +P9Tm where Tp is pavement temperature at H cm, Ta is air temperature, Q is solar radiation, kW/m2, Ta5 is average air temperature for the previous 5 h, Q5 is average solar radiation for the previous 5 h, kW/m2, H is the depth of prediction points in cm, P1–P8 are the undetermined regression coefficients for the prediction model, Tm is the monthly historical average air temperature for the past 20 years.	• The model has many variables, which makes it impractical for fieldwork. This model can be improved to make it more suitable for use in fieldwork.
Tabatabaie et al. (2008)	Iran	T = 0.94Sur + 0.94Sin (2π t/24) -2.99 log(d) - 0.02 comp + 0.02Air +0.32BP+ 0.17BT - 0.34 where T is asphalt temperature (^{O}C) air is air temperature (^{O}C), S is surface temperature (^{O}C), t is time of day in a 24-h system, d is depth (cm), comp is level of compaction (number of blows), BP is bitumen content, BT is bitumen type (1 for 40/50 and 2 for 60/70), and BP is bitumen content	• One drawback of this model is that it is not able to give the maximum and minimum asphalt temperature, which is crucial in the design of asphalt pavement. • The relationship between asphalt temperature and climate influences is linear.
Zheng et al. (2011)	China	Tpave-rising = 1.170 T air-rising- 0.50h + 3.55 Tpave-falling = 1.085 Tair-falling - 0.07h + 4.3 Tpave = 1.118Tair - 0.23h + 4.1 where Tpave-rising is temperature of asphalt pavement at depth h during the period of rising air temperature (^{O}C). Tair-rising is a period of rising air temperature, and h is a depth of pavement (cm). Tpave-falling asphalt pavement temperature at depth h during period of falling air temperature (^{O}C). Tpave-falling is a falling of air temperature (^{O}C), and h is a depth of pavement (cm). Tair is air temperature, and h is the depth of pavement (cm).	• The resulting models are practical and straight-forward. A comparison of the measured and predicted data shows a very accurate application value. This model cannot be used in all countries
Al-Hamed and Maryam (2011)	Iraq	TPave = 3.175 + 0.04866Z + 0.946Tair where Tpave is pavement temperature (^{O}C), Z is depth below pavement surface (cm), and Tair is air temperature (^{O}C).	• This linear regression is a simple and practical model but was not validated.

Matic et al. (2013)	Serbia	ymax = 0.963288xmax – 0.151137xd + 4.452996 ymin = 1.004801xmin - 0.1992731xd + 0.051532 where ymax is maximum pavement temperature (^{O}C), xmax is maximum air temperature, xmin is air temperature (^{O}C), ymin is minimum pavement temperatures (^{O}C), and Xd is depth (cm).	The equation is linear in the first order without complications. • The model can be used in fieldwork and is preferred by road design engineers. • Serbia is located in Europe, and the temperature is low throughout the year. The developed model cannot be used in other parts of the world.
Salem (2015)	Libya	Tmaxpav, d = 7.059 + 0.7764246Tmaxsur d + 0.054628Day -0.000141Day^{2} +0.000006CumSR - 0.053402Lat Tminpav, d = 9.8364 + 0.0.668591Tminsur + 0.259098d + 0.099289Day + 0.000261Day2-0.000025CumSR - 0.053402Lat where Tmaxpav.d is maximum daily pavement temperature (^{O}C), Tmax sur is maximum daily surface temperature (_C), d is distance from surface (cm), is day of the year, Day2 Day2 is the square of the day of the year, CumSRCumSR is cumulative solar radiation (W/m2), and Lat is latitude of the section (degrees). Tmin pav. d is minimum daily pavement temperature at distance d from the surface (^{O}C) and Tmin sur is minimum daily surface temperature (^{O}C).	• The researcher uses a small amount of data from a short period and therefore is not reliable for developing models. • Libya has more than one climate (marine and desert); the difference in air temperatures is enormous, and thus the reactions of asphalt pavement cannot be integrated into standardized models
Ariawan et al. (2015)	Indonesia	T.00 = 10.813 + 0.919 RH T.20 = 6.898 + 0. 687T.Air + 0.640 T.00 T.70 = 1.965 + 0. 755T.Air + 0.331 T.00 where RH is humidity, T. Air is air temperature (^{O}C), T.00 is surface temperature (^{O}C), T.20 is temperature at a depth of 20 mm (_C), and T.70 is temperature at a depth of 70 mm (^{O}C).	• Indonesia has a tropical climate, plenty of sunshine, rain, and high humidity during the year. • The model is accurate, practical and straight-forward but is limited to the depths stated in the equations; the temperature at any other depths cannot be determined.

Viljoen algorithms (Mokoena et al., 2019)	South Africa	$T_{d(max)}$ = Ts(max) *(1*-4.237* 10^{-3} d +2.95 * 10^{-5} d^2- 8.53 *10^{-8} d^3*)* *T (min)* = 0.89 T air(min) +5.2 Where: (Mokoena et al., 2019) Td(max) = Maximum daily asphalt temperature at depth d in ºC Ts(max) = Maximum daily asphalt surface temperature in ºC from d = depth in mm. Td(max) = Maximum daily asphalt temperature at depth d in ºC Ts(max) = Maximum daily asphalt surface temperature in ºC from	• This equation for Calculating the minimum pavement temperature is purely empirical.
LTPP (Long term Pavement performance Model)		$Tpav, h, d$ = 54.32 + 0.78$Tair$ − 0.0025Lat^2 − 15.14 $log10(d + 25)$ + z (9 + 0.61σ^2air)$^{0.5}$ $Tpav, l$= −1.56 + 0.72$Tair$ − 0.004Lat^2 + 6.26 $log10$(d + 25) − z (4.4 + 0.52σ^2air)$^{0.5}$ $Tpav, h$= High AC pavement temperature at 20 mm from surface, °C $Tpav, h, d$=High AC pavement temperature at depth$d$ from surface, °C $Tair$= High 7-day mean air temperature, °C Lat = Latitude of the section, degrees d= Pavement depth, mm , $Tpav, l$ = Low AC pavement temperature, °C $Tair$=1-day minimum mean air temperature, °C σ air= Standard deviation of the 7-day maximum air temperature, °C z = 2.055 for 98% reliability, and z = 0.0 for 50% reliability	This model: • develop a data base of pavement temperatures using the Long-Term Pavement Performance Study's Seasonal Monitoring Program (LTPP-SMP) data; and • develop low and high pavement temperature models for the purpose of improving the Strategic Highway Research Program's (SHRP) asphalt binder selection procedure used in SUPERPAVE.

Source: (Adwan et al., 2021)

In 2014 Egyptian researcher were Compare models to predict pavement temperatures from air temperatures. The Long-Term Pavement Performance (LTPP) model was chosen to forecast low pavement temperatures, leading to the determination of lower Performance Grade (PG) asphalt binder grades. As for the high pavement temperature prediction, both LTPP and the performance model were used to select the high PG grade. The later was an improved performance model applied to identify the high temperature PG grade for asphalt binders based on the rutting damage concept but later model are conservative (Safwan A. Khedr, ,2014)

The high and the low pavement temperatures calculated using the SHRP-SP2 algorithm, the high and the low pavement temperatures calculated using the FHWA–LTPP (Long-term Pavement Performance), bind program algorithm. it is noted that both algorithms produce almost the same results. It should be noted that reliability should be considered when calculating the high and low temperatures. In the SHRP models, there is no reliability, whereas in the FHWA–LTPP models, the reliability has been considered. In addition, the differences in the maximum pavement temperature between the SHRP models and FHWA–LTPP models are due to modelling computations.(Ghuzlan & Al-Khateeb, 2013)

The Superpave pavement temperature predictions algorithms, as contained in Kennedy et al (1994), and the algorithms developed for temperature prediction in the South African climate by Viljoen (2001), are compared(Mokoena et al., 2019). the Viljoen model predictions show less scatter and have a lower standard deviation compared to the Superpave model (CSIR International Convention Centre, Pretoria, South Africa, 2007.).

A. Maximum Pavement Temperature Prediction Model.

For this study the Following are the high temperature model developed under SHRP and LTPP are used because of it is well known around the world.

- **SHRP- Model**

$$Tpav, h = (Tair - 0.00618Lat^2 + 0.2289Lat + 42.4)\,(0.9545) - 17.78 + z\,\sigma\,\text{air} \quad \text{……Equation 2-4}$$

(Kharbuja et al., 2020)

- **LTPP – Model**

$$Tpav,\ h,\ d = 54.32 + 0.78Tair - 0.0025Lat^2 - 15.14\ log10(d + 25) + z\ (9 + 0.61\sigma^2 air)^{0.5} \quad \text{……..Equation 2-5}$$

where,

$Tpav, h$= High AC pavement temperature at 20 mm from surface, °C

$Tpav, h, d$=High AC pavement temperature at depth$d$ from surface, °C

$Tair$= High 7-day mean air temperature, °C

Lat = Latitude of the section, degrees d= Pavement depth, mm

σ air= Standard deviation of the 7-day maximum air temperature, °C

z = 2.055 for 98% reliability, and z = 0.0 for 50% reliability

There are different maximum asphalt surface temperature predictions equations in Superpave (Kennedy ,1994), LTPP and other but thus, are quite uncomplicated in their final form. They are based however, on the energy balance concept, and calibration of the equations involves identifying the best fit of values for the asphalt surface absorptivity, the transmission coefficient of air, the emissivity of air, the emissivity of the asphalt surface, the asphalt surface heat transfer coefficient and the conductivity of the asphalt material (Arangi & Jain, 2015).

B. Low pavement Temperature Prediction Model.

- **Model developed by SHRP**(Kharbuja et al., 2020)

Tpav, l= $Tair$ + 0.051 d − 0.000063 d^2 − z σ air ……. Equation 2-6

- **Model developed by LTPP**

$Tpav, l$= −1.56 + 0.72$Tair$ − 0.004Lat^2 + 6.26 log10(d + 25) − z (4.4 + 0.52σ^2air)$^{0.5}$ ……. Equation 2-7.

where,

$Tpav, l$ = Low AC pavement temperature, °C

$Tair$=1-day minimum mean air temperature, °C

σ air= Standard deviation of the 1-day minimum air temperature, °C.

2.3 Previous Study in different country in Performance Grade (PG) Development

A. In Middle East

Development of Performance Grading Map of Nepal While making performance grading map, maximum and minimum pavement temperature (design pavement temperature) determined by SHRP and LTPP model based on 98% level of reliability were used.(Kharbuja et al., 2020)

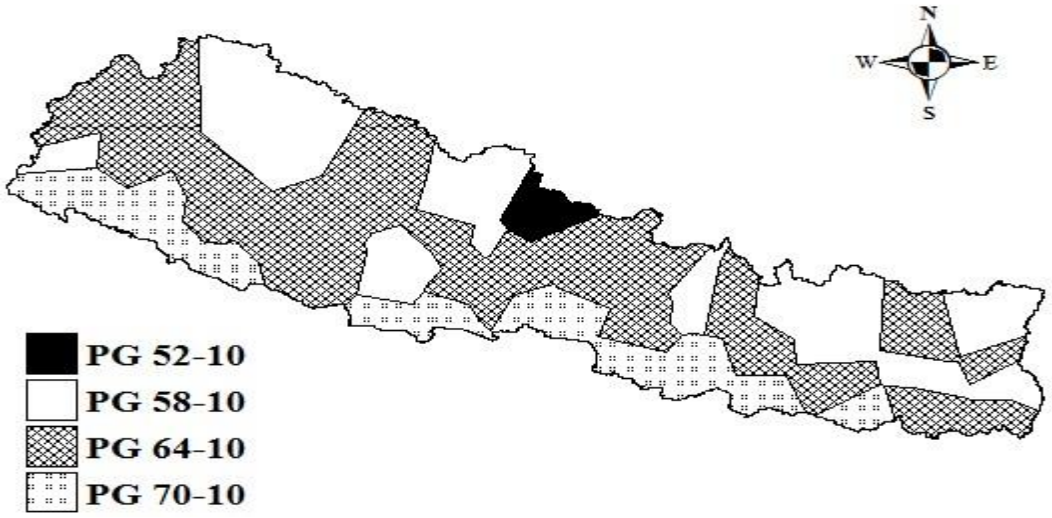

Figure 2-5: Performance grading map of Nepal using SHRP model

Figure 2-6 : Performance grading map of Nepal using LTPP model

the prediction of pavement temperatures using both the models with SHRP models being more severe compared to LTPP models. In Pakistan, a significant number of regions experience moderate to elevated temperatures, resulting in the most common pavement distress being rutting caused by high temperatures and unregulated traffic loads. it was decided to use SHRP models for the purpose of temperature zoning on 98% level of reliability(Pak.j. Engg &Appl.Sci, 2021)

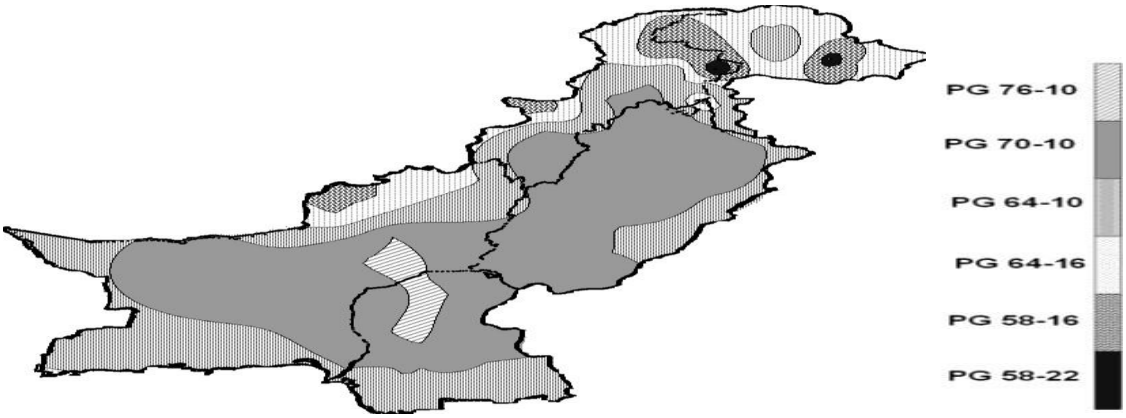

Figure 2-7: Temperature Zoning for PG System in Pakistan

Temperature zoning, a prerequisite for performance-based specification for the Gulf countries, was developed. Temperature zones range from PG 50-10 to PG 76- 10.(Abo-Hashema et al., 2016)

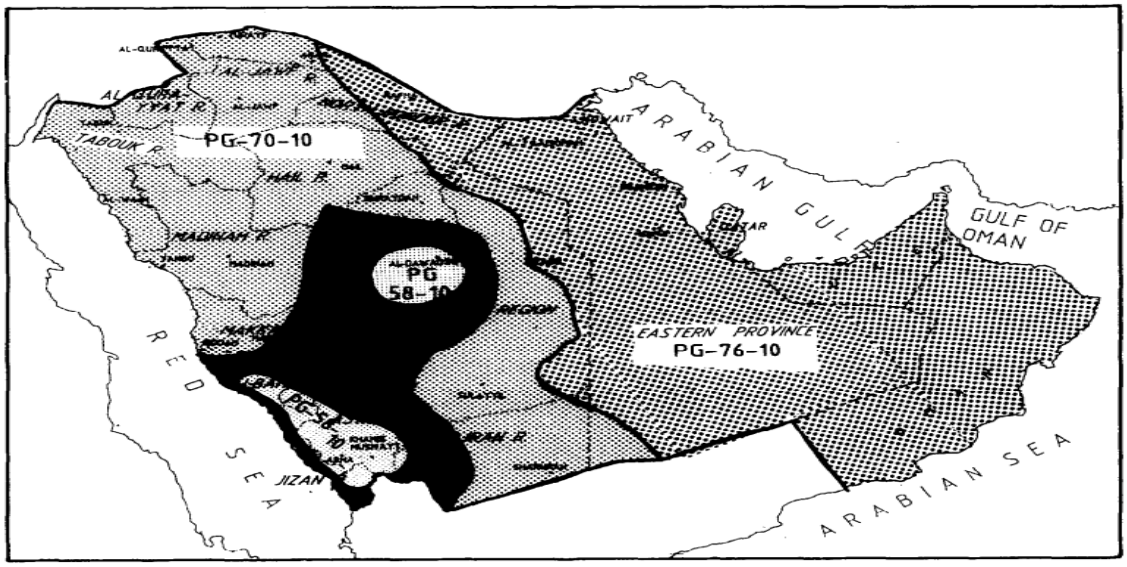

Figure 2-8: Recommended temperature zoning for bitumen specification for the Gulf region

The asphalt binder PGs map of the Yemeni region was derived from the SHRP model, with a reliability level of 50%, and 98%, respectively. In this study, the most common PGs recommended for low volume roads and heavy traffic volume at 50% and 98% reliability level, respectively, are PG52-10, PG58-16, and PG64-10(Ali Hussain et al., 2020)

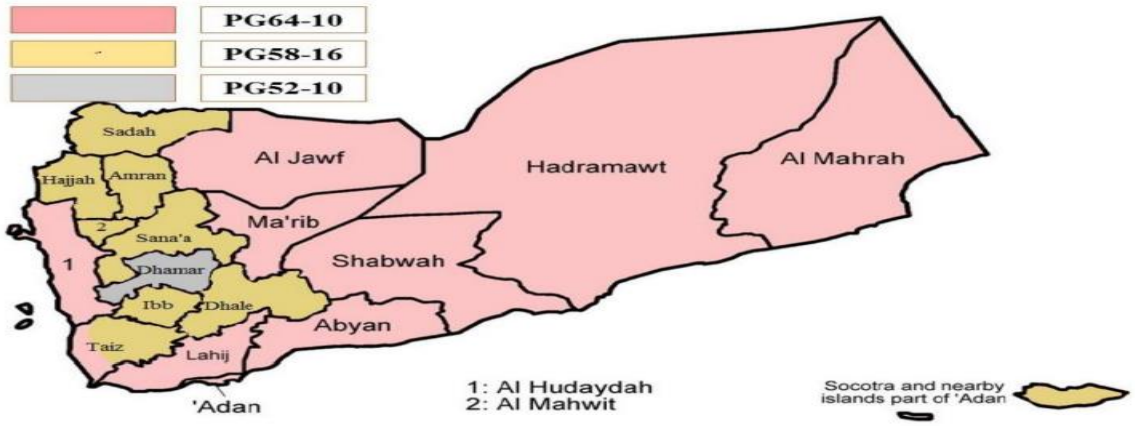

Figure 2-9 : Map of PGs for Yemen based on SHRP model with 98% reliability.

B. East Africa (Uganda, Kenya, Tanzania, Rwanda, Burundi, Malawi, D.R of Congo)

In east Africa of Great Lakes region of Africa studied considered 26 weather stations across the selected states, which includes seven countries, experiences a tropical climate with high precipitation throughout the year. The air temperatures in the region rarely fall below 10 ºC and do not exceed 37 ºC. The hottest areas in the region reported a high pavement design temperature of not more than 64 ºC, while the rest of the areas reported high design temperatures ranging from 52 to 58 ºC. This information is crucial in developing Superpave pavement specifications that can withstand the expected traffic loads and environmental stresses in the region, considering the local climate conditions. (Ronald & Chehab, 2020)

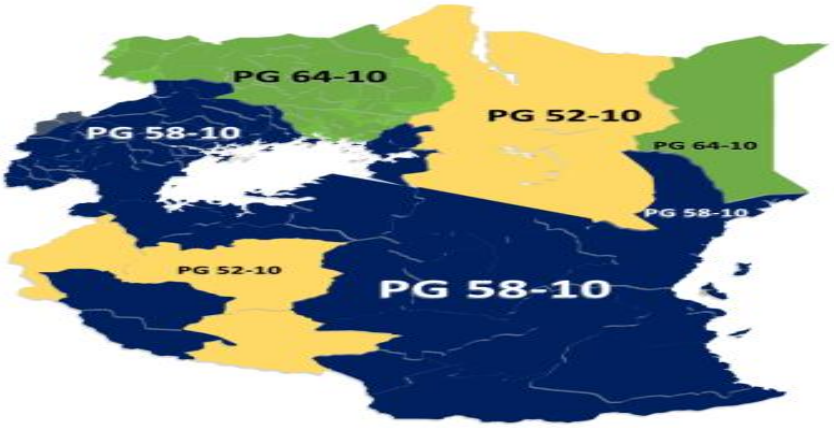

Figure 2-10: East Africa's PG zoning map

2.4 Impact of climate change in Performance grade of Asphalt grade

Roadway design aims to maximize functionality, safety, and durability. Construction materials are typically chosen based on the expectation of a stable climate. However, the impact of human-induced climate change can lead to swift infrastructure deterioration, leading to higher maintenance expenses. This is especially true for paved roads, where temperature is a crucial factor in material selection. As climate patterns become more volatile due to anthropogenic factors, it becomes imperative to reevaluate material choices and adapt construction practices to ensure the longevity and resilience of infrastructure. Failure to do so may result in accelerated infrastructure failure and a subsequent rise in maintenance cost (Underwood et al., 2017)

In recent years, with the use of newly available technology all over the world, prediction of climate change effects has become more convenient. Most of the studies related to climate change explain the increases in the frequency and severity of many types of extreme weather, such as changes in air temperature, rainfall, sea-level rise and hurricanes, all of which have direct effects on pavement performance. and There are many tools that can simulate climate change globally. Most of these climate change models consider the increase in Green House Gases (GHG) to predict the climate change. Some of the models consider climate change at a global average level(T. Swarna et al., 2021).

Given the projected intensification of climate trends under current CO2 emission scenarios, scientists anticipate significant impacts on various aspects of the environment. It is widely

acknowledged that asphalt binder, being highly sensitive to climate factors, is particularly vulnerable to these changes. Consequently, a crucial step in mitigating pavement deterioration involves reviewing and adjusting asphalt binder grades. This proactive measure can help slow down the rate of pavement degradation and extend the lifespan of road infrastructure ((S. T. Swarna et al., 2021)

Viola and Celauro in Italy to evaluate the asphalt binder upgrade at 71 different locations ((Viola & Celauro, 2015)). In this study, the year 2013 was established as the starting point for analysis, serving as the baseline for assessing asphalt binder grades. The focus was on estimating the required upgrades in asphalt binder grades for the year 2033. Notably, the findings revealed that more than a quarter (27%) of the Italian territory experienced an increase of one grade in the high-temperature grade. On the other hand, there was no noticeable change in low-temperature grades in this territory ((Viola & Celauro, 2015)). A similar study was carried out for the binder selection in Chile, total of 94 weather stations were considered in the selection of asphalt binder grades throughout the country ((Delgadillo et al., 2020)).

Researchers in Canada conducted a study to evaluate the impact of future climate change on asphalt binder grades and to understand how the change in binder grade would affect pavement performance of pavements in Canada by extract the daily maximum, and minimum temperature from the climate change models for the selected sixteen locations.(S. T. Swarna et al., 2021)

Table 2-2 : Asphalt binder grade determined for the 1980--2100 in Canada

Province	City	LTPP Section	Base Binder	Upgraded Binder		
			1980-2010	2010-2040	2040-2070	2070-2100
BC	Vancouver**	BC 82-6006	PG 52-16	PG 58-16	PG 58-16	PG 58-10
AB	Calgary**	AB 81-8529	PG 52-40	PG 58-40	PG 58-34	PG 58-28
AB	Edmonton**	AB 81-1804	PG 52-46	PG 58-40	PG 58-40	PG 58-34
SK	Saskatoon***	SK 90-6410	PG 52-52	PG 58-40	PG 58-34	PG 64-34
MB	Brandon***	MB 83-6454	PG 52-46	PG 58-34	PG 58-34	PG 64-28
MB	Winnipeg**	MB 83-6450	PG 58-40	PG 58-40	PG 58-34	PG 64-28
ON	Toronto**	ON 87-1806	PG 58-28	PG 58-28	PG 58-22	PG 64-22
ON	Ottawa**	ON 87-0901	PG 58-34	PG 58-34	PG 58-28	PG 64-28
QC	Montreal**	QC 89-3001	PG 58-34	PG 58-34	PG 58-28	PG 64-22
QC	Quebec City*	QC 89-1125	PG 58-34	PG 58-28	PG 58-28	PG 58-22
QC	Saguenay*	QC 89-0902	PG 58-34	PG 58-34	PG 58-34	PG 58-28
NB	Fredericton**	NB 84-1684	PG 58-34	PG 58-28	PG 58-28	PG 64-22
PEI	Charlottetown**	PEI 88-1646	PG 52-34	PG 58-28	PG 58-22	PG 58-16
NS	Halifax**	NS 86-6802	PG 52-28	PG 58-22	PG 58-22	PG 58-16
NL	Corner Brook*	NL 85-1803	PG 52-28	PG 52-28	PG 52-28	PG 52-22
NL	St. John's**	NL-DTW	PG 52-28	PG 52-22	PG 52-22	PG 58-16

Source: - (S. T. Swarna et al., 2021)

A researcher in the United States has highlighted the economic implications of projected temperature changes on asphalt roads across the contiguous United States. By utilizing an ensemble of 19 global climate models driven by RCP 4.5 and 8.5 scenarios, the study examined the potential costs. The findings indicated that relying on stationary assumptions for material selection over the past two decades resulted in incorrect choices for 35% of the observed locations. As temperatures continue to rise, the standard practice of material selection through maintenance is projected to significantly increase pavement costs. Specifically, it is estimated that under the RCP 4.5 scenario, the additional costs will amount to approximately US$13.6 billion, US$19.0 billion, and US$21.8 billion by 2010, 2040, and 2070, respectively. For the RCP 8.5 scenario, these costs are expected to rise to US$14.5 billion, US$26.3 billion, and US$35.8 billion for the

same time periods. It is worth noting that these costs will disproportionately affect local municipalities with limited resources to address the impacts. Failing to revise engineering standards and practices in light of climate change presents a substantial risk to the integrity of the pavement infrastructure in the United States.(Underwood et al., 2017)

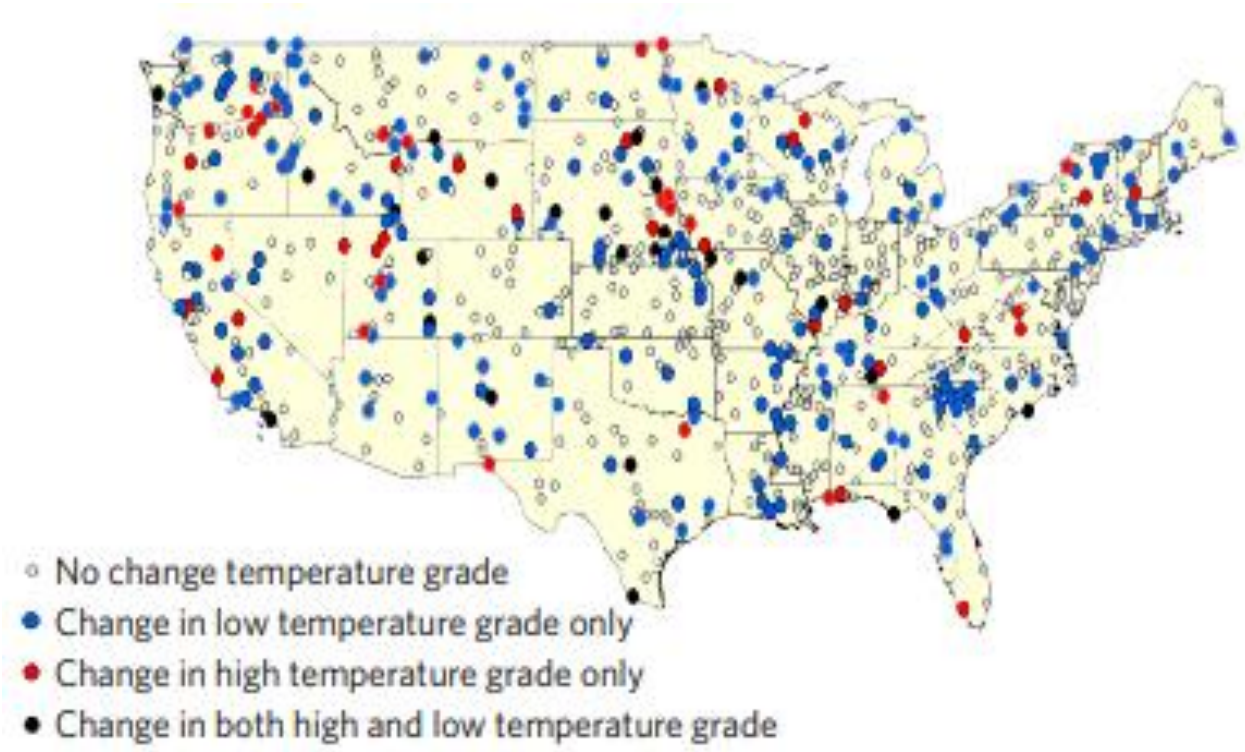

Figure 2-11 : Temperature performance grade change in United states of America

Source: -(Underwood et al., 2017)

2.4.1 Global Climate Model (GCM) Assessment.

In brazil researcher asses the performance of CMIP 6 Models performance in simulating present climate and finally conclude that the models with the highest ability in simulating monthly rainfall, aggregating all five Brazilian regions, were HadGEM3-GC31-MM, ACCESS-ESM1-5, IPSL-CM6A-LR, IPSL-CM6A-LR-INCA, and INM-CM4-8, while for monthly temperatures, they were CMCC-ESM2, CMCC-CM2-SR5, MRI-ESM2- 0, BCC-ESM1, and HadGEM3-GC31-MM. (Ongoma et al., 2022)

The researchers (Yonas Abebe Balcha, Andreas Malcherek, and Tena Alamirew) conducted a study in Ethiopia where they evaluated and ranked 12 Global Climate Models (GCMs) selected from the CMIP6 project. The evaluation and ranking were based on the GCMs' ability to accurately represent the historical observed climate data. Various techniques were employed, including the probability distribution function technique and trend analysis using the Mann-Kendall (MK) test. Four performance metrics were utilized to assess and compare the simulated series against the observed data. These metrics included the coefficient of determination (R2), root mean squared error (RMSE), mean absolute error (MAE), and BIAS. (Balcha et al., 2022)

Table 2-3 Ranking of GCM for Ethiopia Climate

Model	PDF Rank	Trend-Rank	PM-rank
Maximum Temperature			
ECEARTH	4	6	3
INM-CM5-0	4	2	2
INM-CM4-8	4	6	4
MPI-ESM1-2-HR	4	9	6
TaiESM1	4	2	1
ECEARTH3-CC	2	12	5
ECEARTH3-Veg	4	6	8
CMCC-ESM2	4	2	11
GFDL-CM4	1	9	9

GFDL-ESM4	2	1	7
NorESM2-MM	4	2	12
MRI-ESM2	4	9	10
Minimum Temperature			
GFDL-CM4	2	1	1
MPI-ESM1-2-HR	1	5	2
TaiESM	5	1	3
GFDL-ESM4	2	9	8
MRI-ESM2	5	9	7
CMCC-ESM2	2	1	9
INM-CM5-0	5	9	6
INM-CM4-8	5	7	4
NorESM2-MM	5	5	10
ECEARTH3-Veg	5	7	5
ECEARTH3-CC	5	1	12
ECEARTH3	5	9	11

Source (. (Balcha et al., 2022)).

2.5 Performance-Based Binder Tests.

The performance of asphalt pavements is not easily characterized by physical properties as they are subjected to complex environmental and loading conditions. In addition, various modified binders cannot necessarily be characterized by empirical properties. It is important to understand the stress-strain behavior of bituminous binders over a wide range of temperatures and loading time conditions.(Izzi & Yusoff, 2012) .

2.5.1 Dynamic Shear Rheometer (DSR) Test

The dynamic shear rheometer is test machine used to for specification purposes to measure the complex modulus and phase angle of asphalt binders at intermediate to upper pavement service temperatures and a frequency of 10 rad/s which has been related to a traffic speed of 100 km/hr. Where the complex modulus is approximately 10 MPa or larger(Jung et al., 1994).

The dynamic shear rheometer (DSR) test (AASHTO T315–02) is used to measure the elastic, viscoelastic and viscous nature of bituminous binders within the linear viscoelastic (LVE) region over a wide range of temperatures and frequencies (time of loadings)(Izzi & Yusoff, 2012) . it is utilized to evaluate the rutting and cracking potential of asphalt by applying a torque on a thin asphalt binder sample between a fixed and an oscillating parallel plate to apply a shear loading.(Robeam, 2020)

The **absolute value of the complex shear modulus, |G*|,** is the ratio of peak stress divided by peak strain. It represents the stiffness of the bitumen under the conditions of testing. **The phase angle,** defined as the phase difference between the peak stress and strain, represents the time delay from applying a stress to when the material responds, with limiting values of 0^O for purely elastic behavior and 90^O for purely viscous behavior(Airey et al., 1999)

$$\gamma = \frac{\theta r}{h} \quad \text{..... Equation 2-8}$$

$$G^* = \frac{\tau_{max}}{\gamma_{max}} \quad \text{..... Equation 2-9}$$

$$\tau = \frac{2T^2}{\pi r^3} \quad \text{.....Equation 2-10}$$

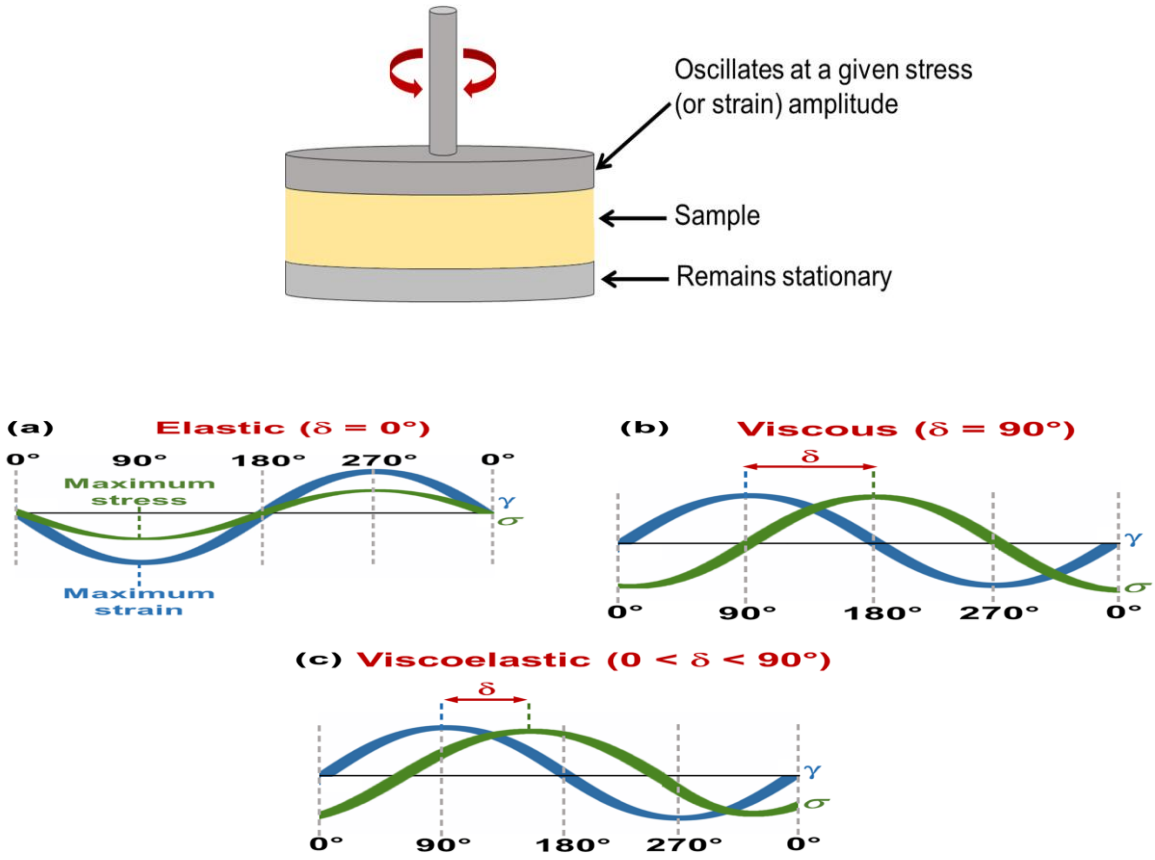

Figure 2-12 : Dynamic Shear Rheometer (SHRP-410)

There are two general types of dynamic shear Rheometers: **controlled-strain** and **controlled stress.**(Jung et al., 1994)

Strain Control Mode--When operating in a strain-controlled mode, determine the strain value according to the value of the complex modulus. Control the strain within +/-20 % of the target value calculated by(Joshi et al., 2013; Jung et al., 1994)

equation given below:

$$\gamma = \frac{12}{(G^*)^{0.29}} \quad \text{.....Equation 2-11}$$

γ = shear strain in percent

G* **= complex modulus in kPa**

Stress-Controlled Mode: When operating in a stress-controlled mode, determine the stress level according to the value of the complex modulus. Control the stress within +/-20% of the target value calculated by ***equation below***:(Joshi et al., 2013; Jung et al., 1994)

$$\tau = \frac{0.12}{(G^*)^{0.71}} \quad \text{Equation 2-12}$$

Where:

τ = shear stress in kPa

Sinusoidal varying stress and strain expression in DSR Test

These components are formulating from the sinusoidally varying stress and strain can be shown as(Gordon da airey, 1997; Izzi & Yusoff, 2012)

Stress

$$\sigma_{(t)} = \sigma_0 \sin(\omega t) \quad \text{Equation 2-13}$$

Strain

$$\gamma(t) = \gamma_0 \sin(\omega t + \delta) \quad \text{Equation 2-14}$$

Where

σ_0 is the peak stress (Pa)

γ_0 is the peak strain,

ω is the angular frequency (rad/s)

t is the time (seconds) and

δ is the phase angle of the measured material response in degree.

The angular frequency, ω, also known as the rotational frequency, is expressed as.

$$\omega = 2\pi f \quad \text{Equation 2-15}$$

The sinusoidally varying stress and strain can also be presented in complex notation(Poole, 2012)

- **Sinusoidally varying stress**

$$\sigma^* = \sigma_0 e^{i\omega t} \text{.....Equation 2-16}$$

- **Sinusoidally varying strain**

$$\gamma^* = \gamma_0 e^{i\omega t+\delta} \text{..... Equation 2-17}$$

The G* has a real and an imaginary part that defines the elastic and viscous behavior of the linear viscoelastic material(Poole, 2012)

$$G^* = \frac{\sigma^*}{\gamma^*} = \frac{\sigma_0}{\gamma_0} e^{i\delta} \text{.....Equation 2-18}$$

Therefore Equation () express as follow

$$G^* = \left(\frac{\sigma_0}{\gamma_0}\right) \cos\delta + i \left(\frac{\sigma_0}{\gamma_0}\right) \sin\delta \text{.....Equation 2-19}$$

Complex modulus (G*) express

$$G^* = G' + i\ G'' \text{..... Equation 2-20}$$

The magnitude of complex modulus $|G^*|$

$$|G^*| = \sqrt{G'^2 + G''^2} \text{..... Equation 2-21}$$

Storage modulus (G')

$$G' = |G^*| \cos(\delta) \text{..... Equation 2-22}$$

Loss modulus (G'')

$$G'' = |G^*| \sin(\delta) \text{..... Equation 2-23}$$

Phase angle

$$(\delta) = \tan^{-1}(G''/G') \text{..... Equation 2-24}$$

Relationship between($|G^*|, G'$, G'' and δ) are expressed

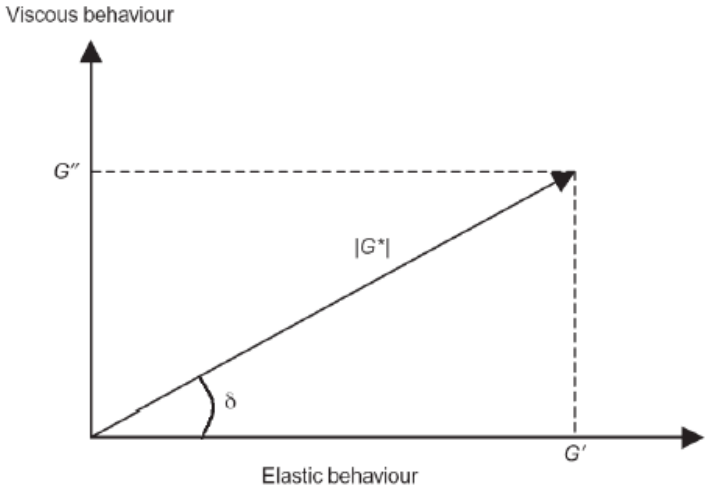

Figure 2-13 Relationship between (shear modulus and phase angle δ) (source: - (Gordon da airey, 1997; Izzi & Yusoff, 2012; Robert N Hunter, 2015))

The storage and loss moduli are sometimes misinterpreted as the elastic and viscous modulus respectively.

2.5.2 Performance Graded Binder Specifications

Table 2-4 : Performance parameter and specification

Test	Performance Parameter	Asphalt Binder Condition State	Specification	Specification Limit	Test Temp. ºC
DSR	Rutting resistance	Neat	G*/sinδ @10 rad/sec.	1.0kPa (Min.)	High
DSR	Rutting resistance	RTFO-aged	G*/sinδ @ 10 rad/sec	1.0kPa (Min.)	High
DSR	Fatigue cracking resistance	PAV-aged	G*/sinδ @ 10 rad/sec	5000kPa (Max.)	Intermediate

Source (FHWA,1994)

2.6 Literature Summary

The literature review explores various aspects of bitumen binder, including its composition, refining methods, and properties. It also discusses different types of bituminous materials and their specifications, such as penetration and viscosity. The Superpave specification for superior performing asphalt pavements is examined, along with the development of pavement temperature prediction models. Previous studies on performance grade (PG) development in different countries are reviewed, highlighting the impact of climate change on asphalt grade performance. Additionally, the review discusses performance-based binder tests. Overall, the literature review provides a comprehensive overview of the relevant topics related to bitumen binder and asphalt pavement performance.

CHAPTER THREE

3 Research Methodology.

3.1 Introduction

Ethiopia, one of Africa's largest countries, boasts diverse landscapes that exhibit striking variations in terrain and altitudes. These variances span from the depths of Assale Lake in the Danakil depression, which lies approximately 155 meters below sea level, to the heights of Ras Dejene at an elevation of about 4,533 meters above sea level. Consequently, Ethiopia's climate is primarily influenced by the seasonal movement of the Intertropical Convergence Zone (ITCZ) and the accompanying atmospheric circulations, along with the intricate topography of the nation. The distinct physiography and elevations found within Ethiopia, such as the highlands and lowlands, give rise to a multitude of climates, ranging from desert-like conditions to those typically observed in equatorial mountainous regions. (National Meteorological Agency, 2020)

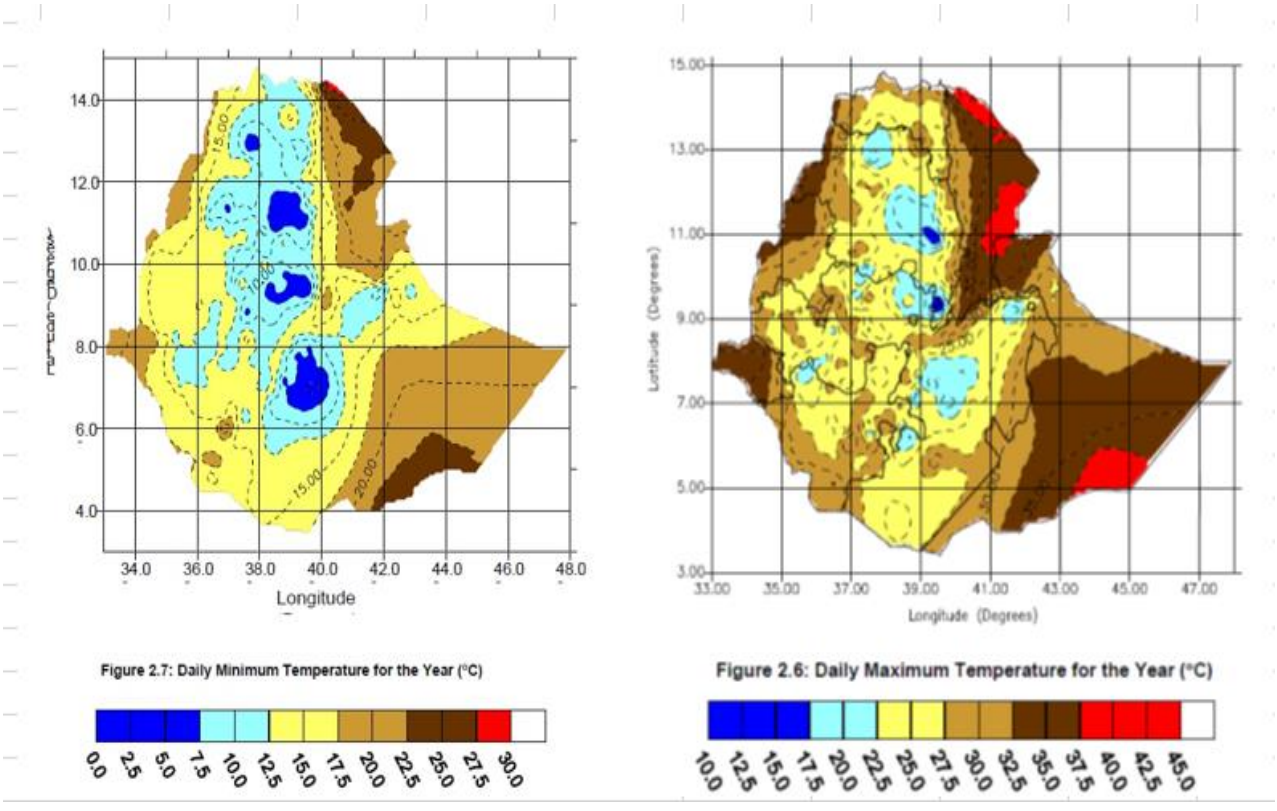

Figure 3-1:Daily max and mini Temperature in Ethiopia for the year. (source NMA,2001)

Table 3-1:Ethiopia elevation and its coverage area.

Elevation(m)	Area_km2	Percent (%)
<500	150,594.6	13.293
500-1500	597943.52	52.782
>1500	384325.32	33.925
Total	**1,132,863.44**	**100**

The traditional climate classifications of the country based on altitude and temperature shows the presence of five climatic zones namely: **wurch** (cold climate at more than 3000 M. altitude), **Dega** (temperate like climate -highlands with 2500-3000 Mts.), **woina dega** (warm-1500-2500), Kola (hot and arid type, less than 1500m in altitude), and **Berha** (hot and hyper-arid type) climates. (NMA,2001)(Daba, 2018)

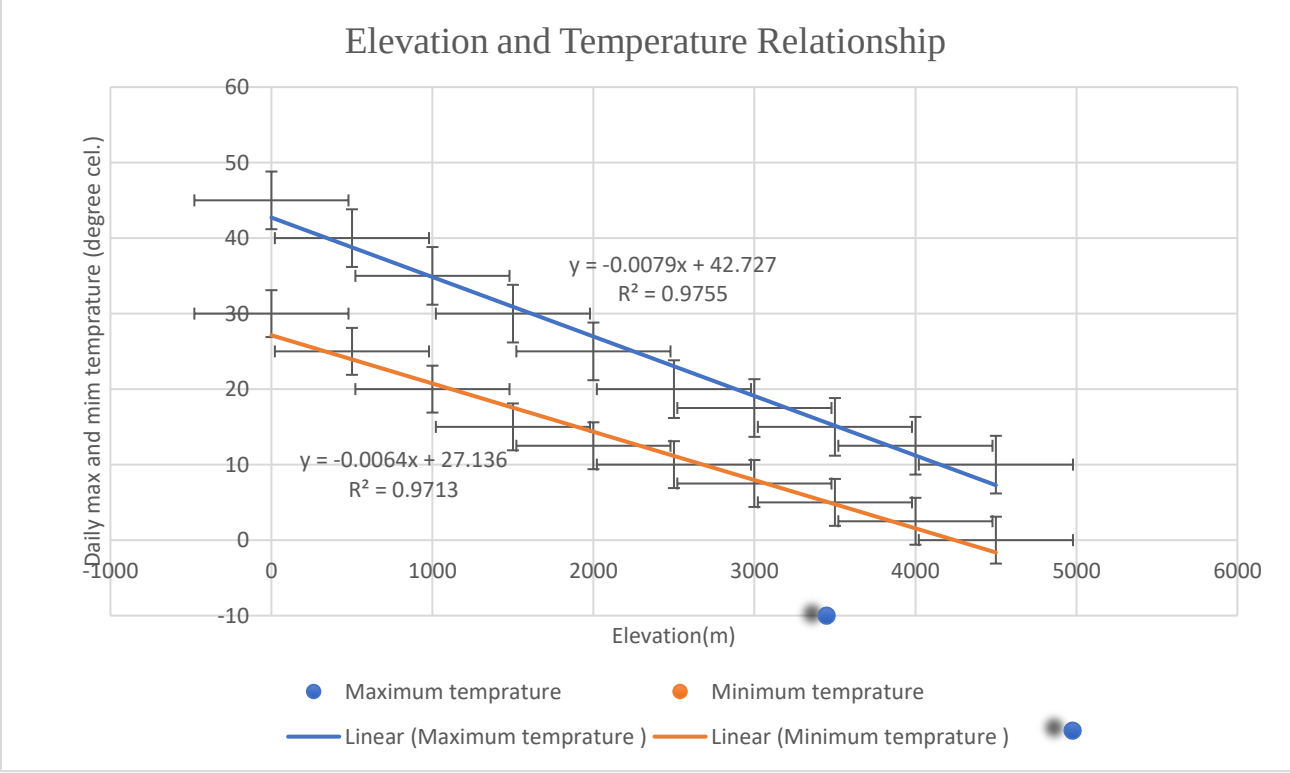

Figure 3-2 :Elevation and Temperature Relationship.

3.2 Study Area

The study focuses on determining the performance grade of Superpave bitumen specification in Ethiopia. The research considers various approaches to achieve specific objectives. The study area encompasses the geographical coordinates of Ethiopia, which lie between 4.05° to 14.277° latitude and 34.5° to 42.8° longitude. Moreover, the location of station points within the study area corresponds to the administrative zones of Ethiopia.

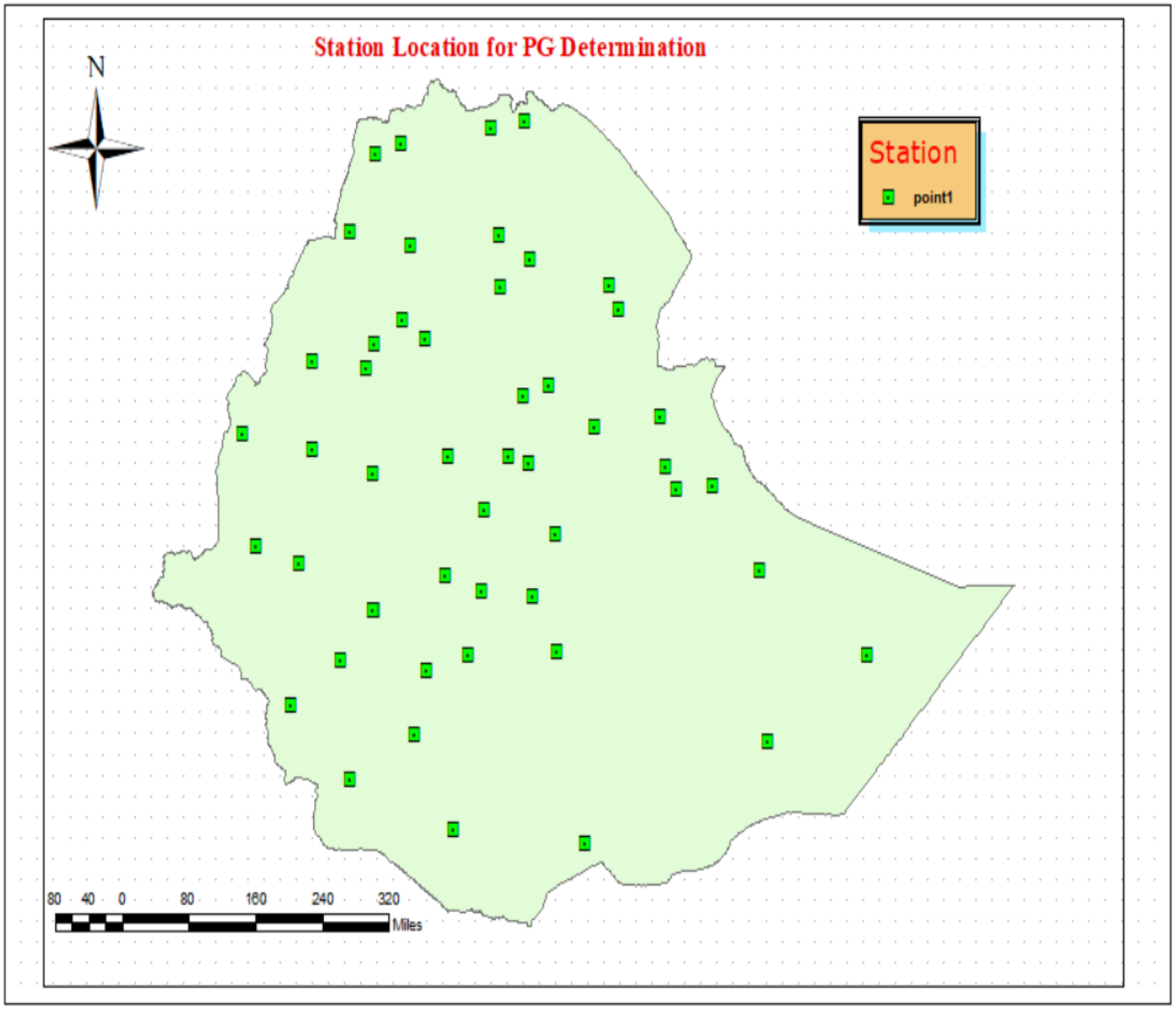

Figure 3-3: Metrological Station Location in Ethiopia.

3.3 Research Design (Procedure)

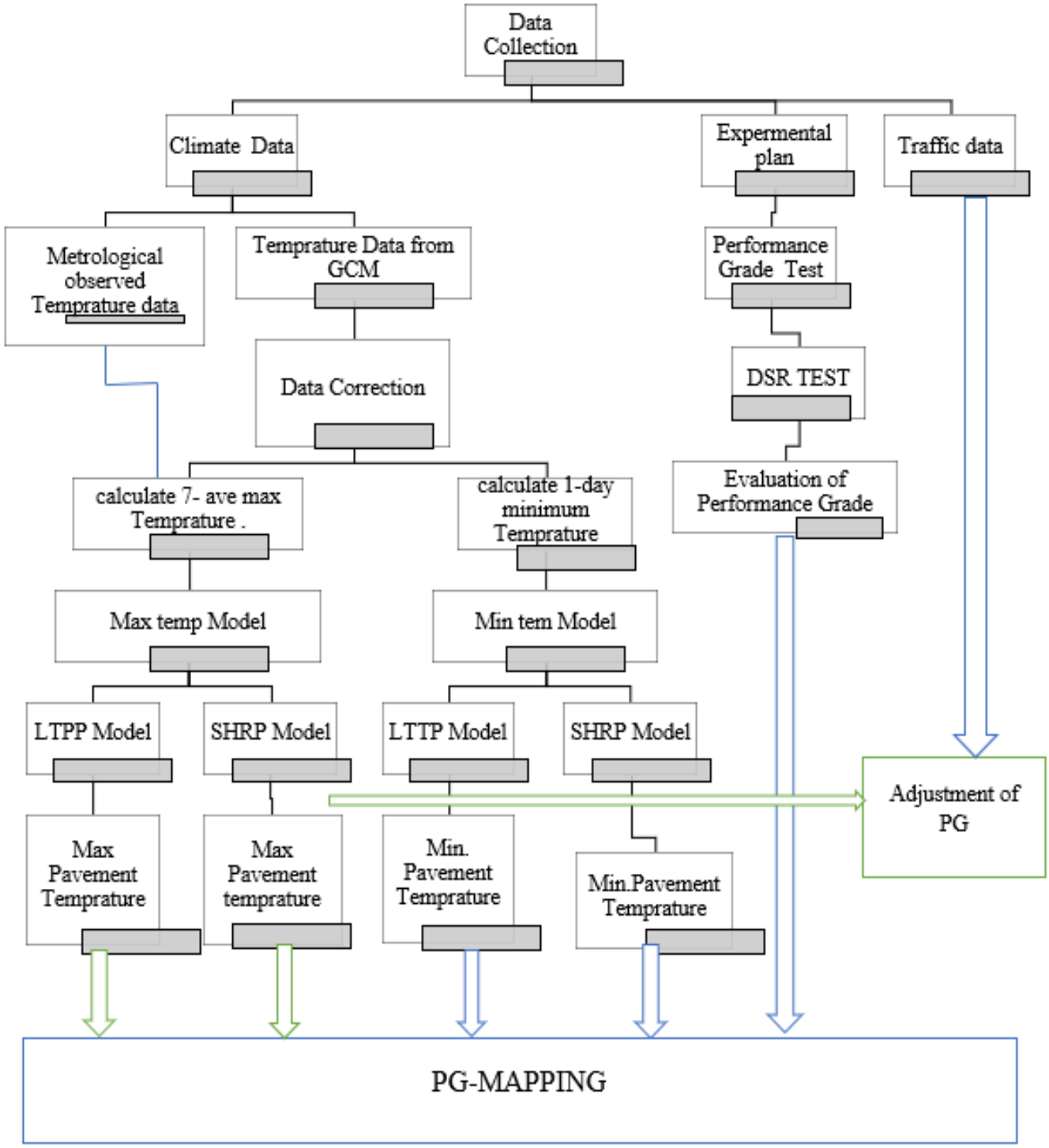

Figure 3-4 : Research General Work Flow.

3.4 Data Collection.

This paper has two sequential work first Statistical analysis of Climate (temperature) data and determine Max and Min pavement temperature to determine performance grade (PG) for Ethiopia and latter Conducting Laboratory Test determine the performance grade of currently used Asphalt grade. The study uses both primary and secondary Source of data Requires The data requires for study collecting from 3 road project (Kaliti-Tulidimtu, Lemi Alem ketema and Menda-Bure) project collect bitumen sample of different grade and temperature data collected from National Meteorological Agency and Global climate model (GCM) as mention later to developing Base line and future performance grade (PG) of asphalt respectively. daily Maximum and Minimum Temperature data analysis for each study area using Excel and traffic volume Range data from Ethiopia Road Authority (ERA) manual. For this research purpose The daily observed maximum and minimum temperature data from National Meteorological Service Agency of Ethiopia from(1990-2020) of the 51 meteorological stations In figure (3-3) with temperature records were used for to determine present asphalt super pave pavement grade and future projection data generate GCM-data from https://esgf-node.llnl.gov/search/cmip6/ daily maximum temperature from (2020-2100) with two different scenario(SSP 2 4.5 and SSP 5 8.5) for the above two global climate model (INM-CM5-0and CMCC-ESM2). The station list is listed on APPENDEX (A).

3.5 Pavement Temperature Data Analysis Method

3.5.1 Pavement Temperature Grade.

The SUPERPAVE system stands out due to its approach of specifying asphalt binder based on the anticipated maximum and minimum pavement temperatures it will encounter. This system ensures that the binder chosen is suitable for the specific temperature range it will be exposed to. However, it is important to note that the mechanical properties, such as stiffness and shear modulus, remain consistent across all grades of binders, regardless of temperature requirements.

Table 3-2 : Super pave bitumen specification.

High Design Temperature (^{O}c)	PG Designation (xx)	Low design Temperature (^{O}c)	PG Designation (yy)
< 46	46	>-10	-10
< 52	52	>-16	-16
< 58	58	> -22	-22
< 64	64	> -28	-28
< 70	70	> -34	-34
< 76	76	>-40	-40
< 82	82	> -46	-46

Source: SHRP-410

The temperatures given in Table correspond to the pavement temperature and can be estimated from the air temperature data collected over the years. SUPERPAVE defines the high and low temperatures by 7-day average maximum air and l-day minimum air temperature. The 7-day average maximum temperature is defined as the average highest air temperature for a period of 7 consecutive days within a given year. The 1-day minimum temperature is defined as the lowest air temperature recorded in a given year. The data are collected over multiple years and the design high and low pavement temperature values are then estimated using the average and standard deviations of the data collected for a desired reliability level.

the factor "z and σair" is included to introduce reliability in the selection of binder grade. For instance, a high pavement temperature grade of 58 ^{O}C at 98% reliability level means that 98% of times the pavement temperature will not exceed 58 ^{0}C

3.5.2 Reliability Determination

In this research, the asphalt binder Performance Grades (PGs) were calculated using two reliability levels: 50% and 98%. The PGs with a 50% reliability level are more cost-effective compared to those with a 98% reliability level. However, binders with 50% reliability are more susceptible to temperature-induced damage on the pavement. The selection of either reliability level depends on various factors, such as the cost situation and traffic conditions of the road. This choice is influenced by the Superpave pavement design method commonly adopted by many states in the US.(Ali Hussain et al., 2020)

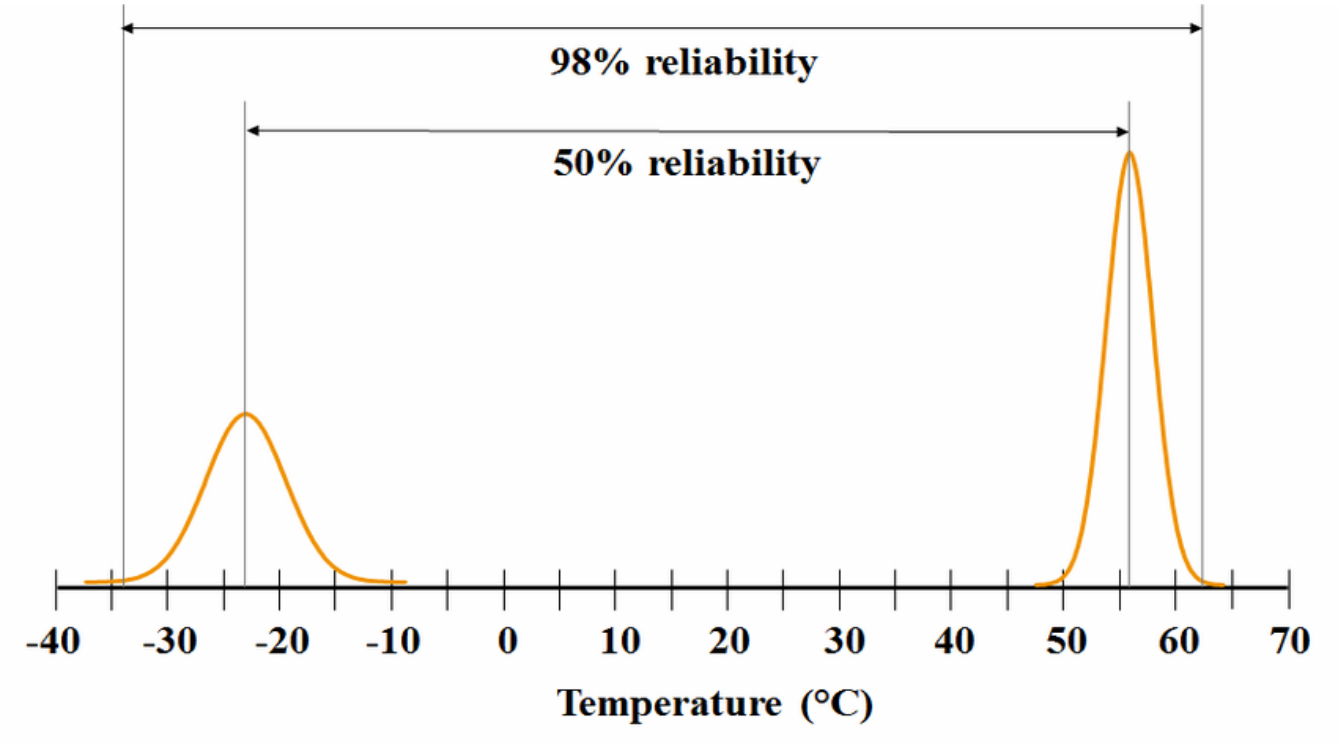

Figure 3-5. Pavement temperature prediction reliability

Source (AASHTO-SP-1)

3.5.3 Current (Baseline) Performance Grade (PG) Determination

- The daily observed maximum and minimum temperature data from National Meteorological Service Agency of Ethiopia from (1990-2020) are collected
- Calculate mean of 1-day minimum air temperature.
- Calculate Mean of Seven-day Maximum Consecutive daily air Temperature
- Calculate standard deviation.
- Select the reliability percentage and determine the Z -value.
- Using Pavement Temperature model (LTPP and SHRP) calculate pavement temperature.
- Select the Maximum and Minimum pavement temperature from AASHTO-SP1.

3.5.4 Climate change assessment on performance grade of asphalt

Temperature is a major factor affecting pavement materials and their deterioration. Rising temperatures can negatively impact the Dynamic Modulus (E*) of the surface HMA layer, leading to a decrease in pavement service life. Climate change is causing significant shifts in weather patterns, including higher temperatures, altered precipitation patterns, and more frequent extreme weather events like heavy rainfall and floods. These changes have important implications for the choice of asphalt grades used in road construction and maintenance. Asphalt, a vital component of road surfaces, is highly sensitive to temperature. Different grades of asphalt are designed to perform optimally within specific temperature ranges. With ongoing climate warming, selecting appropriate asphalt grades becomes crucial to ensure roads can withstand higher temperatures and other climate-related strains.

Therefore, it is essential to carefully consider the impact of climate change on asphalt performance when selecting asphalt grades for road construction and maintenance. Engineers and planners must consider the changing climate conditions and use appropriate materials and techniques to ensure the durability and longevity of the road network. Environmental factors are one of the primary causes of pavement deterioration.

Ethiopia climate change with in different Scenario (SSP)

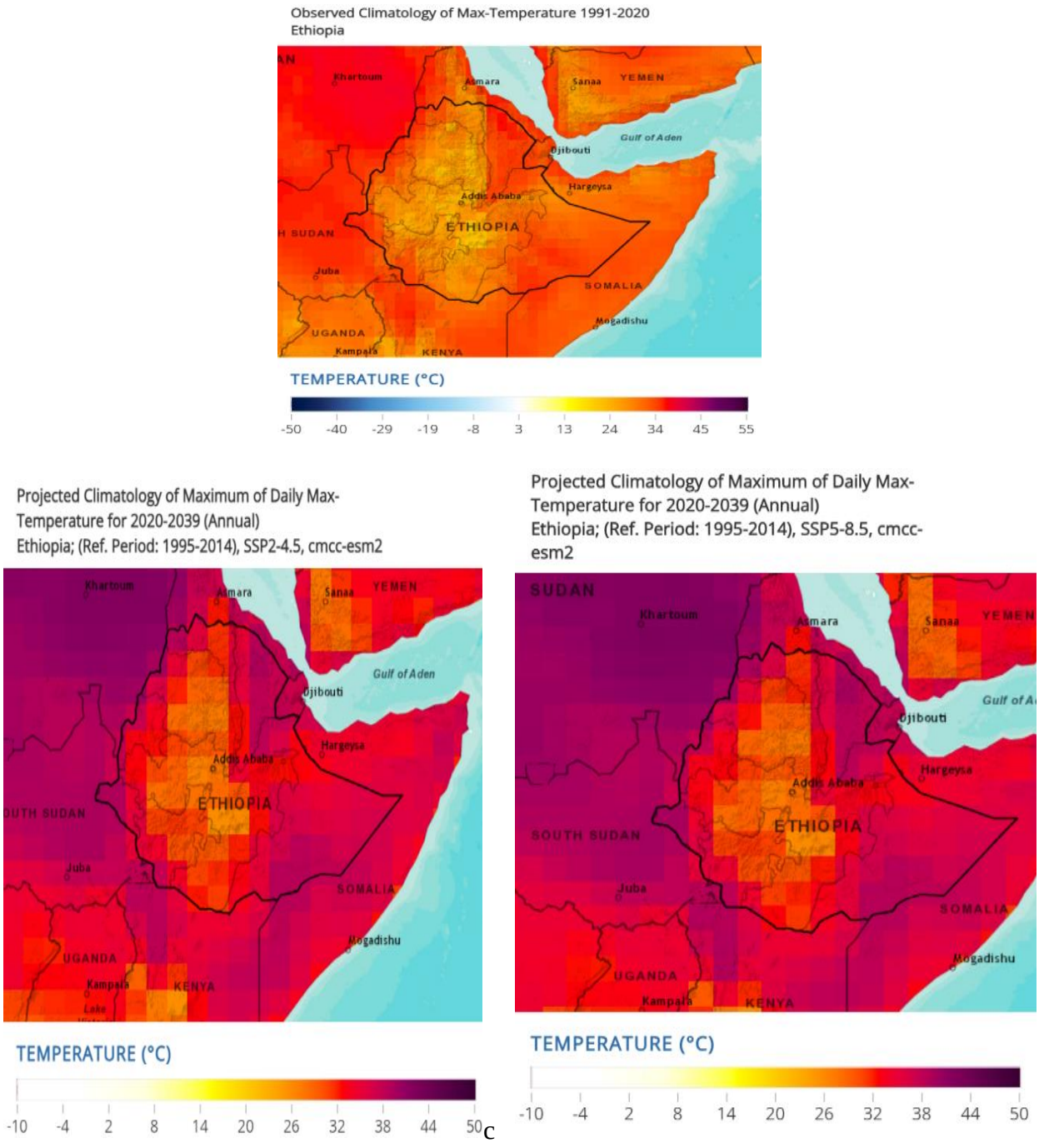

Figure 3-6 : Ethiopia Max temperature of 1991-2020, 2020-2039 of different scenario.

Source: (https://climateknowledgeportal.worldbank.org/country/ethiopia/)

When attempting to estimate how future global warming will contribute to climate change, several elements must be considered. A significant variable is the quantity of future greenhouse gas emissions. according to (IPCC,2021) AR-6 (IPCC, 2021)

Table 3-3 : Scenario description (IPCC, 2021)

SSP	Scenario	Radioactive forcing in the year 2100	Estimated warming (2041–2060)	Estimated warming (2081–2100)	Very likely range in °C (2081–2100)
SSP1-1.9	very low GHG emissions: CO2 emissions	1.9 Watt/m^2	1.6 °C	1.4 °C	1-1.8 °C
SSP1-2.6	low GHG emissions: CO2 emissions	2.6 Watt/m^2	1.7 °C	1.8 °C	1.3-2.4 °C
SSP2-4.5	intermediate GHG emissions: CO2 emissions	4.5 Watt/m^2	2 °C	2.7 °C	2.1-3.5 °C
SSP 3-7	high GHG emissions: CO2 emissions double by 2100	7 Watt/m^2	2.1°C	3.6 °C	2.8-4.6 °C
SSP5-8.5	very high GHG emissions: CO2 emissions	8.5 Watt/m^2	2.4 °C	4.4 °C	3.3-5.7 °C

Source ((IPCC, 2021)

The most important GHG generated by human activity is CO2 for this reason, the GHG emissions are usually expressed as CO2 equivalent. Since it is not possible to know for sure what are the amounts of CO2 that will be generated in the future, climate change studies generally assume possible global warming scenarios. The scenarios vary from Moderate to very hottest. The first one assumes that immediate and significant actions are taken to reduce GHG emissions

globally. The latter one assumes that no significant actions are taken, so the GHG emissions continue to increase in the future(Delgadillo et al., 2020).

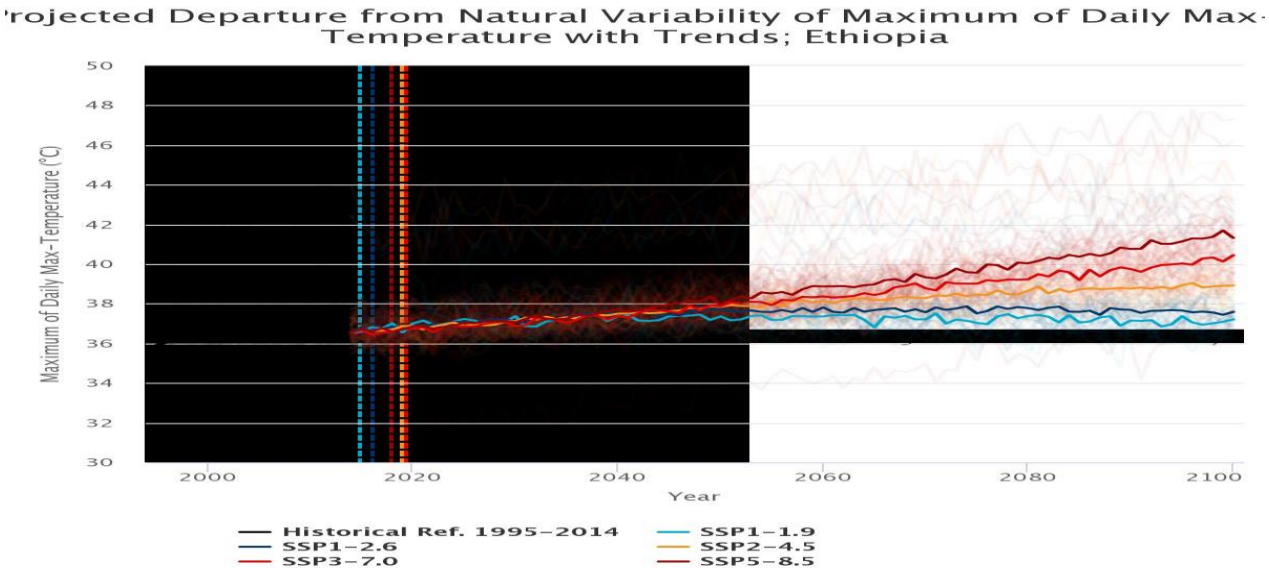

Figure 3-7 : Scenario variability for Ethiopia future temperature. source:(https://climateknowledgeportal.worldbank.org/country/ethiopia/)

Based on the five scenarios defined by the IPCC, the Working Group Coupled Modelling WGCM, member of the WMO, carried out a project called Coupled Model Intercomparing Project Phase 6 (CMIP6) the Coupled Model Intercomparing Project Phase 6 (CMIP6) is a large international research effort involving climate models and their simulations of past, present, and future climate. The project is designed to improve our understanding of the Earth's climate system and its response to various factors, such as greenhouse gases, aerosols, and land use changes.(IPCC, 2021)

CMIP6 involves the participation of many climate modeling groups from around the world and includes simulations from a wide range of models, including both Earth System Models (ESMs) and Earth System Models of Intermediate Complexity (EMICs). The project aims to produce a comprehensive and up-to-date set of climate model simulations that can be used to assess the state of the Earth's climate system, evaluate the impacts of different climate change scenarios, and inform policy decisions.

There are 49 different modelling groups participating in CMIP6, the map below shows the location of the modelling groups participating in CMIP6.

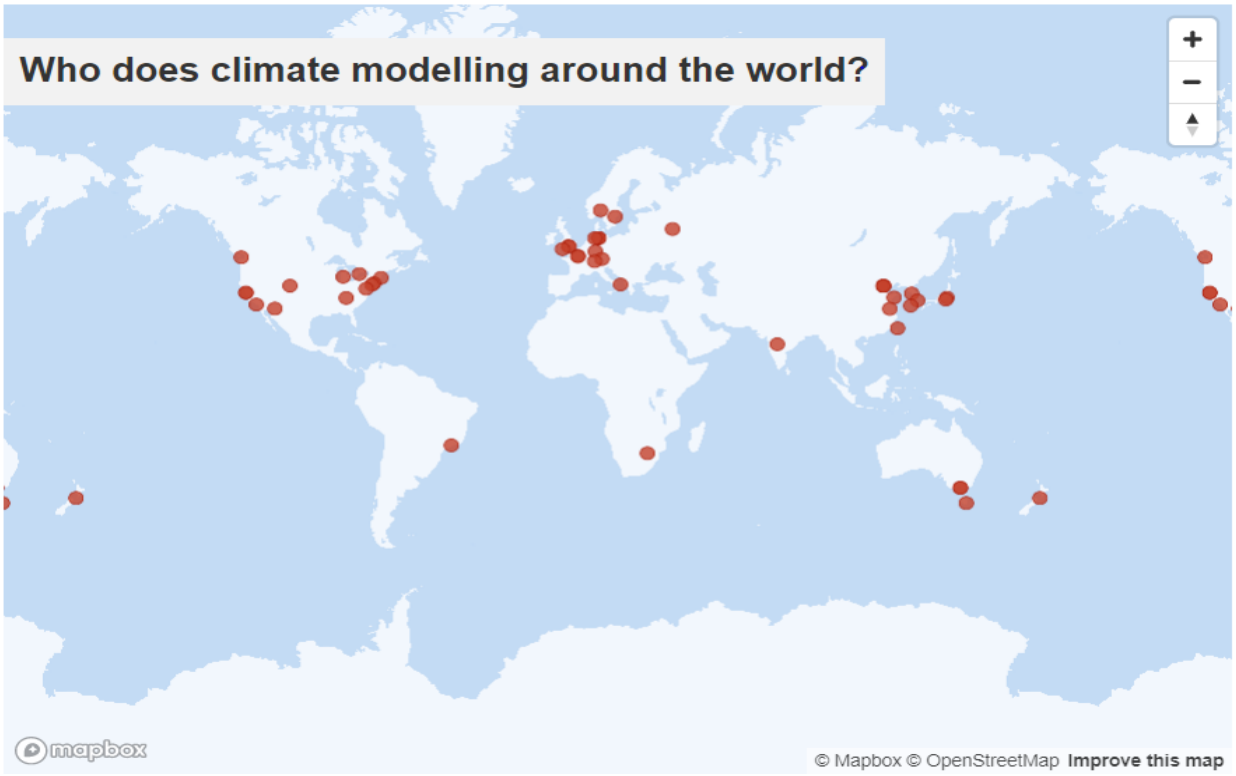

Figure 3-8:Country of modelling groups participating in CMIP6

Source (https://www.carbonbrief.org/cmip6-the-next-generation-of-climate-models-explained/)

3.5.5 Global Climate Model Selection

The Coupled Model Intercomparing Project Phase 6 (CMIP6) models More than 100 GCMs obtained from the CMIP6 archives (https://esgf-node.llnl.gov/search/ cmip6/). Based on table (2-3) and model availability for all variables (Tmax, and Tmin) for the historical time period. The criteria used to filter the models were daily data, nominal resolution, and source type: AOGCM and from the r1i1p1f1 variant and select due to number of data for less time consume for extraction. Therefore, two climate models were selected from the WCRP CMIP6 archive (https://esgf-node.llnl.gov/search/cmip6/ used for this study Model set as shown below within its country to Develop future asphalt pavement grade (PG).

Table 3-4 Selected GCM- Model list

S/N	CMIP6 Model-Name	Country
1	INM-CM5-0	Russia
2	CMCC-ESM2	Italy

3.6 Determination of future Asphalt grade (PG)

3.6.1 Analysis Method of future climate data to determine Asphalt Binder Grade

Available climate change models are very useful tools to investigate possible future trends in global warming and to assess climate change. Their predictions are not intended to be exact forecasts, but to serve as a guide for the possible effects of GHG in climate change (Delgadillo et al., 2020) ,Both Global and Regional Climate models (GCM, RCM) have **systematic errors** (biases) in their output. To use it for specific purpose we should be downscaling or bias correction.

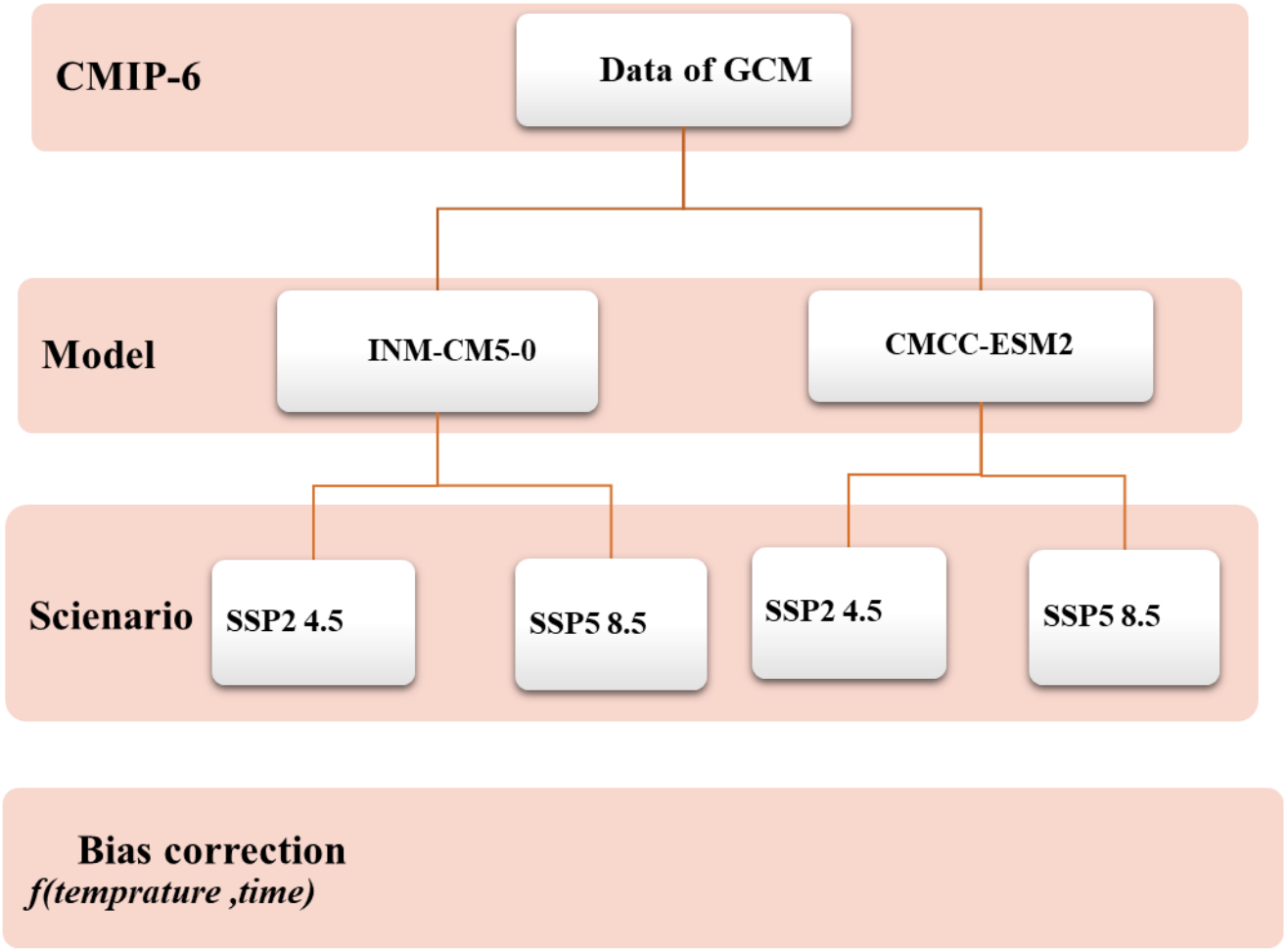

Figure 3-9 : Flow chart of method of analysis for future pavement grade determination

In this paper follow the following procedure to determine future pavement performance grade (PG).

Method of analysis step is shown as below

1. Data from the GCM sources available in **World Climate Research program (WCRP-CMIP -6)** from https://esgf-node.llnl.gov/search/cmip6/ Database were download.
2. **Climate change data extraction**

   To develop superpave performance grade for Ethiopia using future projected max temperature data collect from two GCM (INM-CM5-0 and CMCC-ESM2) from 2020-2040, (2040 -2070) and 2070-2100 in two climate model scenarios (SSP 2 4.5 and SSP 5

8.5). the data generate in form of (NetCDF file format (.nc)) format for extracting this format or to convert the file into (**csv or .xls) File** format. there is different method thus are by using writing programming language in R, Python, using MATLAB's and using ArcGIS Software (Multi-Dimensional tool) by convert to table form. For this study use the ArcGIS software using each area location (**longitude and latitude**) to convert **NetCDF file format (.nc)** into (**csv or .xls) to calculate 7-day daily maximum temperature.**

3. Bias correction the GCM Data

Global climate models (GCMs) are computer simulations used to predict future climate scenarios by simulating the Earth's climate. However, these models are not perfect and can have biases, which can affect the accuracy of the predictions. To improve the accuracy of GCM predictions and ensure their usefulness for climate research and policy-making, bias correction is an important step. Bias correction involves adjusting GCM output to better match observed data. There are different methods of bias correction, but they all aim to correct systematic errors in the model output. To determine the Superpave pavement performance grade, climate data must be extracted. However, before using this data, it is important to perform downscaling or bias correction adjustments to ensure its accuracy. This can be achieved through various statistical downscaling methods, which aim to correct any systematic errors in the climate data.

A. **Delta Method and**
B. Bias-Correction Spatial Disaggregation (BCSD)
C. Bias Correction/Constructed Analogues with Quantile mapping reordering (BCCAQ).
D. EQM (Empirical Quantile Mapping) method

Based on the available bias correction downscaling methods, you have chosen to use the delta method. This method is preferred because it is simple to apply and preserves the observed pattern of temporal and spatial variability. This will help ensure the accuracy of the extracted data for determining the Superpave pavement performance grade.

$$T_{Sd\ Delta} = T_{Gcm\ SSP} + (T_{m\ Obs} - T_{m\ Gcm\ his}) \quad \text{..... Equation 3-1}$$

where,

T (SD, Delta) = downscaled data of temperature,

T_m (Obs) = the average monthly observed

T_m ($_{GCMhist}$) =average monthly GCM simulation historical data of Temperature.

Subscript GCMssp represents the GCM's SSP outputs over the future period and

subscript Obs represents the observation values.

Method of Temperature data adjustment-The correction factor determines using equation (3-1) and add in the forecasting temperature data example for Addis Ababa.

Table 3-5: Example of Bias correction index calculation

Bias Correction for Temperature

Calculation of correction factor			
Month	Obs	GCM	factor
1	24.294	24.306	-0.012
2	25.731	26.942	-1.211
3	26.338	27.246	-0.907
4	25.437	24.952	0.485
5	24.348	23.359	0.989
6	23.790	20.607	3.182
7	20.871	20.644	0.228
8	20.090	20.736	-0.645
9	20.559	20.987	-0.428
10	21.339	22.568	-1.229
11	21.992	23.312	-1.320
12	23.020	24.093	-1.073

Future projected temperature data adjust using the above correction factor. for instance, in Addis Ababa to the future daily maximum temperature of monthly adjustment factor for January = -0.012 ^{o}c add in every and each year of January GCM forecasting temperature data and correct it.

Table 3-6: Example Corrected Forecast Temperature data Addis Ababa January ,2040.

Day	Month	Year	Forecast	corrected =forecast + correction factor of monthly index
1	January	2040	26.9	26.89
2	January	2040	26.18	26.17
3	January	2040	25.19	25.18
4	January	2040	25	24.99
5	January	2040	25.71	25.70

4. **Calculate the average seven-day maximum.**

   After step-2 the extracted daily maximum temperatures, the average seven-day high air temperatures are determined for two different time periods of1990-2020(Baseline), 2020 - 2040, 2040-2070 and 2070-2100, then average seven-day high pavement temperatures are estimated for the considered time periods using two different pavement temperature prediction models (SHRP and LTPP) in two different Scenario.

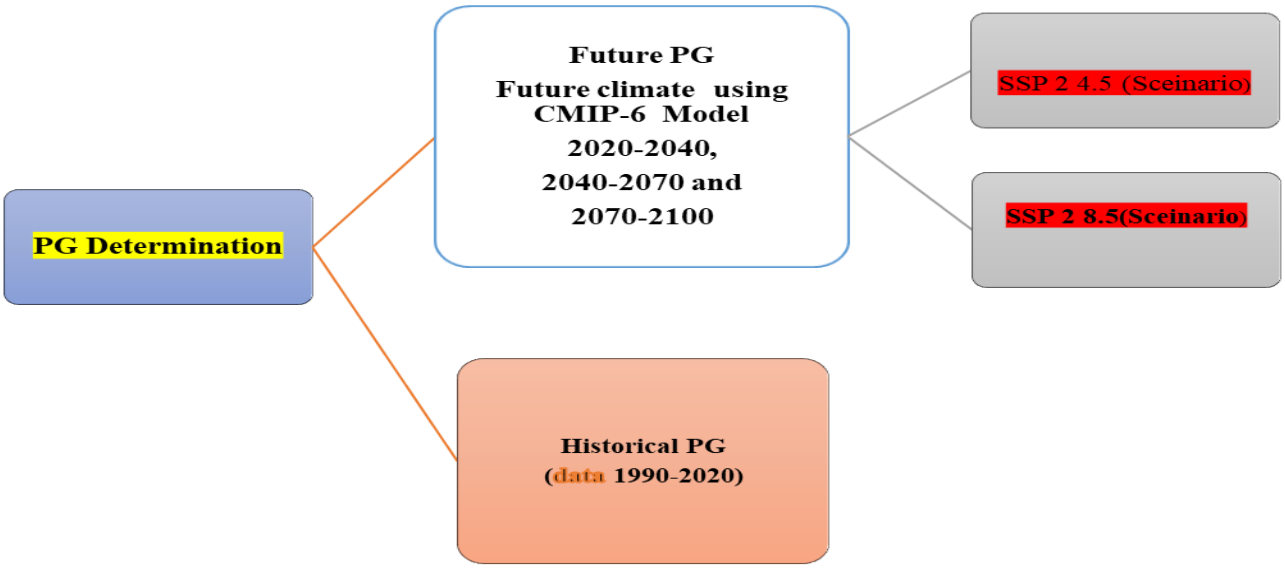

Figure 3-10 : Future PG determination flow chart.

5. Selection of Asphalt Binder Grade

Calculating the mean of each year of maximum consecutive 7-Day maximum temperature and using two model calculate the predicted pavement temperature. but as per Asphalt Institute Superpave Performance Graded Asphalt Binder Specifications (SP-1), the Superpave grades were assigned in a 6°C increment format for both high temperatures and low temperature and select the recommended pavement temperature.

Performance grade determination pavement temperature for Addis Ababa

Table 3-7: Example of calculation of PG XX-YY

Maximum temperature Prediction pavement Temperature for Addis Ababa					
SHRP Model (Strategic Highway Research Program**)**					
$Tpav$, 20mm= ($Tair$ − 0.00618Lat^2 + 0.2289Lat + 42.4) (0.9545) − 17.78 + z σair					
Variable	value	Reliability	z	Critical Temp.	PG Value
$Tair$	29.92	50%	0	52.7	PG-58-YY
Lat	9.01891	98%	2.055	55.1	PG-58-YY
σair	1.16				
LTPP Model (Long-Term Pavement Performance**)**					
$Tpav, h$ = 54.32 + 0.78$Tair$ − 0.0025Lat^2 − 15.14 $log10(d$ + 25) + z (9 + 0.61σ^2air) ^0.5					
Variable	value	Reliability	z	Critical Temp.	PG Value
$Tair$	29.92	50%	0	52.4	PG-58-YY
Lat	9.01891	98%	2.055	58.9	PG-64-YY
σair	1.16				

Minimum Temperature Prediction Pavement Temperature for Addis Ababa

SHRP Model (Strategic Highway Research Program**)**

$T pav, l = Tair + 0.051\ d - 0.000063\ d^2 - z\ \sigma$ air

Variable	value	Reliability	z	critical value	PG Value
$Tair$	value	50%	0	3.6	PG-XX-10
Lat	9.01891	98%	2.055	1.7	PG-XX-10
σair	0.88				
1-day-mean temperature	2.56				

LTPP Model (Long-Term Pavement Performance**)**

$Tpav, l = -1.56 + 0.72Tair - 0.004Lat^2 + 6.26\ log10(d + 25) - z\ (4.4 + 0.52\sigma^2 air)0.5$

Variable	value	Reliability	z	critical value	PG Value
$Tair$	value	50%	0	10.3	PG-XX-10
Lat	9.01891	98%	2.055	5.8	PG-XX-10
σair	0.88				
1-daymean temperature	2.69				

3.7 Method of Model comparation SHRP and LTPP

For comparation of two model result only use the baseline pavement temperature of 98% reliability Using **t-test** to compare the results of the SHRP and LTPP pavement temperature prediction models, we can perform a hypothesis test to determine if there is a significant difference between the mean predicted pavement temperatures from the two models. Using **Paired t-test**: This test is used to compare the means of two related groups (in this case, the same sample of data run through both models) to determine if there is a significant difference between them.

To perform This a hypothesis test:

- **Define the null hypothesis**: The null hypothesis (H0) is that there is no significant difference between the mean predicted pavement temperatures from the SHRP and LTPP models.
- **Define the alternative hypothesis**: The alternative hypothesis (Ha) is that there is a significant difference between the mean predicted pavement temperatures from the SHRP and LTPP models.
- **Select a significance level**: We select a significance level (α) of 0.05. This means that we are willing to accept a 5% chance of making a type I error (rejecting the null hypothesis when it is actually true).
- **Calculate the p-value**: calculate the p-value, where n1 and n2 are Number of pavement prediction temperature from the SHRP and LTPP models.
- **Make decision**

3.8 Superpave Performance Based test

3.8.1 Experiment Plan

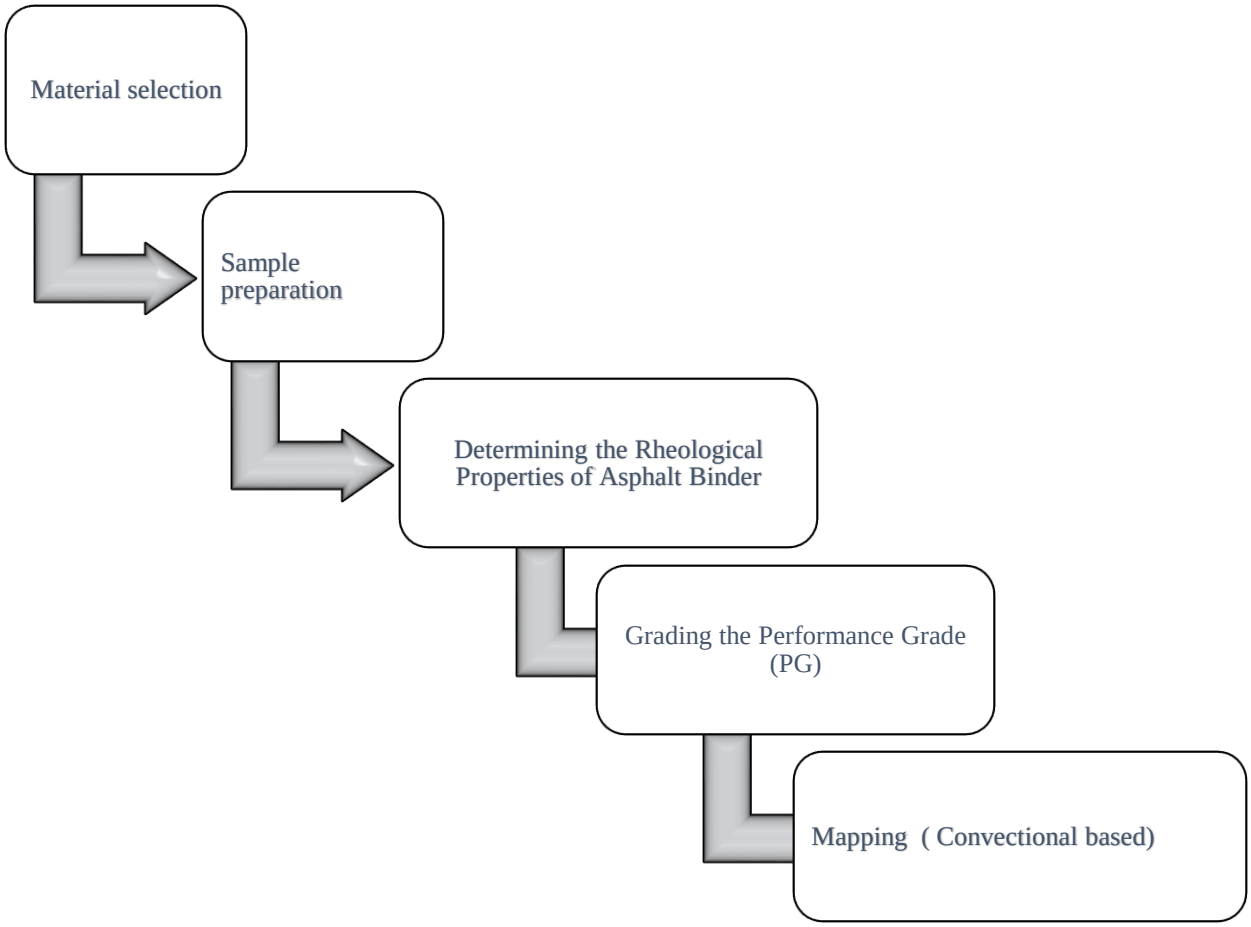

Figure 3-11 Flow chart of experiment design

3.8.1.1 Material selection and Sample preparation

The research is grading of neat current available bitumen sample and the testing required to determine the performance grade (PG) of an asphalt binder. This practice can be used to determine the PG of an unknown asphalt binder, or to verify the PG of a known material.

Table 3-8 sample of currently available in Ethiopia.

S/N	sample grade	Binder condition	Source	Origin
1	Penetration-grade 40/50	unaged /Aged	Menda -Bure project	Arab Emirate
2	Penetration-grade 60/70	unaged /Aged	Kality - Tulidimtu project	Arab Emirate
3	Penetration-grade 80/100	Unaged/Aged	Lemi -Alem Ketema	Arab Emirate
4	Penetration-grade 85/100	unaged /Aged	Kality - Tulidimtu project	Arab Emirate

3.8.1.1 Determining the Rheological Properties of Asphalt Binder.

Dynamic Shear Rheometer (DSR)

A parallel plate geometry is used to test the samples, and the plate diameter is 25 mm for neat bitumen, the DSR test, is used to determine the complex shear modulus and phase angle of asphalt at temperatures ranging from 3 to 88°C. The complex shear modulus and phase angle together are used to characterize the binder at high and intermediate temperatures in order to determine the performance grade. The complex shear modulus, G*, is calculated by dividing the maximum stress by the maximum strain that occurs during the loading cycle. The phase angle of the material, δ, represents the delay in the material's response to the applied load.

Figure 3-12. Dynamic Shear Rheometer (DSR) Machine

3.8.1.2 Grading the Performance Grade (PG) of an Asphalt Binder.

DSR test measures the viscoelastic properties of asphalt binders, which are crucial indicators of their performance under varying temperature and loading conditions. The test involves subjecting the binder to oscillatory shear forces at different temperatures and frequencies. By measuring the complex shear modulus (G*) and phase angle (δ), it provides valuable information for determining the high-temperature (PG High) and low-temperature (PG Low) performance grades of asphalt binders.

On this study the High-Temperature Performance Grade reflects the binder's resistance to rutting and deformation at elevated temperatures. enables researchers to assess the complex shear modulus at high frequencies and temperatures, simulating the actual conditions experienced by asphalt pavements during hot summer months. The research results obtained through DSR testing allow for accurate determination of the PG High grade, ensuring the selection of binders suitable for the targeted environmental conditions and working project.

- Mode of loading: controlled-strain •
- Temperature: 46 to 82 ºC (with the interval of 6 ºC)
- Spindle geometries: and 25 mm (diameter) and 1 mm gap
- Strain amplitude: within the LVE response, dependent on |G*| of each material used.

CHAPTER FOUR

4 Result and Discussion

4.1 Temperature data

From analysis pavement temperature performance grade (PG) determination using historical and future projection temperature data for different locations in Ethiopia developed a Superpave bitumen specification. This specification is based on two different models. The Strategic Highway Research Program (SHRP) model and the Long-Term Pavement Performance (LTPP) model. The analysis revealed that the pavement temperature grade varied significantly across the study locations. The historical temperature data showed that some locations experienced temperature fluctuations graphically shown on (appendix). Future temperature projections also showed that locations are likely to experience significant temperature increases in the coming years.

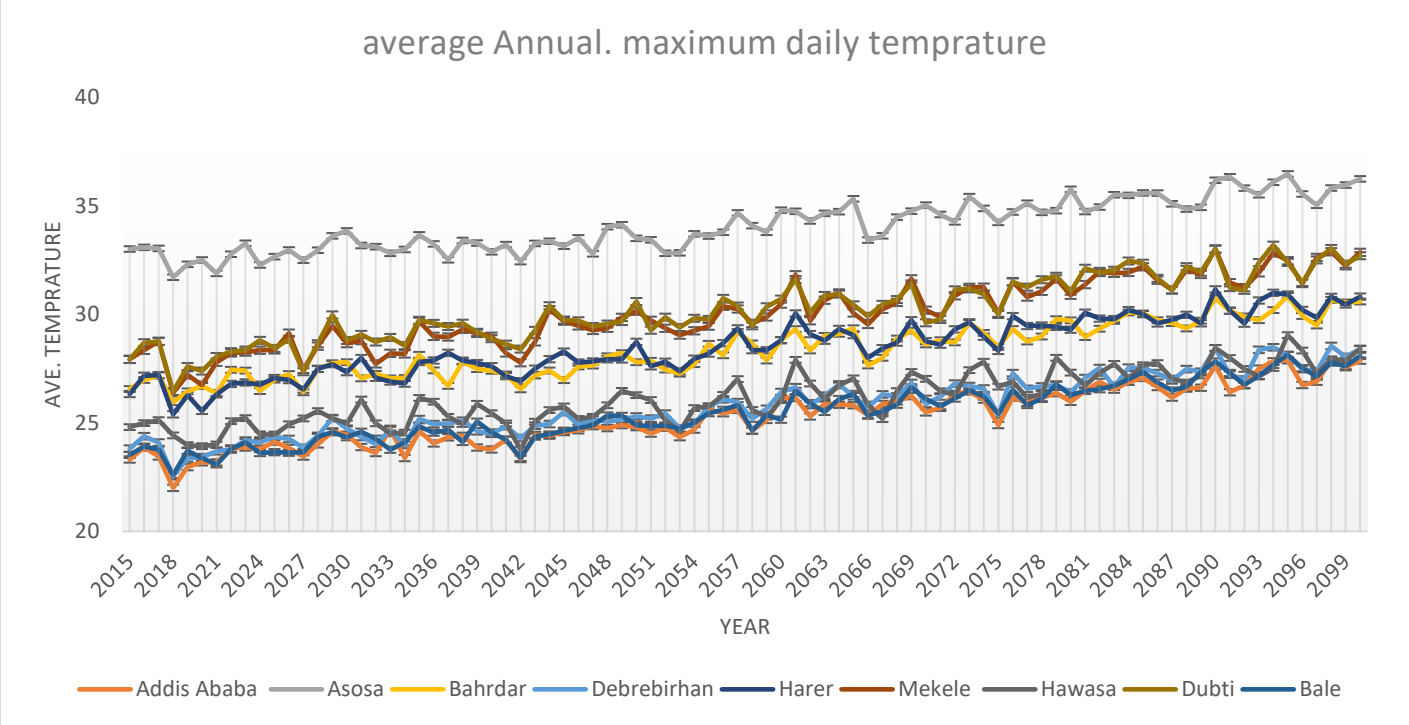

Figure 4-1: Ave.Anually Max. daily Air temperature fluctuation in some selected area

4.1.1 Historical and Future projection 7-Daily temperature data

A. Shared socio-economic pathways (SSP2(4.5))

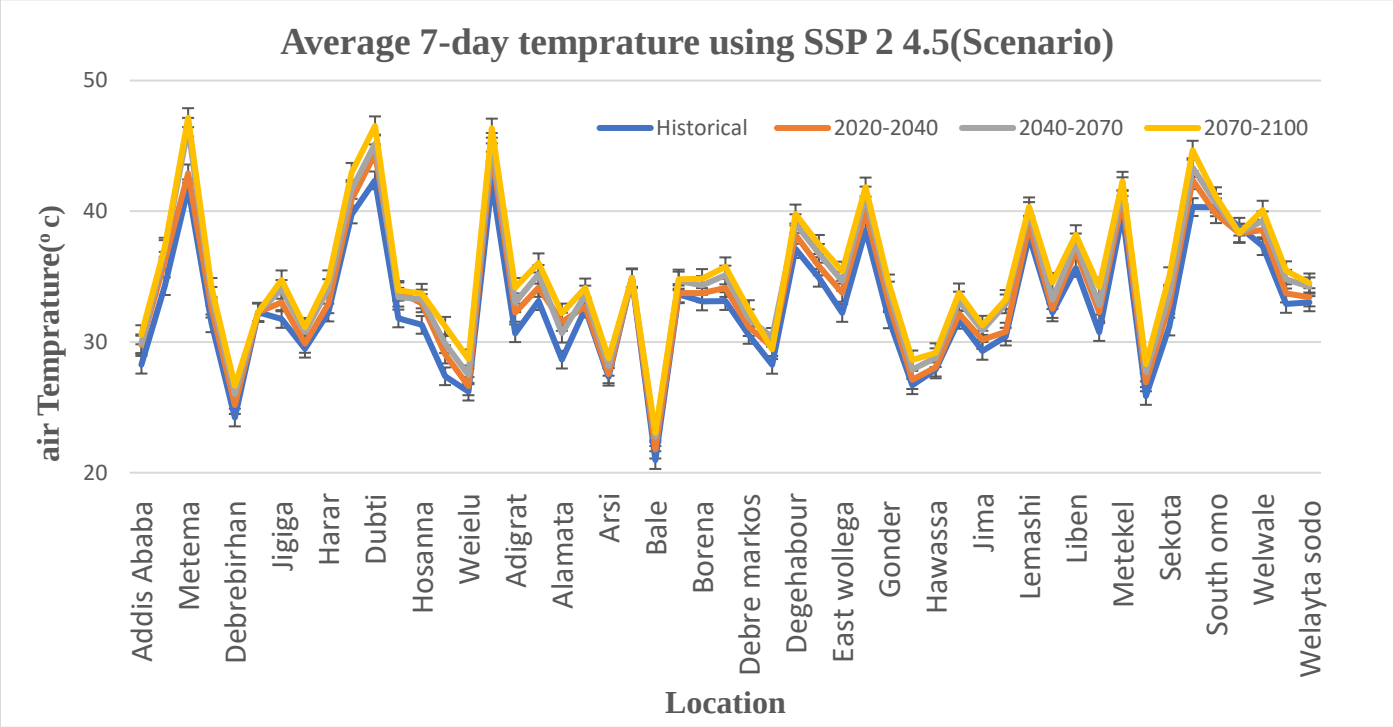

Figure 4-2: Air temperature Historical and Bias corrected future projection data in SSP 2(4.5)

After select the Seven-day consecutive max daily air temperature the analysis result show that the hottest region in the country is Afar (Dubti, Elidar), with maximum temperatures ranging from 40.31°C to 42.37°C during the historical period (1990-2020). Looking ahead to the future, the temperature projections indicate an increase in the range from 42.37°C to 44.55°C for the period of 2020-2040, from 42.27°C to 45.5°C for 2040-2070, and from 42.27°C to 47.67°C for 2070-2100.Another region experiencing high maximum temperatures is Metema, where the observed temperatures range from 39.14°C to 41.76°C historically. The future projections for Metema indicate temperature ranges of 41.76°C to 44.94°C for 2020-2040, 42.94°C to 45.94°C for 2040-2070, and 43.23°C to 46.82°C for 2070-2100.

On the other hand, the coldest region in the country is found in Bale Robe, where the observed temperatures range from 19.16°C to 20.97°C during the historical period. Looking ahead, the

temperature projections suggest a range of 20.97°C to 21.78°C for 2020-2040, 22.76°C to 23.95°C for 2040-2070, and 22.86°C to 23.95°C for 2070-2100 in Bale Robe for this scenario.

Shared socio-economic pathways (SSP 5(8.5))

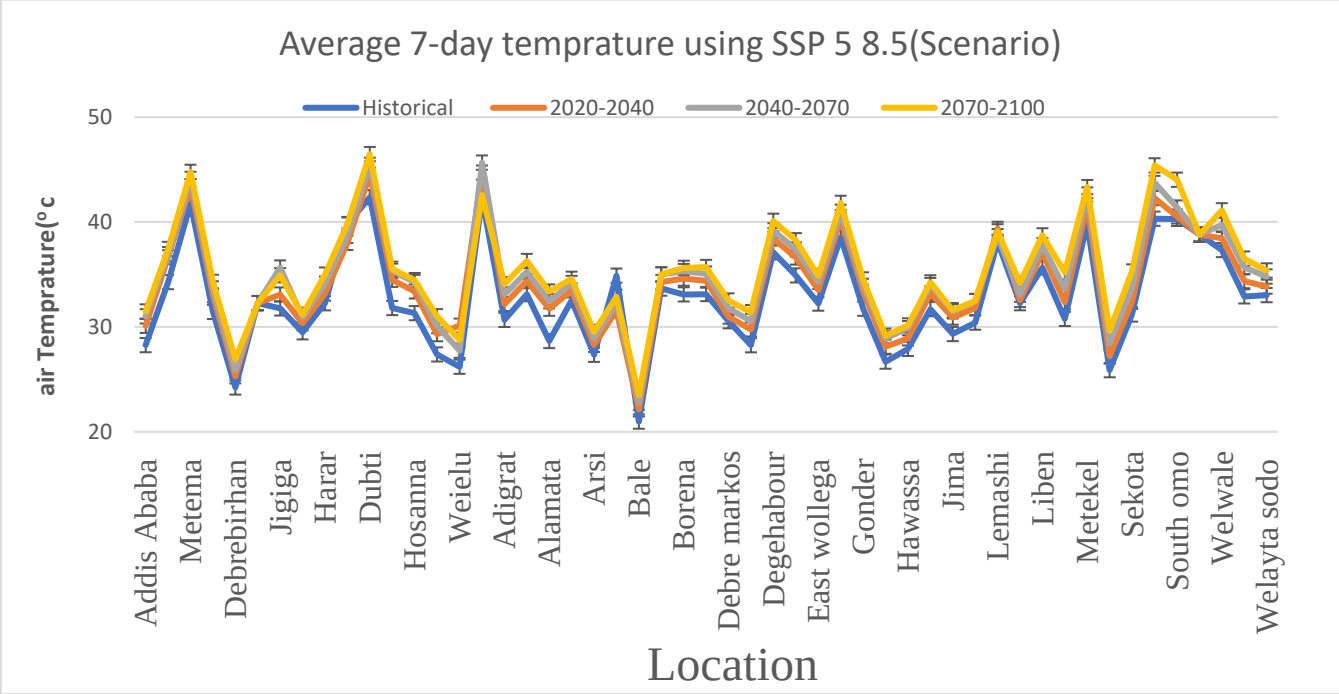

Figure 4-3. Air temperature Historical and Bias corrected future projection data for SSP5(8.5)

According to the analysis based on the Shared Socio-economic Pathways (SSP5) scenario with a radiative forcing pathway of 8.5, the hottest region in the country is Afar (Dubti, Elidar) with maximum temperatures of 42.37°C and 42.27°C, and Metema station with a temperature of 41.76°C. These temperatures are compared to the historical period (1990-2020). For the future projection from 2020 to 2100, the maximum seven daily maximum temperatures in Afar region and Metema station are expected to increase by 2.0°C to 4.0°C.

On the other hand, the coldest region in the country, Bale Robe station, has observed temperatures ranging from 19.16°C to 20.97°C during the historical period (1990-2020). Looking at the future projection from 2020 to 2100, the temperature in Bale Robe is expected to increase by 2.0°C to 3. 0°C.Overall, the analysis indicates a temperature increment ranging from 2.0°C to 6.0°C from

2020 to 2100 for Ethiopia under the SSP5 (8.5) scenario. These projections illustrate the potential changes in temperature relative to the historical period based on the chosen socio-economic pathway.

4.2 Determination of super pave Performance Grade (PG)

To developed a Superpave bitumen specification that considers the unique temperature characteristics of each location. The models were used to create a comprehensive and accurate specification that will ensure optimal performance of the pavement in each location. The results of this analysis are significant because they provide a roadmap for improving the durability and longevity of pavements in different locations. By considering the unique temperature characteristics of each location, we can create more effective and efficient pavement designs that will withstand extreme temperature fluctuations and last longer to do the future PG grade using Global climate model data by correct its systematic error (bias).

The bias correction method used in this study was Delta method, which is commonly used to adjust global climate model temperature data for local conditions. By applying this method to the temperature data for the 51 places in Ethiopia, we were able to calculate the future pavement temperature grade for each location. However, it is important to note that the accuracy of the bias correction method is dependent on several factors, such as the quality and availability of local climate data and on the forecasting of GCM, the choice of reference period, and the assumptions made during the correction process. Therefore, it is possible that our results may have some degree of uncertainty, and also climate change models are developed based on interaction between the atmosphere, the oceans, the land surface and the biosphere Depending on the methodology of interaction, different climate change models predict the climate change in different pattern. Considering one climate change model in a study may lead to high degree of uncertainty therefore, the average of two different climate model are use as to reduce this uncertainty.

The SHRP model is based on the Superpave system, which uses the high-temperature grade and the low-temperature grade to determine the performance grade. The LTPP model is based on the Long-Term Pavement Performance (LTPP) program, which uses the high-temperature grade and the low-temperature grade to determine the performance grade. The future PG in the table refers to the future scenario projection of the asphalt's performance grade using the Shared

Socioeconomic Pathways (SSP2) 4.5 and (SSP5) 8.5. SSP2 4.5 is a scenario that assumes a **moderate level** of mitigation and adaptation to climate change and (SSP5) 8.5**high challenge for mitigation (Resource /fossil fuel intensive)** and low for adaptation.

For the computed average cumulative seven-day high and low pavement temperatures, the asphalt binder grades are assigned following the Asphalt Institute Superpave Performance Graded Asphalt Binder Specifications. PG binders that differ in the high and low temperature specification by 90°C or more generally require some sort of modification.

High Temperature, °C

Low Temprature, °C	46	52	58	64	70	76
-10	46-10	52-10	58-10	64-10	70-10	76-10
-16	46-16	52-16	58-16	64-16	70-16	76-16
-22	46-22	52-22	58-22	64-22	70-22	76-22
-28	46-28	52-28	58-28	64-28	70-28	76-28
-34	46-34	52-34	58-34	64-34	70-34	76-34
-40	46-40	52-40	58-40	64-40	70-40	76-40

= Crude Oil
= High Quality Crude Oil
= Modifier Required

Figure 4-4 : Prediction of Super Pave PG grades for different crude oil blends.

Source: (Mahlet Gashaw, 2018)

From table (4-1and 4-2) the asphalt grade in Ethiopia not need of modification consider for only climate factor, maximum performance grade is PG 76-10 in afar region (Dubti, and Elidar station) and Metema with minimum asphalt grade occur in Mountainous area of Ethiopia in bale robe

PG 46-10 from analysis result of this study in historical and future performance grade. other factor includes like traffic, speed of vehicle this analysis result is changed.

Historical						Future Data SSP 2(4.5)											
S/N	Location	SHRP-Model		LTPP-Model		SHRP-Model		LTPP-Model		SHRP-Model		LTPP-Model		SHRP-Model		LTPP-Model	
		HISTORICAL (1990-2020)				2020-2040				2040-2070				2070-2100			
		50%	98%	50%	98%	50%	98%	50%	98%	50%	98%	50%	98%	50%	98%	50%	98%
1	Addis Ababa	PG-58-10	PG-58-10	PG-58-10	PG-58-10	PG-58-10	PG-58-10	PG-58-10	PG-64-10	PG-58-10	PG-58-10	PG-58-10	PG-64-10	PG-58-10	PG-58-10	PG-58-10	PG-64-10
2	Assosa	PG-64-10	PG-64-10	PG-64-10	PG-64-10	PG-64-10	PG-64-10	PG-58-10	PG-70-10	PG-64-10	PG-64-10	PG-58-10	PG-70-10	PG-64-10	PG-64-10	PG-58-10	PG-70-10
3	Metema	PG-70-10	PG-70-10	PG-64-10	PG-70-10	PG-70-10	PG-70-10	PG-64-10	PG-70-10	PG-70-10	PG-76-10	PG-70-10	PG-76-10	PG-70-10	PG-76-10	PG-70-10	PG-76-10
4	Bahr Dar	PG-58-10	PG-58-10	PG-58-10	PG-64-10	PG-58-10	PG-64-10	PG-58-10	PG-64-10	PG-58-10	PG-64-10	PG-58-10	PG-64-10	PG-58-10	PG-64-10	PG-58-10	PG-64-10
5	Debre Birhan	PG-52-10	PG-52-10	PG-52-10	PG-58-10	PG-52-10	PG-52-10	PG-52-10	PG-58-10	PG-52-10	PG-52-10	PG-52-10	PG-58-10	PG-52-10	PG-52-10	PG-52-10	PG-58-10
6	Dire Dawa	PG-58-10	PG-58-10	PG-58-10	PG-64-10	PG-58-10	PG-58-10	PG-58-10	PG-64-10	PG-58-10	PG-58-10	PG-58-10	PG-64-10	PG-58-10	PG-58-10	PG-58-10	PG-64-10
7	Jigiga	PG-58-10	PG-58-10	PG-58-10	PG-64-10	PG-58-10	PG-64-10	PG-58-10	PG-64-10	PG-58-10	PG-64-10	PG-58-10	PG-64-10	PG-58-10	PG-64-10	PG-58-10	PG-64-10
8	Tipi	PG-58-10	PG-58-10	PG-58-10	PG-64-10	PG-58-10	PG-58-10	PG-58-10	PG-64-10	PG-58-10	PG-58-10	PG-58-10	PG-64-10	PG-58-10	PG-58-10	PG-58-10	PG-64-10
9	Harar	PG-58-10	PG-64-10	PG-58-10	PG-64-10	PG-58-10	PG-64-10	PG-58-10	PG-64-10	PG-58-10	PG-64-10	PG-58-10	PG-64-10	PG-58-10	PG-64-10	PG-58-10	PG-64-10
10	Gewane	PG-64-10	PG-70-10	PG-64-10	PG-70-10	PG-64-10	PG-70-10	PG-64-10	PG-70-10	PG-64-10	PG-70-10	PG-64-10	PG-70-10	PG-70-10	PG-70-10	PG-64-10	PG-70-10
11	Dubti	PG-70-10	PG-70-10	PG-64-10	PG-70-10	PG-70-10	PG-76-10	PG-64-10	PG-76-10	PG-70-10	PG-76-10	PG-70-10	PG-76-10	PG-70-10	PG-76-10	PG-70-10	PG-76-10
12	Zeway	PG-58-10	PG-58-10	PG-58-10	PG-64-10	PG-58-10	PG-64-10	PG-58-10	PG-64-10	PG-58-10	PG-64-10	PG-58-10	PG-64-10	PG-58-10	PG-64-10	PG-58-10	PG-64-10
13	Hosanna	PG-58-10	PG-58-10	PG-58-10	PG-64-10	PG-58-10	PG-64-10	PG-58-10	PG-64-10	PG-58-10	PG-64-10	PG-58-10	PG-64-10	PG-58-10	PG-64-10	PG-58-10	PG-64-10
14	Lalibela	PG-52-10	PG-58-10	PG-52-10	PG-58-10	PG-52-10	PG-58-10	PG-52-10	PG-64-10	PG-58-10	PG-58-10	PG-58-10	PG-64-10	PG-58-10	PG-58-10	PG-58-10	PG-64-10
15	Weielu	PG-52-10	PG-58-10	PG-58-10	PG-58-10	PG-52-10	PG-58-10	PG-52-10	PG-58-10	PG-52-10	PG-58-10	PG-52-10	PG-58-10	PG-58-10	PG-58-10	PG-52-10	PG-58-10
16	Elidar	PG-70-10	PG-70-10	PG-64-10	PG-70-10	PG-70-10	PG-76-10	PG-64-10	PG-76-10	PG-70-10	PG-76-10	PG-70-10	PG-76-10	PG-70-10	PG-76-10	PG-70-10	PG-76-10
17	Adigrat	PG-58-10	PG-58-10	PG-58-10	PG-64-10	PG-58-10	PG-58-10	PG-58-10	PG-64-10	PG-58-10	PG-64-10	PG-58-10	PG-64-10	PG-58-10	PG-64-10	PG-58-10	PG-64-10
18	Adawa	PG-58-10	PG-64-10	PG-58-10	PG-64-10	PG-58-10	PG-64-10	PG-58-10	PG-64-10	PG-58-10	PG-64-10	PG-58-10	PG-64-10	PG-64-10	PG-64-10	PG-58-10	PG-64-10
19	Alamata	PG-58-10	PG-64-10	PG-58-10	PG-64-10	PG-58-10	PG-64-10	PG-58-10	PG-64-10	PG-58-10	PG-58-10	PG-58-10	PG-64-10	PG-58-10	PG-64-10	PG-58-10	PG-64-10
20	Arbaminch	PG-58-10	PG-58-10	PG-58-10	PG-70-10	PG-58-10	PG-64-10	PG-58-10	PG-64-10	PG-58-10	PG-64-10	PG-58-10	PG-64-10	PG-58-10	PG-64-10	PG-58-10	PG-64-10
21	Arsi (Asela)	PG-52-10	PG-58-10	PG-52-10	PG-58-10	PG-52-10	PG-58-10	PG-52-10	PG-58-10	PG-52-10	PG-58-10	PG-52-10	PG-58-10	PG-52-10	PG-58-10	PG-52-10	PG-58-10
22	Enjibara (Awi)	PG-58-10	PG-58-10	PG-58-10	PG-64-10	PG-58-10	PG-58-10	PG-58-10	PG-64-10	PG-58-10	PG-58-10	PG-58-10	PG-64-10	PG-58-10	PG-64-10	PG-58-10	PG-64-10
23	Bale Robe	PG-46-10	PG-52-10	PG-52-10	PG-58-10	PG-46-10	PG-52-10	PG-46-10	PG-58-10	PG-46-10	PG-52-10	PG-52-10	PG-58-10	PG-46-10	PG-52-10	PG-52-10	PG-58-10
24	Bench Maji	PG-58-10	PG-64-10	PG-58-10	PG-64-10	PG-58-10	PG-64-10	PG-58-10	PG-64-10	PG-58-10	PG-64-10	PG-58-10	PG-64-10	PG-58-10	PG-64-10	PG-58-10	PG-64-10
25	Borena	PG-58-10	PG-58-10	PG-58-10	PG-64-10	PG-58-10	PG-64-10	PG-58-10	PG-64-10	PG-58-10	PG-64-10	PG-58-10	PG-64-10	PG-58-10	PG-64-10	PG-58-10	PG-64-10
26	Dangila	PG-58-10	PG-64-10	PG-58-10	PG-64-10	PG-58-10	PG-64-10	PG-58-10	PG-64-10	PG-58-10	PG-64-10	PG-58-10	PG-64-10	PG-64-10	PG-64-10	PG-58-10	PG-64-10

27	Debre Markos	PG-58-10	PG-58-10	PG-58-10	PG-64-10	PG-58-10	PG-58-10	PG-58-10	PG-64-10	PG-58-10	PG-58-10	PG-58-10	PG-64-10	PG-58-10	PG-64-10	PG-58-10	PG-64-10
28	Debre tabor	PG-52-10	PG-58-10	PG-64-10	PG-70-10	PG-58-10	PG-58-10	PG-52-10	PG-64-10	PG-58-10	PG-58-10	PG-58-10	PG-64-10	PG-58-10	PG-58-10	PG-52-10	PG-64-10
29	Degehabour	PG-64-10	PG-64-10	PG-64-10	PG-70-10	PG-64-10	PG-64-10	PG-64-10	PG-70-10	PG-64-10	PG-64-10	PG-64-10	PG-70-10	PG-64-10	PG-64-10	PG-64-10	PG-70-10
30	harerge	PG-58-10	PG-64-10	PG-58-10	PG-64-10	PG-64-10	PG-64-10	PG-58-10	PG-64-10	PG-64-10	PG-64-10	PG-58-10	PG-64-10	PG-64-10	PG-64-10	PG-64-10	PG-70-10
31	Nekemte	PG-58-10	PG-64-10	PG-64-10	PG-70-10	PG-58-10	PG-64-10	PG-58-10	PG-64-10	PG-58-10	PG-64-10	PG-58-10	PG-64-10	PG-58-10	PG-64-10	PG-58-10	PG-64-10
32	Gode	PG-64-10	PG-64-10	PG-64-10	PG-70-10	PG-64-10	PG-70-10	PG-64-10	PG-70-10	PG-64-10	PG-70-10	PG-64-10	PG-70-10	PG-64-10	PG-70-10	PG-64-10	PG-70-10
33	Gonder	PG-64-10	PG-64-10	PG-58-10	PG-64-10	PG-58-10	PG-64-10	PG-58-10	PG-64-10	PG-58-10	PG-64-10	PG-58-10	PG-64-10	PG-58-10	PG-64-10	PG-58-10	PG-64-10
34	Gurage	PG-52-10	PG-58-10	PG-52-10	PG-58-10	PG-52-10	PG-58-10	PG-52-10	PG-58-10	PG-52-10	PG-58-10	PG-52-10	PG-58-10	PG-52-10	PG-58-10	PG-52-10	PG-58-10
35	Hawassa	PG-52-10	PG-58-10	PG-58-10	PG-64-10	PG-52-10	PG-58-10	PG-52-10	PG-58-10	PG-52-10	PG-58-10	PG-52-10	PG-58-10	PG-52-10	PG-58-10	PG-52-10	PG-64-10
36	Illubabor	PG-58-10	PG-64-10	PG-58-10	PG-64-10	PG-58-10	PG-64-10	PG-58-10	PG-64-10	PG-58-10	PG-64-10	PG-58-10	PG-64-10	PG-58-10	PG-64-10	PG-58-10	PG-64-10
37	Jima	PG-58-10	PG-58-10	PG-58-10	PG-64-10	PG-58-10	PG-58-10	PG-58-10	PG-64-10	PG-58-10	PG-58-10	PG-58-10	PG-64-10	PG-58-10	PG-58-10	PG-58-10	PG-64-10
38	Kefa	PG-58-10	PG-64-10	PG-58-10	PG-64-10	PG-58-10	PG-58-10	PG-58-10	PG-64-10	PG-58-10	PG-64-10	PG-58-10	PG-64-10	PG-58-10	PG-64-10	PG-58-10	PG-64-10
39	Kemashi	PG-64-10	PG-70-10	PG-64-10	PG-70-10	PG-64-10	PG-70-10	PG-64-10	PG-70-10	PG-64-10	PG-70-10	PG-64-10	PG-70-10	PG-64-10	PG-70-10	PG-64-10	PG-70-10
40	Kemisie	PG-58-10	PG-64-10	PG-58-10	PG-64-10	PG-58-10	PG-64-10	PG-58-10	PG-64-10	PG-58-10	PG-64-10	PG-58-10	PG-64-10	PG-58-10	PG-64-10	PG-58-10	PG-64-10
41	Liben	PG-58-10	PG-64-10	PG-64-10	PG-64-10	PG-64-10	PG-64-10	PG-58-10	PG-70-10	PG-64-10	PG-64-10	PG-64-10	PG-70-10	PG-64-10	PG-64-10	PG-64-10	PG-70-10
42	Mekele	PG-58-10	PG-58-10	PG-58-10	PG-64-10	PG-58-10	PG-64-10	PG-58-10	PG-64-10	PG-58-10	PG-64-10	PG-58-10	PG-64-10	PG-58-10	PG-64-10	PG-58-10	PG-64-10
43	Metekel	PG-64-10	PG-70-10	PG-64-10	PG-70-10	PG-64-10	PG-70-10	PG-64-10	PG-70-10	PG-70-10	PG-70-10	PG-64-10	PG-70-10	PG-70-10	PG-70-10	PG-64-10	PG-70-10
44	Fitch	PG-52-10	PG-58-10	PG-52-10	PG-58-10	PG-52-10	PG-58-10	PG-52-10	PG-58-10	PG-52-10	PG-58-10	PG-52-10	PG-58-10	PG-52-10	PG-58-10	PG-52-10	PG-58-10
45	Sekota	PG-58-10	PG-58-10	PG-58-10	PG-64-10	PG-58-10	PG-64-10	PG-58-10	PG-64-10	PG-58-10	PG-64-10	PG-58-10	PG-64-10	PG-58-10	PG-64-10	PG-58-10	PG-64-10
46	Shinle	PG-64-10	PG-70-10	PG-64-10	PG-70-10	PG-70-10	PG-70-10	PG-64-10	PG-70-10	PG-70-10	PG-70-10	PG-64-10	PG-70-10	PG-70-10	PG-76-10	PG-64-10	PG-76-10
47	South omo	PG-64-10	PG-70-10	PG-64-10	PG-70-10	PG-64-10	PG-70-10	PG-64-10	PG-70-10	PG-64-10	PG-70-10	PG-64-10	PG-70-10	PG-64-10	PG-70-10	PG-64-10	PG-70-10
48	Humera	PG-64-10	PG-70-10	PG-64-10	PG-70-10	PG-64-10	PG-64-10	PG-64-10	PG-70-10	PG-64-10	PG-70-10	PG-64-10	PG-70-10	PG-64-10	PG-70-10	PG-64-10	PG-70-10
49	Welwale	PG-64-10	PG-64-10	PG-64-10	PG-70-10	PG-64-10	PG-64-10	PG-64-10	PG-70-10	PG-64-10	PG-64-10	PG-64-10	PG-70-10	PG-64-10	PG-70-10	PG-64-10	PG-70-10
50	Dembidolo	PG-58-10	PG-64-10	PG-58-10	PG-70-10	PG-58-10	PG-64-10	PG-58-10	PG-64-10	PG-58-10	PG-64-10	PG-58-10	PG-64-10	PG-58-10	PG-64-10	PG-58-10	PG-64-10
51	Welayta sodo	PG-58-10	PG-64-10	PG-58-10	PG-64-10	PG-58-10	PG-64-10	PG-58-10	PG-64-10	PG-58-10	PG-64-10	PG-58-10	PG-64-10	PG-58-10	PG-64-10	PG-58-10	PG-64-10

Table 4-1 PG of asphalt Binder of Two Model Result. SSP2(4.5) Scenario

- yellow-**Higher Grade**
- Green -**Lower Grade**

Historical						Future Data SSP 5(8.5)											
S/N	Location	SHRP-Model		LTPP-Model		SHRP-Model		LTPP-Model		SHRP-Model		LTPP-Model		SHRP-Model		LTPP-Model	
		HISTORICAL (1990-2020)				2020-2040				2040-2070				2070-2100			
		50%	98%	50%	98%	50%	98%	50%	98%	50%	98%	50%	98%	50%	98%	50%	98%
1	Addis Ababa	PG-58-10	PG-58-10	PG-58-10	PG-58-10	PG-58-10	PG-58-10	PG-58-10	PG-64-10	PG-58-10	PG-58-10	PG-58-10	PG-64-10	PG-58-10	PG-64-10	PG-58-10	PG-64-10
2	Assosa	PG-64-10	PG-64-10	PG-64-10	PG-64-10	PG-64-10	PG-70-10	PG-58-10	PG-70-10	PG-64-10	PG-70-10	PG-58-10	PG-70-10	PG-64-10	PG-70-10	PG-64-10	PG-70-10
3	Metema	PG-70-10	PG-70-10	PG-64-10	PG-70-10	PG-70-10	PG-76-10	PG-64-10	PG-76-10	PG-70-10	PG-76-10	PG-64-10	PG-76-10	PG-70-10	PG-76-10	PG-64-10	PG-76-10
4	Bahr Dar	PG-58-10	PG-58-10	PG-58-10	PG-64-10	PG-58-10	PG-64-10	PG-58-10	PG-64-10	PG-58-10	PG-64-10	PG-58-10	PG-64-10	PG-58-10	PG-64-10	PG-58-10	PG-64-10
5	Debre Birhan	PG-52-10	PG-52-10	PG-52-10	PG-58-10	PG-52-10	PG-52-10	PG-52-10	PG-58-10	PG-52-10	PG-52-10	PG-52-10	PG-58-10	PG-52-10	PG-58-10	PG-52-10	PG-58-10
6	Dire Dawa	PG-58-10	PG-58-10	PG-58-10	PG-64-10	PG-58-10	PG-58-10	PG-58-10	PG-64-10	PG-58-10	PG-58-10	PG-58-10	PG-64-10	PG-58-10	PG-58-10	PG-58-10	PG-64-10
7	Jigiga	PG-58-10	PG-58-10	PG-58-10	PG-64-10	PG-58-10	PG-64-10	PG-58-10	PG-64-10	PG-64-10	PG-64-10	PG-58-10	PG-64-10	PG-58-10	PG-64-10	PG-58-10	PG-64-10
8	Tipi	PG-58-10	PG-58-10	PG-58-10	PG-64-10	PG-58-10	PG-58-10	PG-58-10	PG-64-10	PG-58-10	PG-58-10	PG-58-10	PG-64-10	PG-58-10	PG-58-10	PG-58-10	PG-64-10
9	Harar	PG-58-10	PG-64-10	PG-58-10	PG-64-10	PG-58-10	PG-64-10	PG-58-10	PG-64-10	PG-58-10	PG-64-10	PG-58-10	PG-64-10	PG-58-10	PG-64-10	PG-58-10	PG-64-10
10	Gewane	PG-64-10	PG-70-10	PG-64-10	PG-70-10	PG-64-10	PG-70-10	PG-64-10	PG-70-10	PG-64-10	PG-70-10	PG-64-10	PG-70-10	PG-64-10	PG-70-10	PG-64-10	PG-70-10
11	Dubti	PG-70-10	PG-70-10	PG-64-10	PG-70-10	PG-70-10	PG-76-10	PG-64-10	PG-76-10	PG-70-10	PG-76-10	PG-70-10	PG-76-10	PG-70-10	PG-76-10	PG-70-10	PG-76-10
12	Zeway	PG-58-10	PG-58-10	PG-58-10	PG-64-10	PG-58-10	PG-64-10	PG-58-10	PG-64-10	PG-58-10	PG-64-10	PG-58-10	PG-64-10	PG-58-10	PG-64-10	PG-58-10	PG-64-10
13	Hosanna	PG-58-10	PG-58-10	PG-58-10	PG-64-10	PG-58-10	PG-64-10	PG-58-10	PG-64-10	PG-58-10	PG-64-10	PG-58-10	PG-64-10	PG-58-10	PG-64-10	PG-58-10	PG-64-10
14	Lalibela	PG-52-10	PG-58-10	PG-52-10	PG-58-10	PG-58-10	PG-64-10	PG-58-10	PG-64-10	PG-58-10	PG-58-10	PG-58-10	PG-64-10	PG-58-10	PG-58-10	PG-58-10	PG-64-10
15	Weielu	PG-52-10	PG-58-10	PG-58-10	PG-58-10	PG-58-10	PG-58-10	PG-58-10	PG-64-10	PG-52-10	PG-58-10	PG-52-10	PG-58-10	PG-58-10	PG-58-10	PG-52-10	PG-58-10
16	Elidar	PG-70-10	PG-70-10	PG-64-10	PG-70-10	PG-64-10	PG-70-10	PG-58-10	PG-70-10	PG-70-10	PG-76-10	PG-70-10	PG-76-10	PG-70-10	PG-70-10	PG-64-10	PG-70-10
17	Adigrat	PG-58-10	PG-58-10	PG-58-10	PG-64-10	PG-64-10	PG-70-10	PG-64-10	PG-70-10	PG-58-10	PG-64-10	PG-58-10	PG-64-10	PG-58-10	PG-64-10	PG-58-10	PG-64-10
18	Adawa	PG-58-10	PG-64-10	PG-58-10	PG-64-10	PG-58-10	PG-64-10	PG-58-10	PG-64-10	PG-58-10	PG-64-10	PG-58-10	PG-64-10	PG-64-10	PG-64-10	PG-58-10	PG-64-10
19	Alamata	PG-58-10	PG-64-10	PG-58-10	PG-64-10	PG-58-10	PG-64-10	PG-58-10	PG-64-10	PG-58-10	PG-64-10	PG-58-10	PG-64-10	PG-58-10	PG-64-10	PG-58-10	PG-64-10
20	Arbaminch	PG-58-10	PG-58-10	PG-58-10	PG-70-10	PG-58-10	PG-64-10	PG-58-10	PG-64-10	PG-58-10	PG-64-10	PG-58-10	PG-64-10	PG-58-10	PG-64-10	PG-58-10	PG-64-10
21	Arsi(Asela)	PG-52-10	PG-58-10	PG-52-10	PG-58-10	PG-58-10	PG-58-10	PG-58-10	PG-64-10	PG-52-10	PG-58-10	PG-52-10	PG-64-10	PG-58-10	PG-58-10	PG-52-10	PG-64-10
22	Enjibara(Awi)	PG-58-10	PG-58-10	PG-58-10	PG-64-10	PG-58-10	PG-58-10	PG-58-10	PG-64-10	PG-58-10	PG-64-10	PG-58-10	PG-64-10	PG-58-10	PG-64-10	PG-58-10	PG-64-10
23	Bale	PG-46-10	PG-52-10	PG-52-10	PG-58-10	PG-52-10	PG-58-10	PG-52-10	PG-58-10	PG-46-10	PG-52-10	PG-52-10	PG-58-10	PG-52-10	PG-52-10	PG-52-10	PG-58-10
24	Bench Maji	PG-58-10	PG-64-10	PG-58-10	PG-64-10	PG-52-10	PG-58-10	PG-52-10	PG-58-10	PG-58-10	PG-64-10	PG-58-10	PG-64-10	PG-58-10	PG-64-10	PG-58-10	PG-64-10
25	Borena	PG-58-10	PG-58-10	PG-58-10	PG-64-10	PG-58-10	PG-64-10	PG-58-10	PG-64-10	PG-58-10	PG-64-10	PG-58-10	PG-64-10	PG-58-10	PG-64-10	PG-58-10	PG-64-10

26	Dangila	PG-58-10	PG-64-10	PG-58-10	PG-64-10	PG-58-10	PG-64-10	PG-58-10	PG-64-10	PG-58-10	PG-64-10	PG-58-10	PG-64-10	PG-64-10	PG-64-10	PG-58-10	PG-64-10
27	Debre markos	PG-58-10	PG-58-10	PG-58-10	PG-64-10	PG-58-10	PG-64-10	PG-58-10	PG-64-10	PG-58-10	PG-58-10	PG-58-10	PG-64-10	PG-58-10	PG-64-10	PG-58-10	PG-64-10
28	Debre tabor	PG-52-10	PG-58-10	PG-58-10	PG-58-10	PG-58-10	PG-64-10	PG-58-10	PG-64-10	PG-58-10	PG-58-10	PG-58-10	PG-64-10	PG-58-10	PG-58-10	PG-58-10	PG-64-10
29	Degehabour	PG-64-10	PG-64-10	PG-64-10	PG-70-10	PG-58-10	PG-64-10	PG-58-10	PG-64-10	PG-64-10	PG-64-10	PG-64-10	PG-70-10	PG-64-10	PG-70-10	PG-64-10	PG-70-10
30	harerge	PG-58-10	PG-64-10	PG-58-10	PG-64-10	PG-58-10	PG-64-10	PG-58-10	PG-64-10	PG-64-10	PG-64-10	PG-64-10	PG-70-10	PG-64-10	PG-64-10	PG-64-10	PG-70-10
31	Nekemte	PG-58-10	PG-64-10	PG-64-10	PG-64-10	PG-64-10	PG-64-10	PG-58-10	PG-70-10	PG-58-10	PG-64-10	PG-58-10	PG-64-10	PG-58-10	PG-64-10	PG-58-10	PG-64-10
32	Gode	PG-64-10	PG-64-10	PG-64-10	PG-70-10	PG-64-10	PG-64-10	PG-64-10	PG-70-10	PG-64-10	PG-70-10	PG-64-10	PG-70-10	PG-64-10	PG-70-10	PG-64-10	PG-70-10
33	Gonder	PG-64-10	PG-64-10	PG-58-10	PG-64-10	PG-58-10	PG-64-10	PG-58-10	PG-64-10	PG-58-10	PG-64-10	PG-58-10	PG-64-10	PG-58-10	PG-64-10	PG-58-10	PG-64-10
34	Gurage	PG-52-10	PG-58-10	PG-52-10	PG-58-10	PG-58-10	PG-64-10	PG-58-10	PG-64-10	PG-52-10	PG-58-10	PG-52-10	PG-64-10	PG-52-10	PG-58-10	PG-52-10	PG-64-10
35	Hawassa	PG-52-10	PG-58-10	PG-52-10	PG-58-10	PG-58-10	PG-58-10	PG-58-10	PG-64-10	PG-58-10	PG-58-10	PG-58-10	PG-64-10	PG-58-10	PG-58-10	PG-58-10	PG-64-10
36	Illubabor	PG-58-10	PG-64-10	PG-58-10	PG-64-10	PG-58-10	PG-58-10	PG-58-10	PG-64-10	PG-58-10	PG-64-10	PG-58-10	PG-64-10	PG-58-10	PG-64-10	PG-58-10	PG-64-10
37	Jima	PG-58-10	PG-58-10	PG-58-10	PG-64-10	PG-58-10	PG-64-10	PG-58-10	PG-64-10	PG-58-10	PG-64-10	PG-58-10	PG-64-10	PG-58-10	PG-64-10	PG-58-10	PG-64-10
38	Kefa	PG-58-10	PG-64-10	PG-58-10	PG-64-10	PG-58-10	PG-64-10	PG-58-10	PG-64-10	PG-58-10	PG-64-10	PG-58-10	PG-64-10	PG-58-10	PG-64-10	PG-58-10	PG-64-10
39	Kemashi	PG-64-10	PG-70-10	PG-64-10	PG-70-10	PG-58-10	PG-64-10	PG-58-10	PG-64-10	PG-64-10	PG-70-10	PG-64-10	PG-70-10	PG-64-10	PG-70-10	PG-64-10	PG-70-10
40	Kemisie	PG-58-10	PG-64-10	PG-58-10	PG-64-10	PG-58-10	PG-64-10	PG-58-10	PG-64-10	PG-58-10	PG-64-10	PG-58-10	PG-64-10	PG-58-10	PG-64-10	PG-58-10	PG-64-10
41	Liben	PG-58-10	PG-64-10	PG-64-10	PG-64-10	PG-64-10	PG-64-10	PG-64-10	PG-70-10	PG-64-10	PG-64-10	PG-64-10	PG-70-10	PG-64-10	PG-64-10	PG-64-10	PG-70-10
42	Mekele	PG-58-10	PG-58-10	PG-58-10	PG-64-10	PG-58-10	PG-64-10	PG-58-10	PG-64-10	PG-58-10	PG-64-10	PG-58-10	PG-64-10	PG-58-10	PG-64-10	PG-58-10	PG-64-10
43	Metekel	PG-64-10	PG-70-10	PG-64-10	PG-70-10	PG-64-10	PG-70-10	PG-64-10	PG-70-10	PG-70-10	PG-70-10	PG-64-10	PG-70-10	PG-70-10	PG-70-10	PG-64-10	PG-70-10
44	Fitche	PG-52-10	PG-58-10	PG-52-10	PG-58-10	PG-58-10	PG-64-10	PG-52-10	PG-64-10	PG-52-10	PG-58-10	PG-52-10	PG-58-10	PG-58-10	PG-58-10	PG-52-10	PG-64-10
45	Sekota	PG-58-10	PG-58-10	PG-58-10	PG-64-10	PG-64-10	PG-70-10	PG-58-10	PG-70-10	PG-58-10	PG-64-10	PG-58-10	PG-64-10	PG-58-10	PG-64-10	PG-58-10	PG-64-10
46	Shinle	PG-64-10	PG-70-10	PG-64-10	PG-70-10	PG-58-10	PG-64-10	PG-58-10	PG-64-10	PG-70-10	PG-70-10	PG-64-10	PG-70-10	PG-70-10	PG-76-10	PG-70-10	PG-76-10
47	South omo	PG-64-10	PG-70-10	PG-64-10	PG-70-10	PG-64-10	PG-64-10	PG-58-10	PG-64-10	PG-64-10	PG-70-10	PG-64-10	PG-70-10	PG-70-10	PG-70-10	PG-64-10	PG-76-10
48	Humera	PG-64-10	PG-70-10	PG-64-10	PG-70-10	PG-64-10	PG-70-10	PG-64-10	PG-70-10	PG-64-10	PG-70-10	PG-64-10	PG-70-10	PG-64-10	PG-70-10	PG-64-10	PG-70-10
49	Welwale	PG-64-10	PG-64-10	PG-64-10	PG-70-10	PG-64-10	PG-70-10	PG-64-10	PG-70-10	PG-64-10	PG-70-10	PG-64-10	PG-70-10	PG-64-10	PG-70-10	PG-64-10	PG-70-10
50	Dembidolo	PG-58-10	PG-64-10	PG-58-10	PG-70-10	PG-64-10	PG-70-10	PG-58-10	PG-70-10	PG-64-10	PG-64-10	PG-58-10	PG-64-10	PG-64-10	PG-64-10	PG-58-10	PG-70-10
51	Welayta Sodo	PG-58-10	PG-64-10	PG-58-10	PG-64-10	PG-64-10	PG-64-10	PG-58-10	PG-70-10	PG-58-10	PG-64-10	PG-58-10	PG-64-10	PG-58-10	PG-64-10	PG-58-10	PG-64-10

Table 4-2 PG of asphalt Binder of Two Model Result. SSP5(8.5) Scenario

4.3 Interpretation of Asphalt Grade change due to climate change

Table 4-3 increment of PG grade of Middle (SSP 2(4.5) and hottest (SSP5(8.5) model

No. of Grade Increment.	No. of study area Grade change (Location) in Ethiopia											
	2020-2040				2040-2070				2070-2100			
	SHRP		LTPP		SHRP		LTPP		SHRP		LTPP	
	50%	98%	50%	98%	50%	98%	50%	98%	50%	98%	50%	98%
Middle Model (SSP 2(4.5)												
1-Grade	6	13	9	12	8	15	10	13	12	18	11	14
More than 1-Grade	*	*	*	*	*	*	*	*	*	*	*	*
Total no. Location Change Grade	6	13	9	12	8	15	10	13	12	18	11	14
% of Change	**12%**	**25%**	**18%**	**24%**	**16%**	**29%**	**20%**	**25%**	**24%**	**35%**	**22%**	**27%**
Hottest Model (SSP 5(8.5)												
1-Grade	22	25	20	21	11	20	10	14	19	22	13	17
More than 1-grade		2										
Total no. Location Change Grade	22	27	20	21	11	20	10	14	19	22	13	17
% of Change	**43%**	**53%**	**39%**	**41%**	**22%**	**39%**	**20%**	**27%**	**37%**	**43%**	**25%**	**33%**

***=zero**

The table (4-3) shows the impact of climate change on road pavement performance grade different places in Ethiopia using two different models, SHRP and LTPP models. The Superpave system is a widely used method for specifying asphalt binders and mixtures used in road construction, which considers the effects of climate conditions on pavement performance. The results from the table (4-3) show that the performance of road pavements has been significantly affected by climate change in Ethiopia. The increment of one grade (1-Grade)

led to an average percentage of around 20% and 23% and 27 %, for Middle (moderate climate change scenario SSP2 (4.5) and 44%, 27% and 35% (For hottest climate change scenario) of the study area in 2020-2040,2040-2070 and 2070-2100 respectively. are changed in SHRP and LTPP models, from over all study location and Adigrat and Sekota location are increment with two Grade in 2020-2040 in SSP5(8.5) period from determine Performance Grade result.

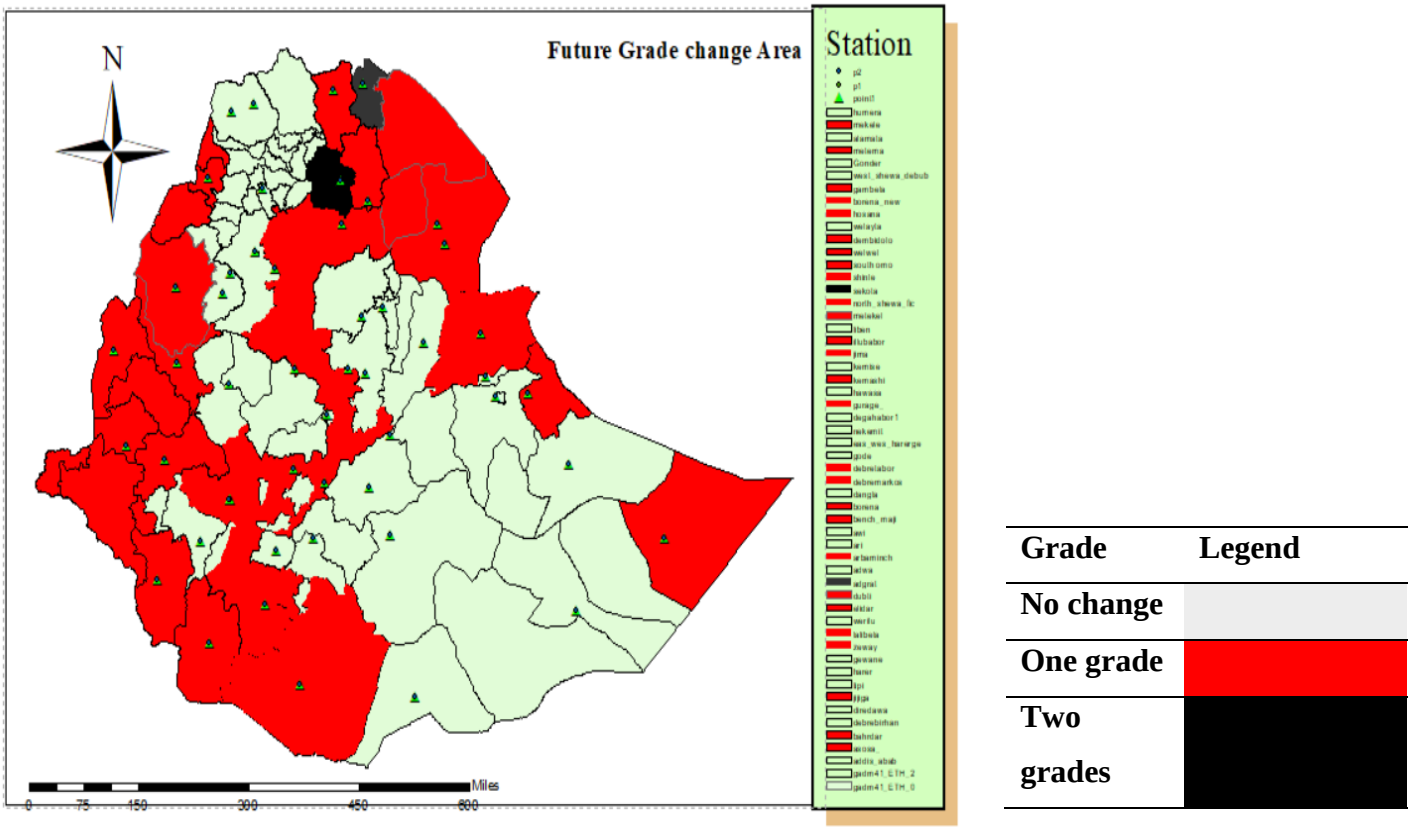

Grade	Legend
No change	
One grade	
Two grades	

Figure 4-5 : Map of Grade Change station SSP 5 (8.5)

These changes indicate need for action to mitigate the impact of climate change on road infrastructure in Ethiopia. The Superpave system can, therefore, be used to design pavements that are better suited to the local climate conditions and are more resilient to the effects of climate change. finally, the findings from the table reinforce the urgent need for policymakers and road infrastructure managers to take appropriate measures to address the impacts of climate change and ensure that road infrastructure remains functional and safe for all users. The Superpave system is a valuable tool for designing pavements that are better suited to the local climate conditions and can help improve pavement performance and reduce the need for frequent maintenance and repairs.

Air temperature increase has a direct impact on pavement temperature. As the air temperature rises, the pavement temperature follows a similar upward trend

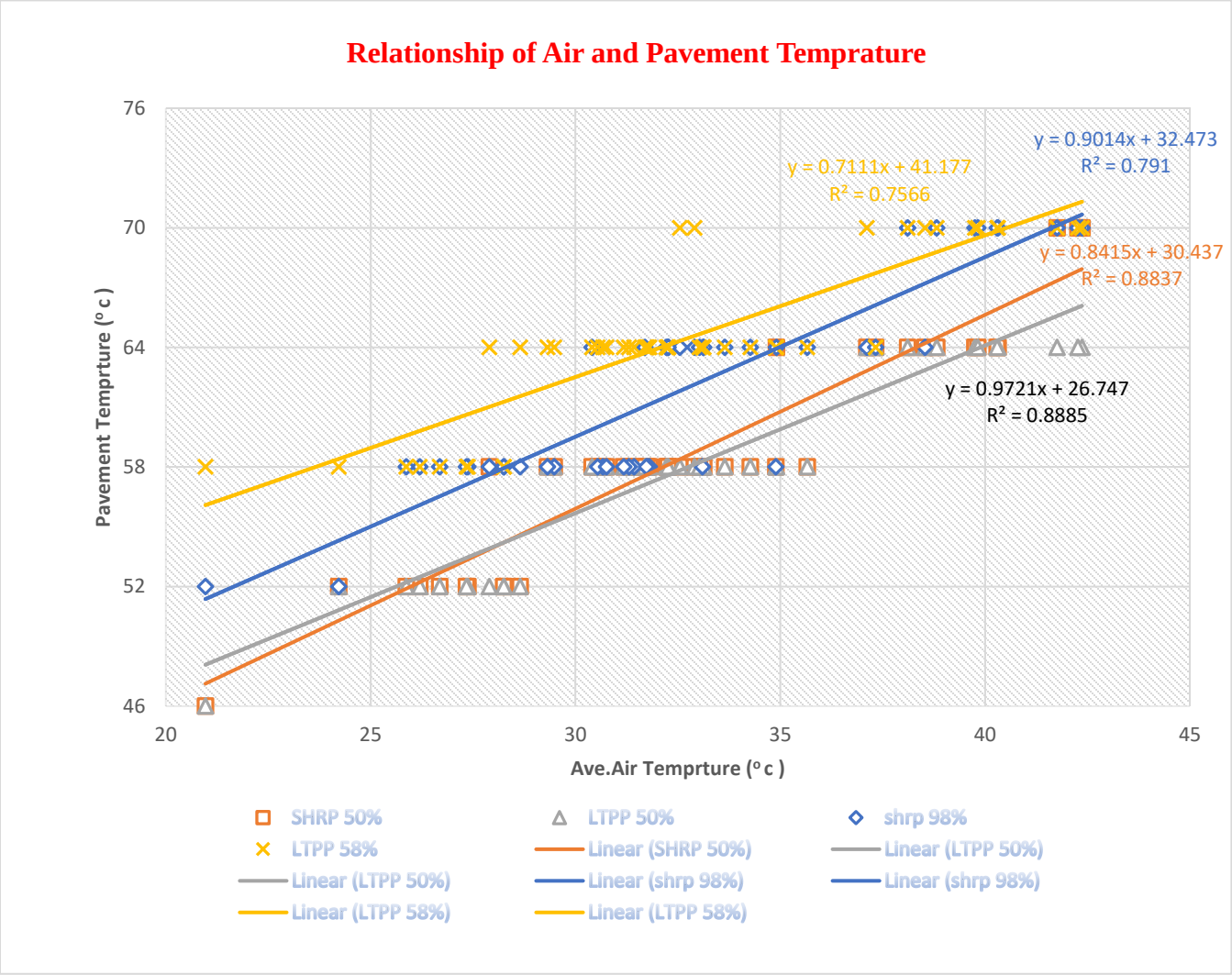

Figure 4-6: SHRP and LTPP Estimated High Pavement Temperatures vs. Air Temperature

. This relationship is depicted in the Graph R^2 =0.8837 R^2 =0.8885 Value shown for 50% reliability of SHRP and LTPP model respectively shown that air temperature more related with 50% reliability than 98 % reliability and for 98%. R^2 =0.791 R^2 =0.7566 but for both model and reliability, the air temperatures highly related.

4.4 Comparation of SHRP &LTPP-Model

Based on Baseline pavement Temperature prediction for both model the result is as shown on the chart for 51 location of Ethiopia

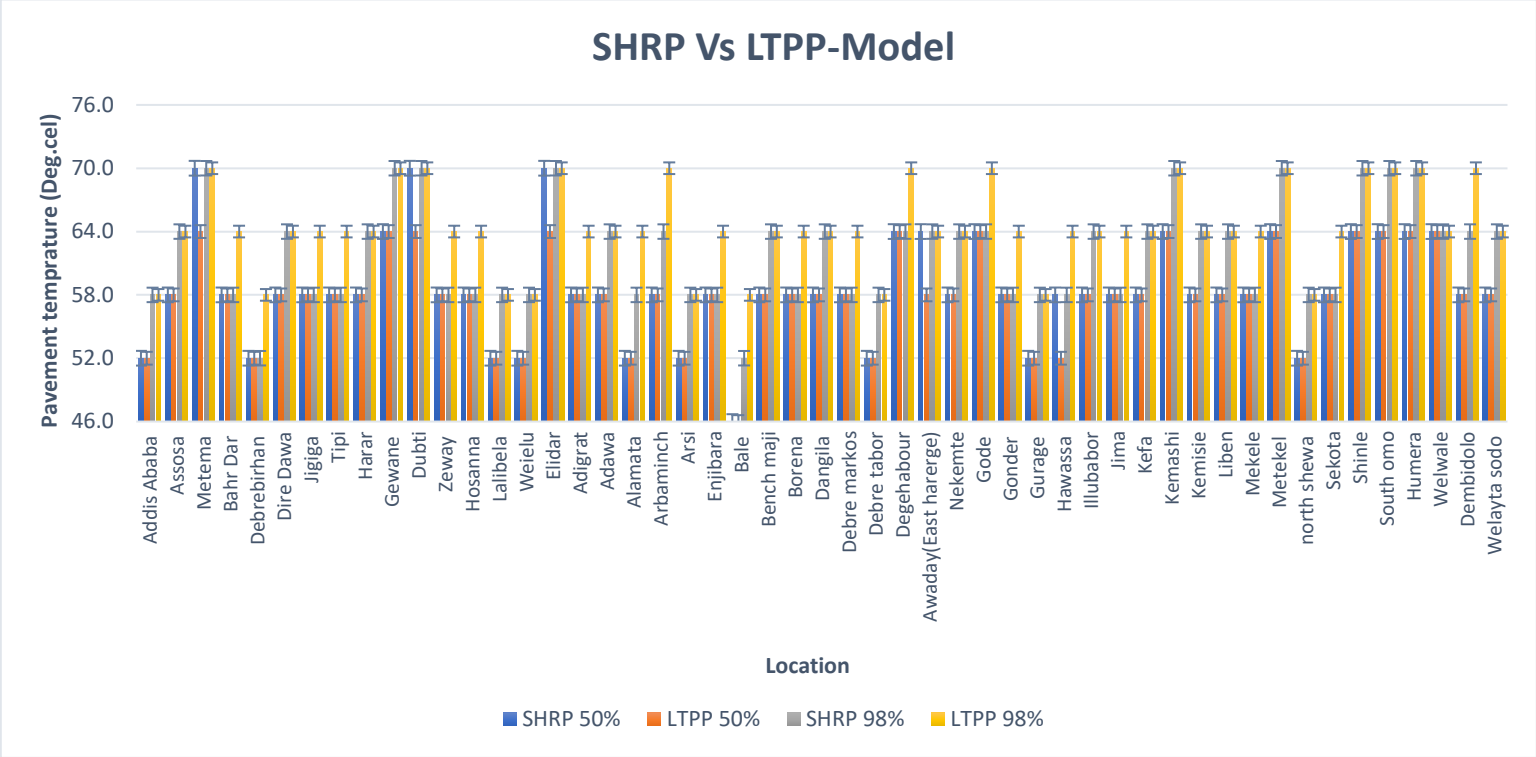

Figure 4-7: Graphical representation of Two model difference at baseline period

The value of the difference between the SHRP and LTPP pavement temperature results for the selected locations ranges one Grade. For instance, the differences are observed in Bahr Dar, Debrebirhan, Bale, and Gode, the SHRP temperature and LTPP results, shown the above LTPP Model are **overestimation** in some location. Therefore, it is important to understand the reasons for the differences in pavement temperature results between the SHRP and LTPP programs and to take these differences into account when designing and maintaining roadways.

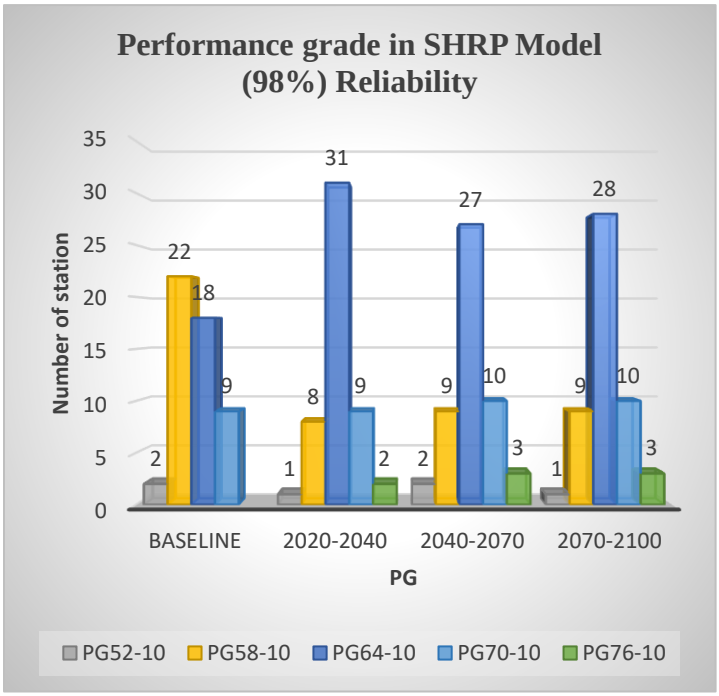

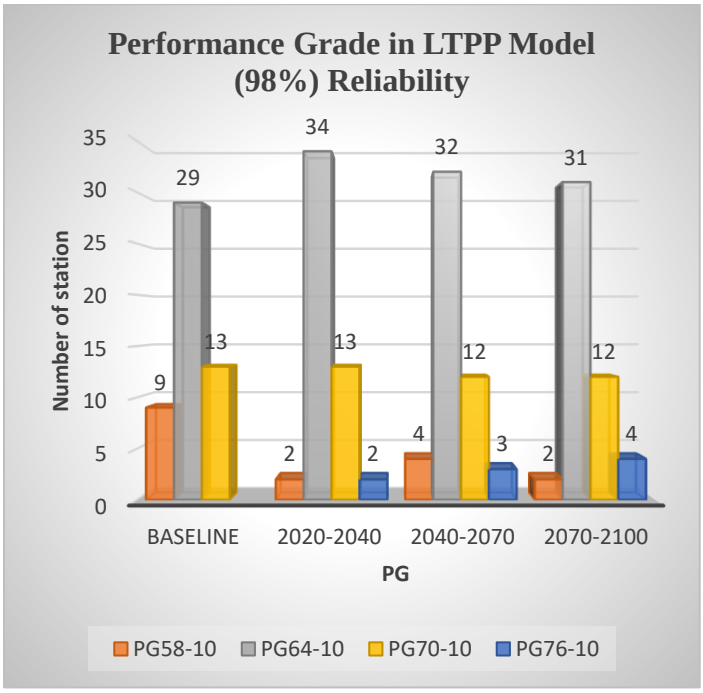

Figure 4-8: Number of station Performance Grade (PG) result Using SHRP and LTPP Model.

Looking at the graph, it appears that there is significant variability in the PG values across the different stations and time periods. For example, the station with PG52-10 has relatively low values in the baseline period, but then shows an increase in performance grade in the later time periods. In contrast, the station with PG64-10 has high in the baseline period.

For both of pavement temperature prediction Model of 98% reliability of performance grade determination result as express in graph in baseline year maximum number of station result are PG 58-10 in SHRP and for LTPP Model is PG 64-10. However, for future PG result Maximum Number of station result is PG64-10 for 2020-2040,2040-2070 and 2070-2100 Asphalt grade determination result.PG76-10 asphalt grade is not occurred in Baseline result, but for future in both scenarios more than 2 station.

4.4.1 Performance Grade (PG) Analysis Result of Area coverage

To interpret the results of my analysis, it is assumed that all selected meteorology stations cover an equal area for observing temperature data, and that the total area of Ethiopia is 1,132,863.44 square kilometers. This will enable the results to be presented for the specified location area.

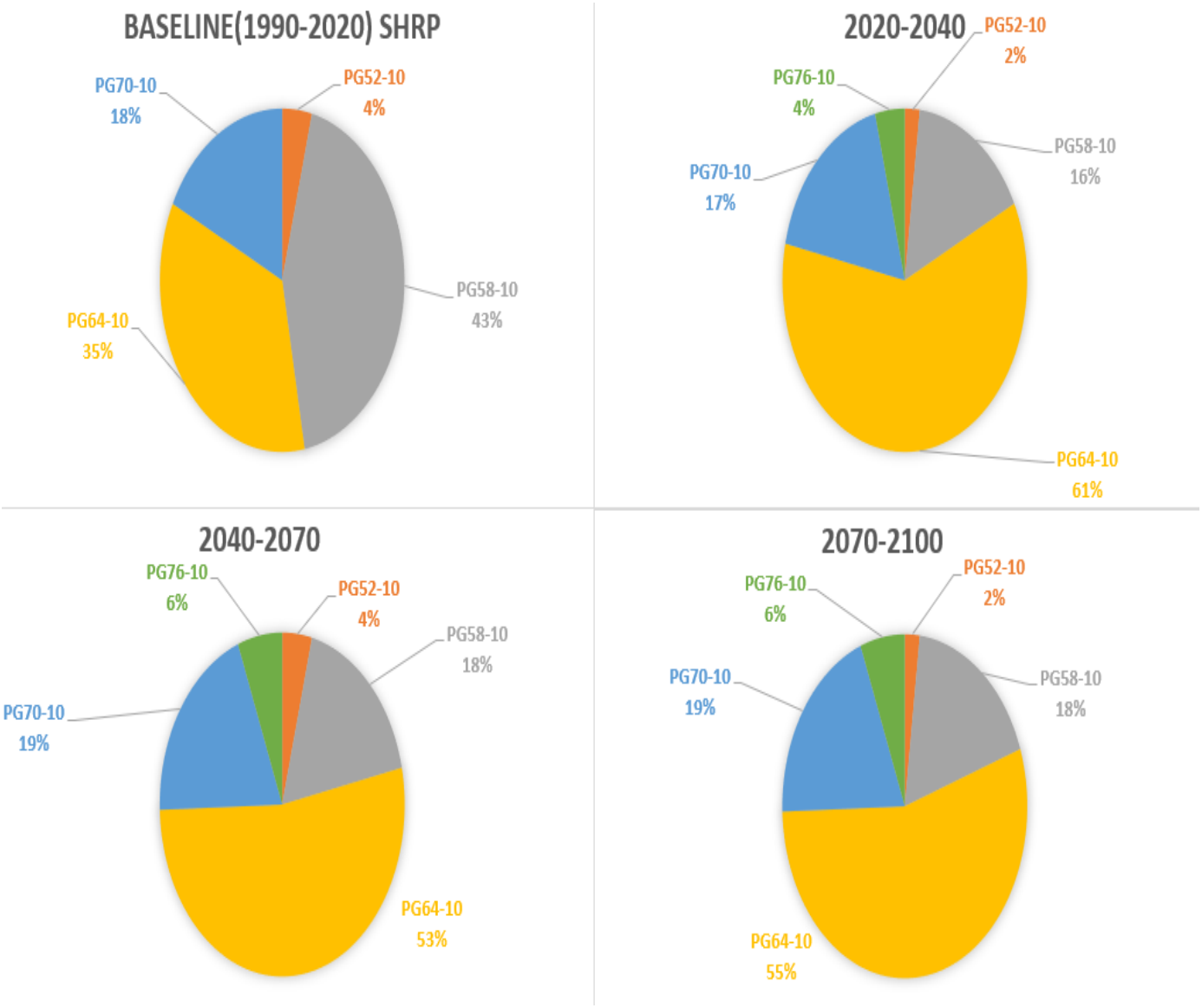

Figure 4-9 SHRP Model of PG Result Percentage expression

From pie chart shown that for this model In Ethiopia, the estimated coverage of higher performance grades of asphalt (PG58-10 and PG64-10) significantly increased over time, while the coverage of lower performance grades (PG52-10) decreased. This trend was observed from 1990-2020, 2020-2040, 2040-2070, and 2070-2100. The coverage of PG46-10 remained at zero throughout all time periods. Overall, the study *suggests* increasing

adoption of higher performance asphalt grades in Ethiopia.

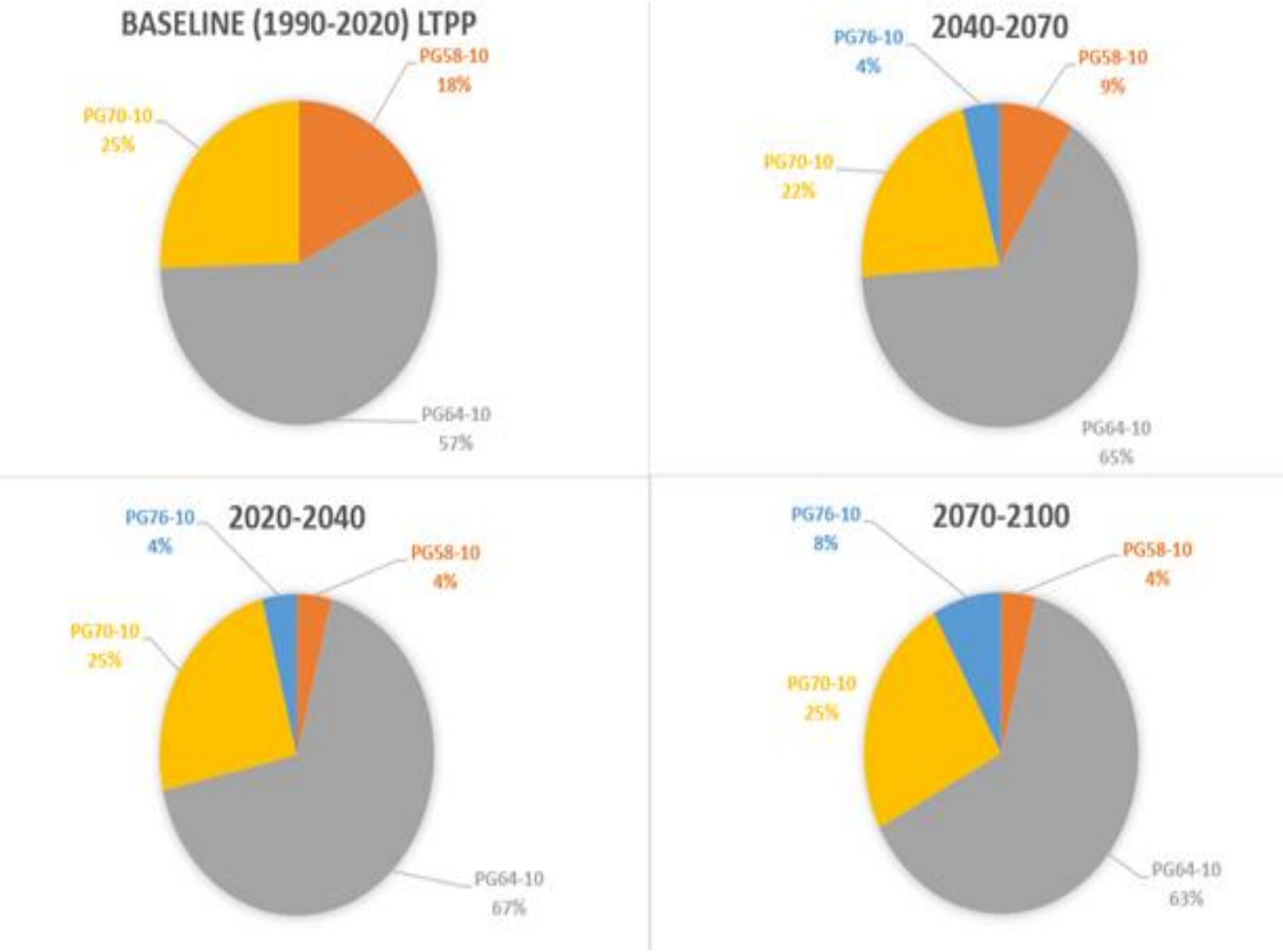

Figure 4-10 : LTPP Model prediction of PG Result Percentage expression

From Above figure or chart shown that for this model In Ethiopia, the estimated coverage of higher performance grades of asphalt (PG64-10 and PG70-10) significantly increased over time, while the coverage of lower performance grades (PG58-10) decreased and PG 76-10 are cover some area. This trend was observed from 1990-2020, 2020-2040, 2040-2070, and 2070-2100. The coverage of PG46-10 remained at zero throughout all time periods. Overall, the study suggests an increasing

The research results of both models suggest that the estimated coverage of different performance grades of asphalt in Ethiopia varied over time, with a shift towards higher performance grades in some cases. The results also

suggest that the use of different performance grades of asphalt may be influenced by factors such as climate change, as seen in the shift towards more resilient asphalt types in the later time periods. These findings can inform discussions on the allocation of resources for road construction and maintenance in Ethiopia, and the need for continued investment in quality road infrastructure

4.4.2 Statistical Comparation of two model PG Result

4.4.2.1 Descriptive statistics of data

To interpreted result of two model more investigation is need similarity and different then first Descriptive statistics can provide valuable insights into the characteristics of a normal distribution of data. To determine if the data is normally distributed, we can look at the skewness and kurtosis values. For a normal distribution, the skewness should be close to zero and the kurtosis should be close to three.

Table 4-4 : Descriptive statistics value of 98% reliability of pavement temperature.

Reliability	***98%***							
Year	**Baseline (1990-2020)**		**2020-2040**		**2040-2070**		**2070-2100**	
Model	**SHRP**	**LTPP**	**SHRP**	**LTPP**	**SHRP**	**LTPP**	**SHRP**	**LTPP**
Mean	59.10	61.54	60.44	62.10	60.21	62.33	61.16	62.91
Standard Error	0.62	0.53	0.77	0.71	0.88	0.80	0.87	0.79
Median	58.54	60.97	60.52	62.06	60.20	62.57	61.27	63.01
Standard Deviation	4.38	3.76	5.45	5.04	6.26	5.64	6.14	5.59
Sample Variance	19.22	14.13	29.74	25.40	39.14	31.82	37.66	31.25
Kurtosis	-0.34	-0.48	10.62	18.79	6.10	12.44	7.24	13.43
Skewness	0.13	0.12	-2.05	-3.33	-1.23	-2.43	-1.55	-2.62
Range	18.30	15.55	38.43	37.11	40.33	38.45	39.59	38.19
Minimum	49.42	53.02	34.15	34.31	33.63	33.98	33.92	34.31
Maximum	67.72	68.57	72.58	71.42	73.96	72.43	73.51	72.50

The table shows that the kurtosis and skewness values for both models in the baseline period are relatively close to zero, indicating that the data is normally distributed and symmetric. However, the kurtosis and skewness values for the different time periods and models vary widely, suggesting that the data may not be normally distributed and that there may be outliers or extreme values affecting the shape of the distribution. For example, the kurtosis value for the SHRP model in the 2020-2040 time period is 10.62, indicating a very peaked distribution, while the kurtosis value for the LTPP model in the same time period is 18.79, indicating an even more peaked distribution. In the future periods of pavement prediction results, the kurtosis and skewness values suggest that the data may not be normally distributed. For instance, the skewness value for the SHRP model in the 2040-2070 time period is -1.23, indicating a moderately negative skew, while the skewness value for the LTPP model in the same time

4.4.2.2 T-test of comparation of Two model Result

for this study from the result of pavement temperature prediction using two model t test result is for 98 % Reliability t-test Result of Baseline pavement temperature prediction.

Table 4-5 T-test result of comparation of Two model (SHRP and LTPP)

Paired t-Test

Reliability	**50%**		**98%**	
Model	***SHRP-Result***	***LTPP-Result***	***SHRP-Result***	***LTPP-Result***
Mean	55.5	54.6	59.0	61.5
Variance	21.7	14.6	19.2	14.1
Observations	51.0	51	51.0	51
Pearson Correlation	1.0		1.0	
Hypothesized Mean Difference	0.0		0.0	
df	50.0		50.0	
t Stat	6.2		-14.9	
P(T<=t) one-tail	0.0		0.0	
t Critical one-tail	1.7		1.7	
P(T<=t) two-tail	0.0		0.0	
t Critical two-tail	2.0		2.0	

From above table shown that to Compare the p-value to the significance level. from the two models. the In this case have a very small p-value (less than 0.001), indicating strong evidence against the null hypothesis that the mean difference is zero. The critical values for both models are 1.7 for a one-tailed test and 2.0 for a two-tailed test, which are not exceeded by the calculated t-statistics. Therefore, the null hypothesis is rejected for both Case at the 0.05 significance level.

4.5 Mapping of pavement Temperature zoning of Performance Grade (PG) for (SHRP & LTPP Model)

4.5.1 Mapping using Historical Temperature data.

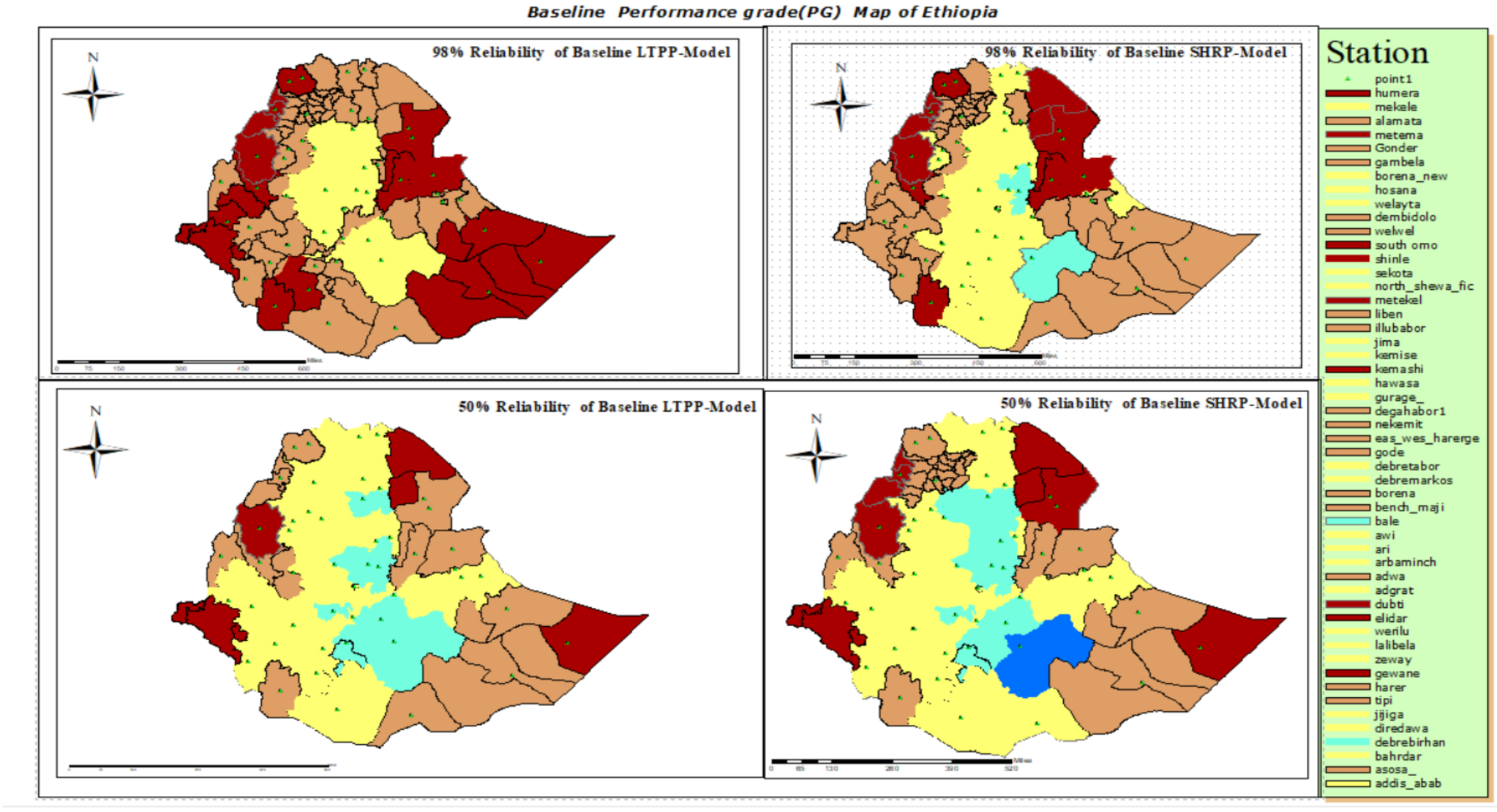

Figure 4-11 Baseline PG of Ethiopia by historical climate data (1990-2020)

4.5.2 Mapping of Future projection temperature data climate change Scenario (SSP2(4.5).

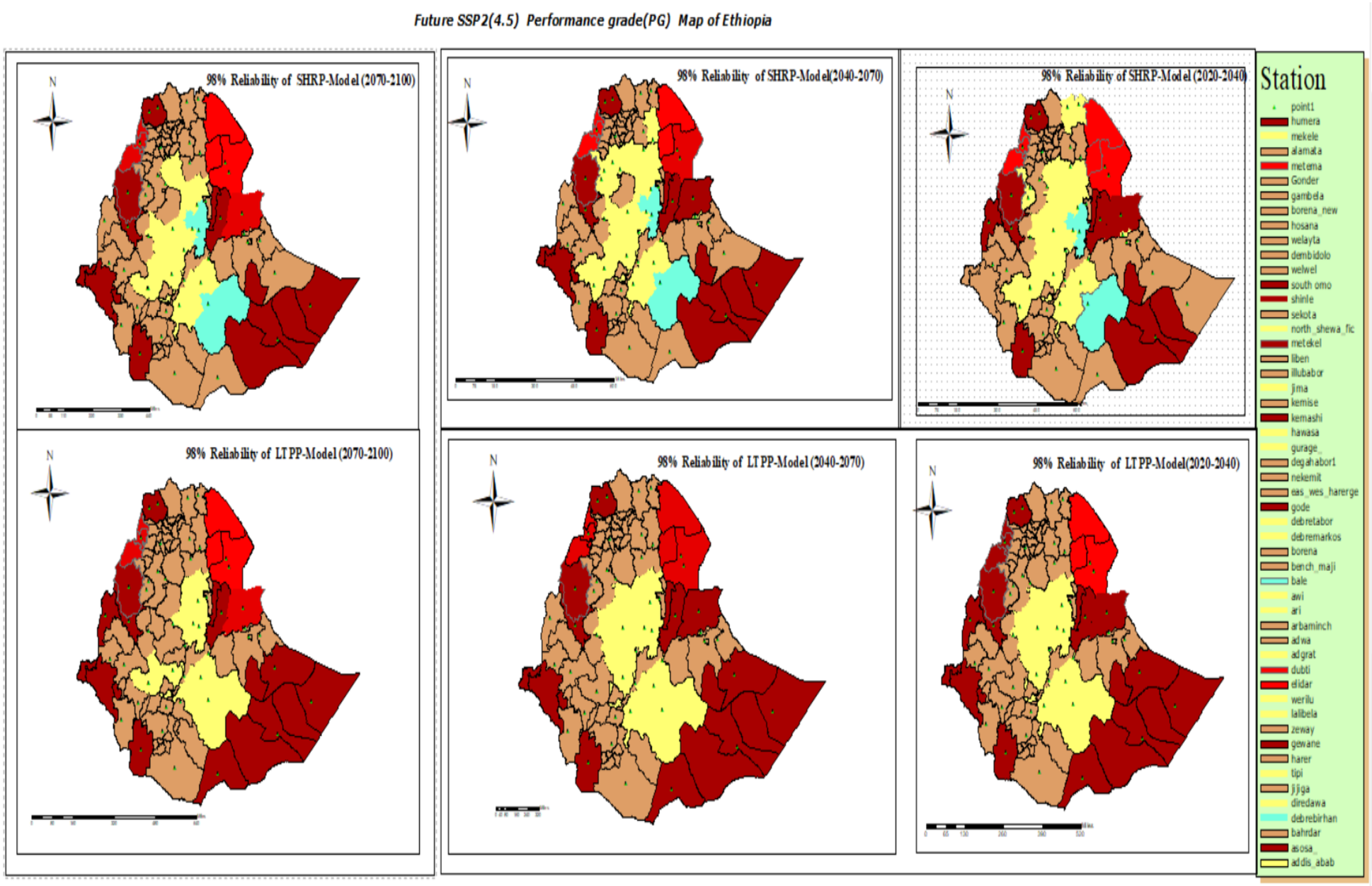

Figure 4-12 : Future PG of Ethiopia SSP 2 (4.5) (2020-2100)

4.5.3 Mapping using Future projection temperature data of climate change Scenario (SSP5(8.5).

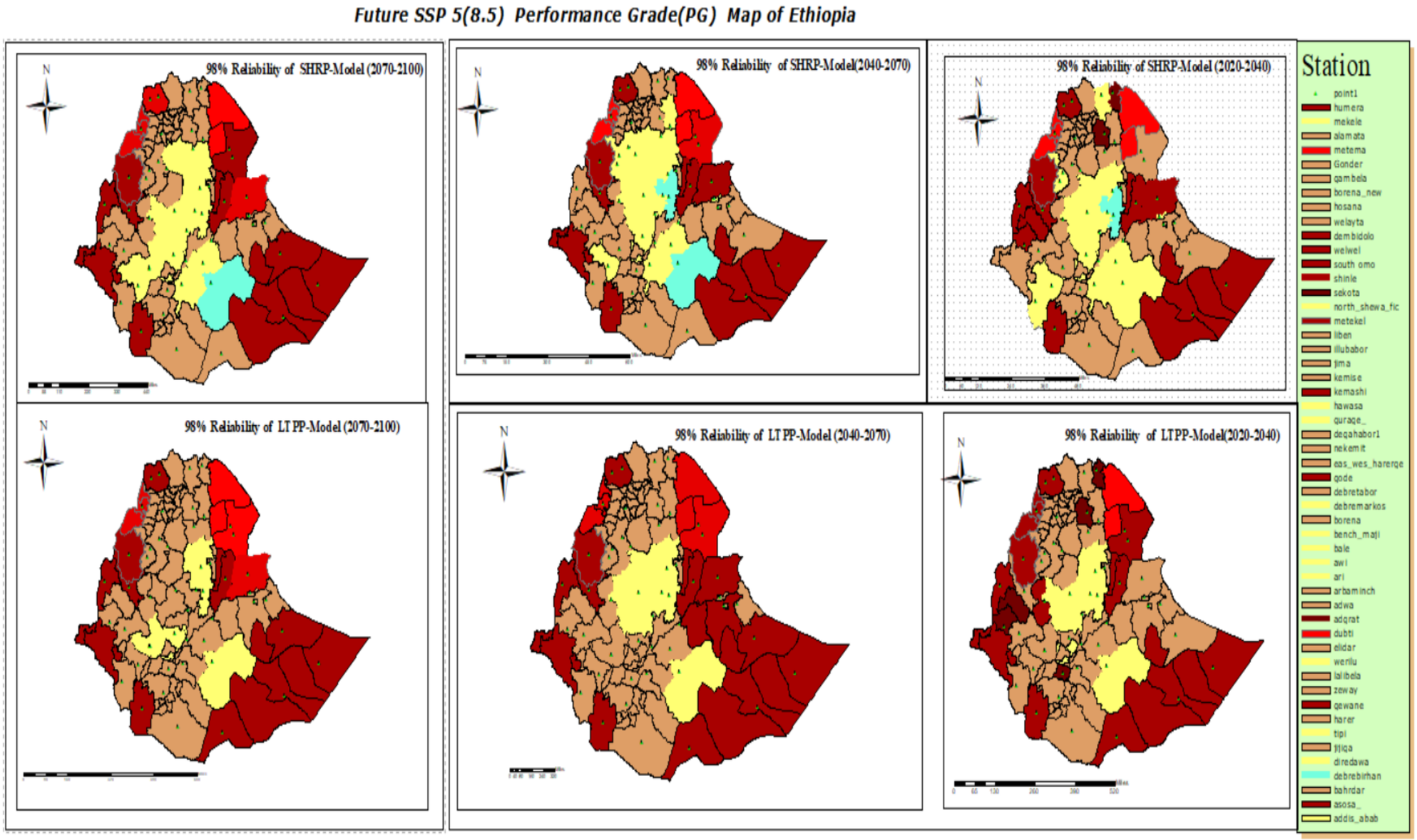

Figure 4-13 : Future PG of Ethiopia SSP 5(8.5) (2020-2100).

4.6 Adjustment of Performance Grade (PG) of Asphalt considering traffic and speed factor

The Performance Grade (PG) of asphalt is a measure of its ability to resist deformation and cracking under different temperature conditions. However, the PG of asphalt can be affected by traffic and speed factors, which can cause additional stress and strain on the pavement. To adjust the PG of asphalt considering traffic and speed factors, Determine the expected traffic volume and speed for the pavement section. This can be done by analyzing traffic data and conducting speed surveys and Calculate the equivalent single axle loads (ESALs) for the expected traffic volume and speed.

In this study, to develop super pave bitumen specification of adjusted performance grade (PG) use the ERA Manual traffic volume for adjusting purpose.

Table 4-6 : Table of Adjusted Binder PG-Grade is provided in AASHTO MP-2

Design ESALs	Adjusted Binder PG-Grade		
	Traffic Load Rate		
	Standing	Slow	Standard
<0.3	-	-	-
0.3 to<3	2	1	-
3 to<10	2	1	-
10 to <30	2	1	
>30	2	1	1

standing Traffic where the average traffic speed is less than 20km /hr., **Slow traffic** where the average traffic speed is range 20-70km /hr. and **Standard Traffic** where the average traffic speed is greater than 70km /hr.

Traffic level and speed are also considered in selecting the project performance grade (PG)binder either through reliability or “grade bumping.” in AASHTO MP-2.the selection of the appropriate asphalt binder for a road construction project is based on a number of factors, including the expected traffic volume and speed, as well as the climate and environmental conditions in the area. The performance grade (PG) of the asphalt binder is determined based on laboratory testing, which

evaluates the binder's performance characteristics under different conditions. In some cases, the expected traffic and environmental conditions may be more severe than what is typically encountered in the area. In these cases, a higher-grade asphalt binder may be selected through grade bumping.

Table 4-7 Traffic Classes for Flexible Pavement Design of Ethiopia

Traffic Classes	Range ESAs(million)
LV1	**<0.01**
LV2	**0.01-0.1**
LV3	**0.1-0.3**
LV4	**0.3-0.5**
LV5	**0.5-0.7**
T3	**0.7-1.5**
T4	**1.5-3**
T5	**3.0-6.0**
T6	**6.0-10**
T7	**10-17**
T8	**17-30**
T9	**30-50**
T10	**50-80**
T11	**>80**

It is possible to adjust the performance grade (PG) of asphalt binders based on the AASHTO MP-2 specification and the ERA manual traffic classification,

Table 4-8 -adjusted performance grade (PG)of Superpave specification in Ethiopia.

Performance Grade (PG)	Speed (Km/hr.)	Number of Additional Grade					
		LV1-LV3	LV4-T_4	T_5 - T_6	T_7	T_8	T_9-T_{11}
PG-46-10	Standing	No adjustment needed	2	2	2	2	2
	Slow		1	1	1	1	1
	Standard						1
PG-52-10	Standing		2	2	2	2	2
	Slow		1	1	1	1	1
	Standard						1
PG-58-10	Standing		2	2	2	2	2
	Slow		1	1	1	1	1
	Standard						1
PG-64-10	Standing		2	2	2	2	2
	Slow		1	1	1	1	1
	Standard						1
PG-70-10	Standard						1
	Slow		1	1	1	1	1
	Standing		Polymer Modification needed				
PG-76-10	Standing		Polymer Modification needed				
	Slow		Polymer Modification needed				
	Standard		Polymer Modification needed				

N.B. 1-means one grade (6 ºC) and 2-means Two Grade (12 ºC)

The above table (4-9) is note that a general adjustment Performance grade from the minimum **(PG46-10)** to higher **(PG76-10), according to above result shown.** it is important to consider all relevant factors and consult with a qualified professional to determine the appropriate PG grade for a specific location

4.7 PG of Penetration Grade currently used Asphalt binder in Ethiopia

4.7.1 Determine PG asphalt Binder using DSR.

To grade an **unknown binder**, begin DSR testing at 58˚C. Determine the results of G*/sin δ. If the sample fails at 58˚C, increase or decrease the temperature by increments of 6˚C until the value of G*/sin δ ≥ 1.00 kPa. The highest temperature where G*/sin δ ≥ 1.00 kPa will determine the starting value for the **PG grade.** Perform the DSR on original asphalt binder in accordance with AASHTO T 315. Test the sample initially at 58°C. Increase the test temperature and repeat the test until G*/sin δ ≤ 1.00 kPa. the flash point of the original binder according to the requirements set forth in AASHTO T 48. The flash point must exceed 230˚C. the viscosity of the original binder in accordance with AASHTO T 316 at 135˚C. The viscosity must not exceed 3 Pa·s.

Table 4-9 : PG Grading of 85/100 original

Test information						
Sample type	85/100-orginal					
Plate diameter	25 mm					
Test Gap	1mm					
Test Frequency, rad/s	10					
Test Mode	12%					
Result						
Trial	Trial-1			Trial -2		
Test Temperature (º c.)	59.95	65.96	72.01	59.45	64.59	71.53
Complex Modulus, G*, for 10 cycles (kPa to three significant figures	1252.40	621.19	348.49	1260.1	617.5	337.6
Phase angle, δ, for 10 cycles (nearest 0.1 degrees)	87.52	87.89	88.29	88.20	88.63	88.93
G*/(sinδ) (nearest 0.01 kPa)	1253.6	621.6	348.6	1260.7	617.7	337.7
Fail temperature (º c.)	62.7			62		
Average	62.35					
PG-Grade	**58**					

The test result shown that equivalent PG grade for unaged 85/100 penetration graded asphalt is determined to be **PG 58-YY**. In addition, the critical temperature, which refers to the specific temperature at which the complex shear modulus (G*) divided by the sine of the phase angle (δ) falls below 1 kilopascal (kPa), are fail in at 62.35^{o} c.

Table 4-10 : PG Grading of 85/100 aged

Test information						
Sample type	85/100-aged					
Plate diameter	25 mm					
Test Gap	1mm					
Test Frequency, rad/s	10					
Test Mode	10%					
Result						
Trial	Trial-1			Trial -2		
Test Temperature (^{o} c)	51.96	58.07	63.90	52.01	57.99	63.92
Complex Modulus, G*, for 10 cycles (kPa to three significant figures	6418.90	2518.60	1078.40	8373.70	3488.10	1499.90
Phase angle, δ, for 10 cycles (degrees)	84.52	86.52	87.80	82.75	85.21	86.75
G*/(sinδ) (Pa)	6448.37	2523.25	1079.20	8441.19	3500.33	1502.32
Fail temperature (^{o} c)	60.37			61.67		
Average (^{o} c)	61.02					
PG-Grade	**58**					

N.B: Another Test result are in APPENDEX-E

Perform the DSR on the RTFO-conditioned material in accordance with AASHTO T 315. Test the sample initially at the starting grade determined. If G*/sin δ ≥2.20 kPa, the temperature from table is the high-temperature grade of asphalt binder. If G*/sin δ ≤ 2.20 kPa, retest the material at a temperature 6°C lower the from the above table the test result shown that material fail at 61.02^{o} C

Therefore, **PG 58-YY** are the equivalent grade of Penetration grade 85/100.

Table 4-11: PG Grading of Penetration binder

S/N	Pen-grade	Unaged (Original)						Aged					over all PG Grade
		Test temp. (º c)	Complex Modulus, G*	Phase angle, δ	G*/(sinδ) (Pa)	Fail Temp.	PG	Complex Modulus, G*	, Phase angle δ (degrees)	G*/(sinδ) (Pa)	Fail Temp (º c).	PG	
1	85/100	58	1338.04	87.39	1339.30	62.35	PG58	4438.50	87.82	4441.71	61.02	PG58	PG58
2	80/100	58	1919.64	86.89	1923.55	59.13	PG58	4669.60	84.95	4687.79	59.66	PG58	PG58
3	60/70	64	2128.27	86.92	2132.88	68.03	PG64	2742.61	87.82	2744.59	64.52	PG64	PG64
4	40/50	64	1900.5	83.89	1902.64	69.29	PG64	2974.24	85.18	2984.79	71.66	PG70	PG64

Based on these results, it can be observed that Pen.Grade 85/100 and Pen.Grade 80/100 have similar **PG58-YY** grades, both in their original and RTFO-aged states, with average fail temperatures in the range of 59-62°C.

Pen.Grade 60/70 and Pen.Grade 40/50 have a higher PG64 grade in their original state, indicating a stiffer asphalt binder. However, after RTFO aging, Pen.Grade 60/70 retains its PG 64 grade, while Pen.Grade 40/50 experiences an increase in average fail temperature and achieves a higher PG70 grade.

In the context of Ethiopia, these PG grades can help in selecting appropriate asphalt binders for different climate and temperature conditions. The selection of an appropriate PG grade ensures

that the asphalt will perform adequately under expected temperature ranges, avoiding issues such as rutting or cracking.

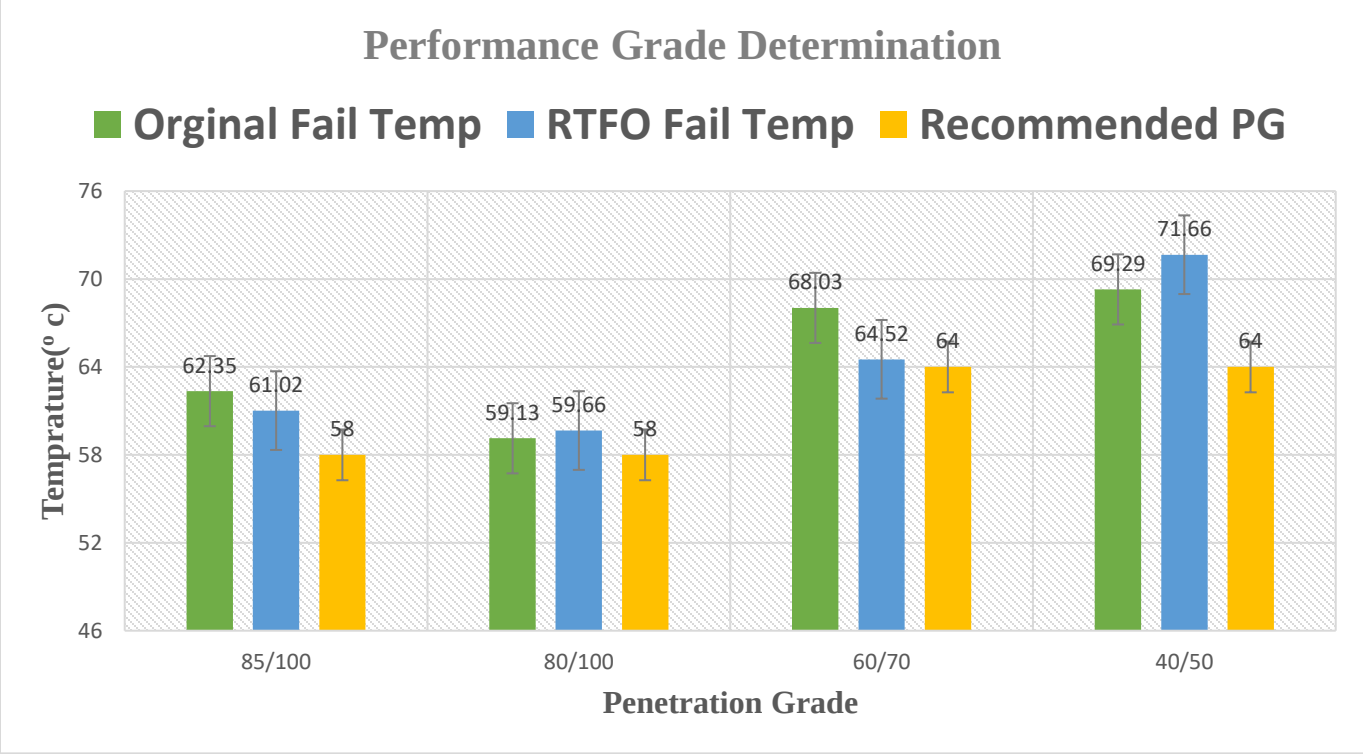

Figure 4-14: Penetration grade bitumen performance fail temperature

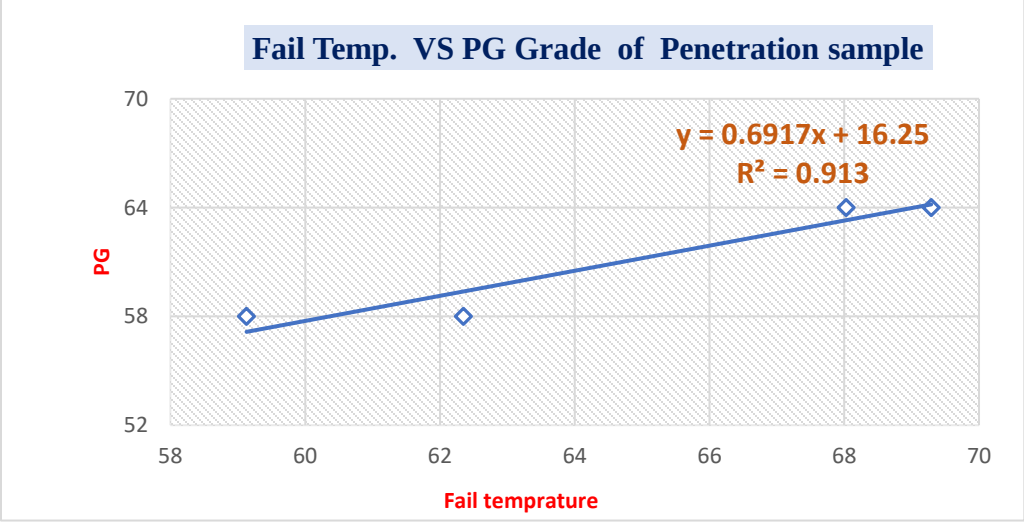

Figure 4-15 : Relationship between fail temperature with PG grade

It's important to note that the selection of the appropriate PG grade depends on various factors such as traffic loads, climate conditions, and pavement design considerations. Further analysis and consideration of these factors are crucial to determine the most suitable PG grade for specific applications in Ethiopia.

4.7.2 Mapping of penetration grade result in Ethiopia

From the result shown to Map penetration grade to temperature zones based on the Performance Grade (PG) system can provide insights into the expected performance of asphalt binders under specific temperature conditions. Here's a general mapping of penetration grades to temperature zones in relation to the PG system according to fail temperature

- PG 58: This grade is typically associated with penetration grades around 80/100.
- PG 64 this grade corresponds to penetration grades around 60/70 and 40/50
- For PG 70 Other bitumen grade or Modified Binder needed.

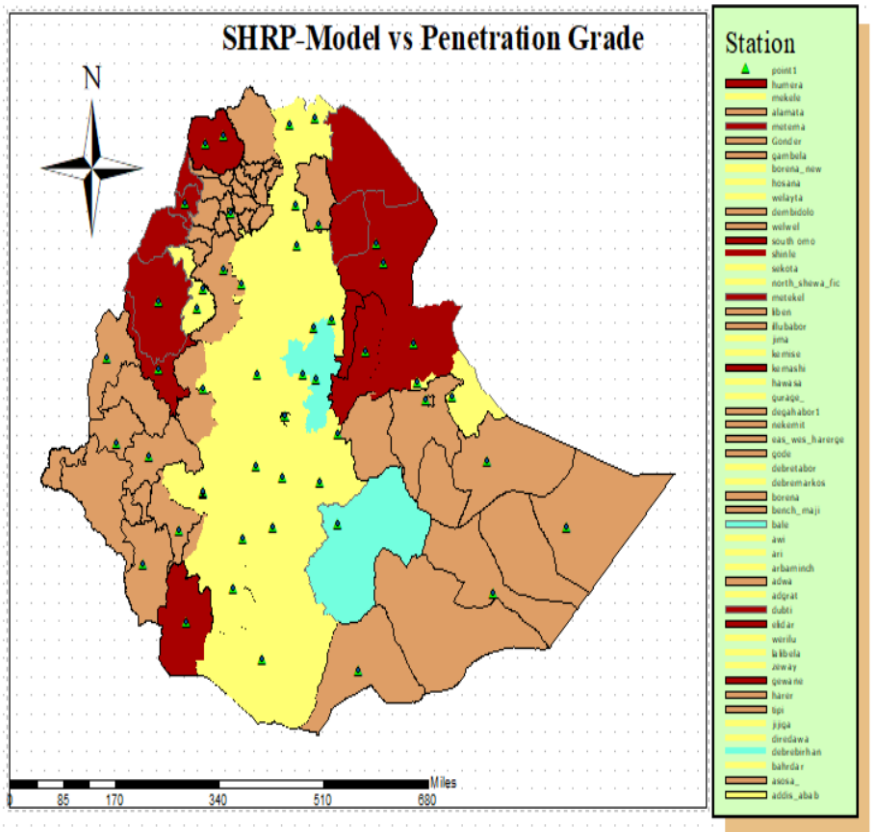

Grade		Legend
PG	Pen-Grade	
PG52	85/100	
PG58	80/100	
PG64	60/70& 40/50	
PG70	Other Bitumen Grade	

Figure 4-16: Penetration grade map for Ethiopia for current

CHAPTER FIVE

5 Conclusion and Recommendation

5.1 Conclusion

The research focused on adapting Superpave bitumen specifications for Ethiopia in response to climate change concerns and its impact on asphalt pavements. Two pavement temperature prediction models, SHRP and LTPP, were used to analyze past and future climate data for different time frames (1990-2020, 2020-2040, 2040-2070, and 2070-2100).

- Statistical methods were employed to determine the appropriate binder grade for each location, considering climate conditions and the impact of climate change on pavement performance grade. Results showed that many locations in Ethiopia would require an increase in binder grade to ensure the durability and longevity of asphalt pavements under future climate conditions.
- The majority of locations would require PG58-10 and PG64-10, while the Afar region and the western part of Ethiopia would require PG76-10 in the future.
- The study revealed that the SHRP and LTPP models produced different temperature predictions, with the LTPP model overestimating in some locations.
- A t-test was conducted to compare the two temperature prediction models, and the null hypothesis was rejected, indicating a statistically significant difference in the Superpave bitumen specifications. This is due to SHRP model is a mechanistic-empirical model, while the LTPP model is a statistical model. Both models were found useful in predicting pavement performance grade (PG).
- The currently used asphalt binder grades in Ethiopia were evaluated using the Dynamic Shear Rheometer (DSR) with SHRP criteria. The evaluation showed that penetration grades 40/50 and 60/70 bitumen were graded as PG64, while penetration grades 80/100 and 85/100 were graded as PG58.

The findings of the research have important implications for infrastructure planning and development in Ethiopia, emphasizing the need for ongoing research in pavement engineering and climate change adaptation.

- The developed Superpave bitumen specifications can serve as a foundation for future infrastructure planning in Ethiopia and as a model for other countries facing similar challenges.
- The study highlights the significance of considering climate change impacts in infrastructure planning and underscores the need for continued research in this field.

5.2 Recommendation

Based on the findings of this study, the following recommendations are suggested

- Update the current bitumen specifications in Ethiopia to incorporate the impact of climate change on pavement performance. The Superpave system is recommended as it considers the climatic conditions of the region and can provide more accurate predictions of pavement performance.
- Conduct further research to validate the findings of this study and to refine the Superpave bitumen specifications for Ethiopia. This could include additional field testing and data collection to improve the accuracy of the temperature prediction models.
- Develop a comprehensive climate change adaptation strategy for infrastructure development in Ethiopia. This should include measures to improve the resilience of pavements to the impacts of climate change, such as increased use of recycled materials and improved drainage systems.
- Increase public awareness of the importance of climate change adaptation in infrastructure development. This could include educational campaigns and outreach programs to inform the public about the risks of climate change and the need for sustainable infrastructure development.

Generally, this study provides valuable insights into the development of Superpave bitumen specifications for Road infrastructure development in Ethiopia. The findings of this study can be used to inform policy decisions and guide future research in this area, with the aim of developing more resilient and sustainable infrastructure that can withstand the challenges of climate change

REFERENCE

Abo-Hashema, M. A., Mousa, R. M., Al-Zedjali, S. A., Al Balushi, A., Metwally, M., & Al-Rashdi, M. H. (2016). *Development of oman performance grade paving map for superpave asphalt mix design*.

Adwan, I., Milad, A., Memon, Z. A., Widyatmoko, I., Zanuri, N. A., Memon, N. A., & Yusoff, N. I. M. (2021). Asphalt pavement temperature prediction models: A review. In *Applied Sciences (Switzerland)* (Vol. 11, Issue 9). MDPI AG. https://doi.org/10.3390/app11093794

Airey, G. D., & Collop, A. (2002). *Linear viscoelastic limits of bituminous binders Towards 100% recycling of Reclaimed Asphalt Pavement (RAP) View project Recycling Tyre Rubber in Civil Engineering applications View project*. https://www.researchgate.net/publication/283412618

Airey, G. D., Collop, A., Singleton, T. M., Airey, * -G D, Widyatmoko, -I, & Collop, -A C. (1999). *Residual Bitumen Characteristics Following Dry Process Rubber-Bitumen Interaction*. https://www.researchgate.net/publication/288798691

Alder, S., Croke, K., Duhaut, A., Marty, R., & Vaisey, A. (2022). *The Impact of Ethiopia's Road Investment Program on Economic Development and Land Use Evidence from Satellite Data*. http://www.worldbank.org/prwp.

Ali Hussain, G. M., Abdulaziz, M. A. G., Xiang, Z. N., & Al-Hammadi, M. A. (2020). Asphalt Binder Performance Grading for the Republic of Yemen Based on Superpave Asphalt Mix-Design. *The Open Civil Engineering Journal*, *14*(1), 365–379. https://doi.org/10.2174/1874149502014010365

Al-Qadi, I. L., Diefenderfer, B. K., Asce, A. M., Asce, F., & Diefenderfer, S. D. (2006). *Model to Predict Pavement Temperature Profile: Development and Validation*. https://doi.org/10.1061/ASCE0733-947X2006132:2162

Anderson, D. (n.d.). *Asphalt Binders, characterization of bitumen material https://trb.org/publications/millennium/00006.pdf.*

Arangi, S. R., & Jain, R. K. (2015). *Journal of Innovative Research in Advanced Engineering International Journal of Innovative Research in Advanced Engineering (I JI RAE) ISSN: 2349-2163 Issue 8* (Vol. 2). www.ijirae.com

Asphalt Institute, & European Bitumen. (2015a). *The bitumen industry: a global perspective: production, chemistry use, specification and occupational exposure.*

Asphalt Institute, & European Bitumen. (2015b). *The bitumen industry: a global perspective: production, chemistry use, specification and occupational exposure.*

Balcha, Y. A., Malcherek, A., & Alamirew, T. (2022). Understanding Future Climate in the Upper Awash Basin (UASB) with Selected Climate Model Outputs under CMIP6. *Climate*, *10*(12). https://doi.org/10.3390/cli10120185

Corbett, L. W. (1984). *Refinery Processing of Asphalt Cement*.

Daba, D. (2018). *Prediction of Maximum Pavement Surface Temperature Using Maximum Air Temperature & Latitude*.

Delgadillo, R., Arteaga, L., Wahr, C., & Alcafuz, R. (2020). The influence of climate change in Superpave binder selection for Chile. *Road Materials and Pavement Design*, *21*(3), 607–622. https://doi.org/10.1080/14680629.2018.1509803

E. Denneman. (2007). *The 26th Annual Southern African Transport Conference: the challenges of implementing policy: CSIR International Convention Centre, Pretoria, South Africa, 9 - 12 July 2007*.

ERA Manual. (2013). *Ethiopia Road Authority flexible Pavement Design Volume -1*. www.era.gov.et

Ghuzlan, K. A., & Al-Khateeb, G. G. (2013). Selection and verification of performance grading for asphalt binders produced in Jordan. *International Journal of Pavement Engineering*, *14*(1–2), 116–124. https://doi.org/10.1080/10298436.2011.650697

Gordon da airey. (1997). Rheological property of polymer Modified and aged Bitumen. *Rheological Characteristic of Bitumen*.

Harman, T. (2002). *Superpave Asphalt Mixture Design Workshop Developed by the Asphalt Team* (Vol. 202, Issue 202).

Hassan, H. F., Al-Nuaimi, A. S., Taha, R., & Jafar, T. M. A. (2005). Development of Asphalt Pavement Temperature Models for Oman. In *The Journal of Engineering Research* (Vol. 2, Issue 1).

IPCC. (2021). *inter-governmental panel on climate change The Physical Science Basis Summary for Policymakers.*

Izzi, N., & Yusoff, M. (2012). *Modelling the Linear Viscoelastic Rheological Properties of Bituminous Binders*.

john read, D. whiteoak. (2003). *Shell Bitumen Handbook*.

Joshi, C., Patted, A., R, A. M., & Amarnath, M. S. (2013). Determining the rheological properties of asphalt binder using dynamic shear rheometer (DSR) for selected pavement stretches. in *ijret: International Journal of Research in Engineering and Technology*. http://www.ijret.org

Jung, D. H., Vinson, T. S., Oregon State University. Department of Civil Engineering., & Strategic Highway Research Program (U.S.). (1994). *Low-temperature cracking: binder validation*. Strategic Highway Research Program, National Research Council.

Kennedy, T. W. (1994). *Superior Performing Asphalt Pavements (Superpave) : The Product of the SHRP Asphalt Research Program*.

Kharbuja, S., Kharbuja[1], S., Shahi[2], T. C., & Duwal[3], R. (2020). *Development of Performance grading map of Nepal based on super pave system* (Vol. 8).

Mahlet Gashaw. (2018). *Mapping Temperature Zone of Ethiopia for Binder Performance Grading System*.

Melaku, R. S. (2020). *Performance Evaluation Of Sustainable Pavement Materials*. https://commons.und.edu/theses/3111

Member of RAHA Group. (2022). Iran Bitumen- Road Bitumen, RAHA Bitumen Co.2022. *Bitumen Binder* .

Mokoena, R., Mturi, G., Maritz, J., Malherbe, J., & O'connell, J. (2019). *Adapting Asphalt Pavements to Climate Change Challenges*.

National Meteorological Agency. (2020). *National Meteorological Agency revised Meteorological station network master plan for 2021-2030*.

O'Malley, C., Piroozfarb, P. A. E., Farr, E. R. P., & Gates, J. (2014). An investigation into minimizing urban heat island (UHI) effects: A UK perspective. *Energy Procedia*, *62*, 72–80. https://doi.org/10.1016/j.egypro.2014.12.368

Ongoma, V., Abatan, A., Lim, K. T. C., Sian, K., Ândrea, M., & Firpo, F. (2022). *Assessment of CMIP6 models' performance in simulating present-day climate in Brazil*. https://esgf-node.llnl.gov/search/

Pak.j.Engg &Appl.Sci. (2021). Temperature Zoning of Pakistan for Asphalt Mix Design,Pak. J. Engg. & Appl. Sci. Vol. 8, Jan., 2011 (p. 49-60). *Temperature Zoning of Pakistan for Asphalt Mix Design*, *Vol. 8*(Jan,2011), 49–60.

pavement interactive. (2023). *Asphalt Production and Oil Refining-Pavement Interactive*. https://pavementinteractive.org/reference.

Poole, R. J. (2012). *The Deborah and Weissenberg numbers Purely-elastic instabilities View project Type III b end leak View project*. https://www.researchgate.net/publication/249993763

Puzinauskas, V. P., Harrigan, E. T., & Leahy, R. B. (1990). *Current Refining Practices for Paving Asphalt Production*.

Quintero, N. M. (2007). *Validation of the Enhanced Integrated Climatic Model (EICM) for the Ohio SHRP Test*.

Remišová, E., Zatkaliková, V., & Schlosser, F. (2016). Study of Rheological Properties of Bituminous Binders in Middle and High Temperatures. *Civil and Environmental Engineering*, *12*(1), 13–20. https://doi.org/10.1515/cee-2016-0002

Robert N Hunter, A. self and jon reed. (2015). The Shell Bitumen Handbook, 6th edition. In *The Shell Bitumen Handbook, 6th edition*. https://doi.org/10.1680/tsbh.58378

Robertson, R. E. (1991). *Chemical Properties of Asphalts and Their Relationship to Pavement Performance*.

Rogers, Martin. (2003). *Highway engineering*. Blackwell Science.

Ronald, M., & Chehab, G. (2020). *Determination of Temperature Zoning for the Great Lakes Region of Africa based on Superpave System*. 495–501. https://doi.org/10.29117/cic.2020.0062

Sabita. (2012). *Bituminous binders for road construction and maintenance.* Sabita.

SAFWAN KKEDR. (2014). *Development of Asphalt Binder Performance Grade in Egypt*.

Salvatore Magnifico. (2014). *Linear viscoelastic properties and fatigue of bituminous mixtures produced with Reclaimed Asphalt Pavement and corresponding binder blends*.

Shiferaw, A., Söderbom, M., Siba, E., & Alemu, G. (2012). *Road Infrastructure and Enterprise Development in Ethiopia*.

Swarna, S. T., Hossain, K., Pandya, H., & Mehta, Y. A. (2021). Assessing climate change impact on asphalt binder grade selection and its implications. In *Transportation Research Record* (Vol. 2675, Issue 10, pp. 786–799). SAGE Publications Ltd. https://doi.org/10.1177/03611981211013026

Swarna, T., John's Newfoundland, S., & Canada, L. (2021). *Influence of Climate Change on Pavement Design and Materials in Canada*.

Underwood, B. S., Guido, Z., Gudipudi, P., & Feinberg, Y. (2017). Increased costs to US pavement infrastructure from future temperature rise. *Nature Climate Change*, *7*(10), 704–707. https://doi.org/10.1038/nclimate3390

Viola, F., & Celauro, C. (2015). Effect of climate change on asphalt binder selection for road construction in Italy. *Transportation Research Part D: Transport and Environment*, *37*, 40–47. https://doi.org/10.1016/j.trd.2015.04.012

APPENDIX. A. Location of Station

Station Coordinate Historical and future Temperatures data Period						
S/N	**Location**	**Latitude**	**Longitude**	**Elevation**	**Historical Observed year**	**Future Data**
1	Addis Ababa	9.01891	38.74689	2386	1990-2020	2020-2100
2	Assosa	10.04556	34.5458	1541	1990-2020	2020-2100
3	Metema	12.7746	36.4139	790	1990-2020	2020-2100
4	Bahr Dar	11.6027	37.322	1827	1990-2020	2020-2100
5	Debrebirhan	9.670278	39.5131	3206	1990-2020	2020-2100
6	Dire Dawa	9.613367	41.8986	1045	1990-2020	2020-2100
7	Jigiga	9.365133	42.7179	1557	1990-2020	2020-2100
8	Tipi	7.204883	35.4375	1208	1990-2020	2020-2100
9	Harar	9.314433	42.0932	1977	1990-2020	2020-2100
10	Gewane	10.15588	40.6583	618	1990-2020	2020-2100
11	Dubti	11.72667	41.0897	381	1990-2020	2020-2100
12	Zeway	7.936389	38.7147	1646	1990-2020	2020-2100
13	Hosanna	7.567788	37.8561	2306	1990-2020	2020-2100
14	Lalibela	12.039	39.0398	2487	1990-2020	2020-2100
15	Weielu	10.57949	39.4367	2708	1990-2020	2020-2100
16	Elidar	12.0497	40.9219	442	1990-2020	2020-2100
17	Adigrat	14.2788	39.4605	2,482	1990-2020	2020-2100

18	Adawa	14.1782	38.878	2235	1990-2020	2020-2100
19	Alamata	12.4184	39.5572	1710	1990-2020	2020-2100
20	Arbaminch	5.996	37.5403	1290	1990-2020	2020-2100
21	Arsi(Asela)	7.86662	39.5944	2355	1990-2020	2020-2100
22	Enjibara	10.9398	36.6973	2080	1990-2020	2020-2100
23	Bale	7.1065	40.0019	2400	1990-2020	2020-2100
24	Bench maji	6.3953	35.4004	1800	1990-2020	2020-2100
25	Borena	4.7224	38.2248	1000	1990-2020	2020-2100
26	Dangila	11.2585	36.8391	2116	1990-2020	2020-2100
27	Debre markos	10.343	37.727	2420	1990-2020	2020-2100
28	Debre tabor	11.834	38.0268	2612	1990-2020	2020-2100
29	Degehabour	8.2220645	43.523238	1070	1990-2020	2020-2100
30	Harerge (Aweday)	8.7038	40.001	1800	1990-2020	2020-2100
31	Nekemit	9.5066	36.8237	2119	1990-2020	2020-2100
32	Gode	5.8977	43.6684	295	1990-2020	2020-2100
33	Gonder	12.6051	37.4693	2133	1990-2020	2020-2100
34	Gurage	8.1484	38.0833	1800	1990-2020	2020-2100
35	Hawassa	7.062	38.4763	1708	1990-2020	2020-2100
36	Illubabor	8.29	35.5396097	2400	1990-2020	2020-2100
37	Jima	7.6671	36.8333	1780	1990-2020	2020-2100
38	Kefa	7.0004	36.2486	1900	1990-2020	2020-2100

39	Kemashi	9.8422	35.7804	1317	1990-2020	2020-2100
40	Kemisie	10.7162	39.8666	1900	1990-2020	2020-2100
41	Liben	4.5331	40.5011	1500	1990-2020	2020-2100
42	Mekele	13.4898	39.4766	2254	1990-2020	2020-2100
43	Metekel	11.0335	35.7741	1500	1990-2020	2020-2100
44	Fitche	9.755	38.1207	2798	1990-2020	2020-2100
45	Sekota	12.7417	39.0191	2200	1990-2020	2020-2100
46	Shinle	10.2987	41.7996	1500	1990-2020	2020-2100
47	South omo	5.3844	36.4189	1000	1990-2020	2020-2100
48	Humera	13.9667	37.3166	550	1990-2020	2020-2100
49	Welwale	7.0636	45.4111	1500	1990-2020	2020-2100
50	Dembidolo	8.530498	34.7857	1811	1990-2020	2020-2100
51	Welayta sodo	6.86	37.7616	1550	1990-2020	2020-2100

APPENDIX-B- Mean and Standard Deviation of Data

S/N	Location	Lat	Ave. max-7-day	σair	Ave.max -7-day	σair	(Ave. max-7-day)	σair)	Ave.max -7-day	σair
			1990-2020		2020-2040		2040-2070		2070-2100	
1	Addis Ababa	9.019	28.260	1.820	29.61	2.051	28.617	1.15	29.403	1.227
2	Assosa	10.046	34.270	2.670	35.98	2.544	36.680	1.86	36.538	1.665
3	Metema	12.775	41.760	1.630	42.30	2.828	43.541	1.17	43.885	1.094
4	Bahr Dar	11.603	31.430	1.565	32.44	2.280	33.245	1.42	33.523	1.389
5	Debre Birhan	9.670	24.220	2.010	24.17	1.383	24.875	1.0	25.606	1.052
6	Dire Dawa	9.613	32.270	1.570	32.195	1.570	32.221	1.53	32.217	1.550
7	Jigiga	9.365	31.760	1.410	32.54	1.568	33.284	0.86	33.735	0.905
8	Tipi	7.205	29.483	2.757	29.03	1.672	29.713	1.20	29.718	1.168
9	Harar	9.314	32.253	1.601	32.47	1.945	33.216	0.99	33.596	0.891
10	Gewane	10.156	39.756	1.514	40.56	1.859	41.093	1.47	41.776	1.315
11	Dubti	11.727	42.368	0.931	43.60	2.262	44.260	1.39	44.792	1.311
12	Zeway	7.936	31.801	1.292	34.10	2.508	32.128	1.25	32.618	1.245
13	Hosanna	7.568	31.310	1.700	32.73	0.000	32.349	0.00	32.570	0.000
14	Lalibela	12.039	27.377	1.196	28.48	1.734	28.951	1.3	29.749	1.042
15	Weielu	10.579	26.200	1.531	25.90	1.712	26.438	1.15	27.161	0.986
16	Elidar	12.050	42.270	1.390	43.57	2.446	44.336	1.35	44.753	1.291
17	Adigrat	14.279	30.670	1.680	31.33	1.346	31.735	0.94	32.417	0.834
18	Adawa	14.178	33.122	1.401	33.68	1.874	34.390	0.86	34.994	0.901
19	Alamata	12.418	28.649	1.811	32.07	2.841	29.400	1.45	30.150	1.159
20	Arbaminch	5.996	32.550	1.410	32.57	2.074	33.195	1.46	33.460	1.224
21	Arsi (Asela)	7.867	27.340	1.420	27.06	1.653	27.352	1.25	27.824	1.211
22	Enjibara(Awi)	10.940	34.890	1.690	30.7	2.291	31.294	1.59	31.733	1.485
23	Bale	7.107	20.966	2.660	21.26	1.798	21.993	1.1	22.207	0.989
24	Bench maji	6.395	33.650	1.900	33.11	1.915	33.900	1.33	33.777	1.304
25	Borena	4.722	33.100	1.070	33.74	1.377	33.994	1.03	34.302	1.111
26	Dangila	11.259	33.130	1.550	33.99	2.458	34.887	1.44	35.074	1.408

27	Debre markos	10.343	30.540	1.680	30.29	2.356	30.777	1.78	31.250	1.636
28	Debre tabor	11.834	28.250	1.250	29.18	1.795	29.782	1.72	26.758	1.035
29	Degehabour	7.020	37.115	1.148	38.19	2.015	38.907	1.14	39.400	1.241
30	Harerge	8.704	34.910	1.480	35.37	1.474	36.094	0.68	36.669	0.875
31	Nekemit	9.507	32.220	2.410	32.49	2.230	33.174	1.40	33.690	1.271
32	Gode	5.898	38.537	0.959	40.23	1.755	40.636	1.3	41.247	1.318
33	Gonder	12.605	31.733	1.255	32.83	2.264	33.634	1.42	33.914	1.383
34	Gurage	8.148	26.690	1.610	26.38	1.894	26.794	1.24	27.303	1.230
35	Hawassa	7.062	27.900	2.200	27.38	1.704	27.663	1.32	28.145	1.248
36	Illubabor	8.321	31.694	3.029	31.23	1.886	31.781	1.37	32.192	1.248
37	Jima	7.667	29.320	2.710	29.34	2.137	29.823	1.39	29.986	1.416
38	Lefa	7.000	30.410	2.840	30.06	2.037	30.534	1.38	30.642	1.431
39	Kemashi	9.842	38.108	2.328	38.84	2.823	39.610	1.90	39.439	1.718
40	Kemisie	10.716	32.260	1.890	31.89	2.093	32.170	1.38	32.905	1.181
41	Liben	4.533	35.661	1.045	37.14	1.120	37.315	1.2	37.898	1.118
42	Mekele	13.490	30.760	1.730	31.23	1.967	31.501	1.19	32.195	0.955
43	Metekel	11.034	39.828	1.574	40.74	3.074	41.582	1.90	41.404	1.718
44	Fitch	9.755	25.870	1.770	26.20	1.684	26.625	1.24	27.347	1.069
45	Sekota	12.742	31.180	1.200	32.29	1.735	32.734	1.27	33.535	1.022
46	Shinle	10.299	40.320	1.280	41.80	2.118	42.463	1.39	42.992	1.325
47	South omo	5.384	40.300	1.280	39.81	2.034	40.357	1.49	40.641	1.357
48	Humera	13.967	38.820	1.280	39.69	1.322	41.320	1.16	41.693	1.125
49	Welwale	7.064	37.330	1.010	38.88	2.184	39.346	1.23	40.219	1.337
50	Denbidolo	9.1762	32.91	2.32	32.81	2.242	33.784	1.4	34.160	1.302
51	Welayta sodo	6.860	33.030	2.180	32.81	2.397	33.337	1.44	33.528	1.488

Minimum Performance Grade (PG)								
S/N	Location	Lat	(Ave.-1-day min temp)	(σair)	PG-SHRP-Model		PG-LTPP-Model	
					Reliability %		Reliability %	
					50%	98%	50%	98%
1	Addis Ababa	9.019	2.56	0.88	PG-XX-10	PG-XX-10	PG-XX-10	PG-XX-10
2	Assosa	10.046	9.58	1.12	PG-XX-10	PG-XX-10	PG-XX-10	PG-XX-10
3	Metema	12.775	14.20	1.42	PG-XX-10	PG-XX-10	PG-XX-10	PG-XX-10
4	Bahr Dar	11.603	7.33	0.86	PG-XX-10	PG-XX-10	PG-XX-10	PG-XX-10
5	Debrebirhan	9.670	0.90	0.79	PG-XX-10	PG-XX-10	PG-XX-10	PG-XX-10
6	Dire Dawa	9.613	8.24	1.31	PG-XX-10	PG-XX-10	PG-XX-10	PG-XX-10
7	Jigiga	9.365	5.75	1.36	PG-XX-10	PG-XX-10	PG-XX-10	PG-XX-10
8	Tipi	7.205	9.67	0.78	PG-XX-10	PG-XX-10	PG-XX-10	PG-XX-10
9	Harar	9.314	8.24	5.83	PG-XX-10	PG-XX-10	PG-XX-10	PG-XX-10
10	Gewane	10.156	14.49	0.83	PG-XX-10	PG-XX-10	PG-XX-10	PG-XX-10
11	Dubti	11.727	13.92	0.98	PG-XX-10	PG-XX-10	PG-XX-10	PG-XX-10
12	Zeway	7.936	7.51	0.83	PG-XX-10	PG-XX-10	PG-XX-10	PG-XX-10
13	Hosanna	7.568	6.33	0.91	PG-XX-10	PG-XX-10	PG-XX-10	PG-XX-10
14	Lalibela	12.039	9.14	0.88	PG-XX-10	PG-XX-10	PG-XX-10	PG-XX-10
15	Weielu	10.579	2.63	0.87	PG-XX-10	PG-XX-10	PG-XX-10	PG-XX-10
16	Elidar	12.050	14.27	0.89	PG-XX-10	PG-XX-10	PG-XX-10	PG-XX-10
17	Adigrat	14.279	5.48	0.95	PG-XX-10	PG-XX-10	PG-XX-10	PG-XX-10
18	Adawa	14.178	8.38	0.96	PG-XX-10	PG-XX-10	PG-XX-10	PG-XX-10
19	Alamata	12.418	5.55	0.82	PG-XX-10	PG-XX-10	PG-XX-10	PG-XX-10
20	Arbaminch	5.996	11.90	0.93	PG-XX-10	PG-XX-10	PG-XX-10	PG-XX-10
21	Arsi(Asela)	7.867	3.67	0.78	PG-XX-10	PG-XX-10	PG-XX-10	PG-XX-10
22	Enjibara (Awi)	10.940	6.24	0.66	PG-XX-10	PG-XX-10	PG-XX-10	PG-XX-10
23	Bale	7.107	-0.31	0.93	PG-XX-10	PG-XX-10	PG-XX-10	PG-XX-10
24	Bench maji	6.395	12.58	0.84	PG-XX-10	PG-XX-10	PG-XX-10	PG-XX-10
25	Borena	4.722	11.96	0.60	PG-XX-10	PG-XX-10	PG-XX-10	PG-XX-10
26	Dangila	11.259	7.97	0.72	PG-XX-10	PG-XX-10	PG-XX-10	PG-XX-10
27	Debre markos	10.343	4.75	1.04	PG-XX-10	PG-XX-10	PG-XX-10	PG-XX-10
28	Debre tabor	11.834	8.48	0.82	PG-XX-10	PG-XX-10	PG-XX-10	PG-XX-10
29	Degehabour	7.020	13.68	0.83	PG-XX-10	PG-XX-10	PG-XX-10	PG-XX-10
30	Harerge	8.704	10.62	1.64	PG-XX-10	PG-XX-10	PG-XX-10	PG-XX-10
31	Nekemit	9.507	7.49	1.06	PG-XX-10	PG-XX-10	PG-XX-10	PG-XX-10
32	Gode	5.898	15.88	1.04	PG-XX-10	PG-XX-10	PG-XX-10	PG-XX-10
33	Gonder	12.605	9.26	0.68	PG-XX-10	PG-XX-10	PG-XX-10	PG-XX-10

34	Gurage	8.148	2.13	0.95	PG-XX-10	PG-XX-10	PG-XX-10	PG-XX-10
35	Hawassa	7.062	4.45	0.87	PG-XX-10	PG-XX-10	PG-XX-10	PG-XX-10
36	Illubabor	8.321	7.99	0.95	PG-XX-10	PG-XX-10	PG-XX-10	PG-XX-10
37	Jima	7.667	7.07	1.14	PG-XX-10	PG-XX-10	PG-XX-10	PG-XX-10
38	Kefa	7.000	9.35	0.85	PG-XX-10	PG-XX-10	PG-XX-10	PG-XX-10
39	Kemashi	9.842	13.36	1.23	PG-XX-10	PG-XX-10	PG-XX-10	PG-XX-10
40	Kemisie	10.716	8.36	0.95	PG-XX-10	PG-XX-10	PG-XX-10	PG-XX-10
41	Liben	4.533	14.03	0.84	PG-XX-10	PG-XX-10	PG-XX-10	PG-XX-10
42	Mekele	13.490	4.67	0.81	PG-XX-10	PG-XX-10	PG-XX-10	PG-XX-10
43	Metekel	11.034	13.58	2.19	PG-XX-10	PG-XX-10	PG-XX-10	PG-XX-10
44	Fitch	9.755	4.49	0.79	PG-XX-10	PG-XX-10	PG-XX-10	PG-XX-10
45	Sekota	12.742	11.61	0.88	PG-XX-10	PG-XX-10	PG-XX-10	PG-XX-10
46	Shinle	10.299	12.64	0.87	PG-XX-10	PG-XX-10	PG-XX-10	PG-XX-10
47	South omo	5.384	17.95	0.70	PG-XX-10	PG-XX-10	PG-XX-10	PG-XX-10
48	Humera	13.967	14.32	1.18	PG-XX-10	PG-XX-10	PG-XX-10	PG-XX-10
49	Welwale	7.064	13.91	0.89	PG-XX-10	PG-XX-10	PG-XX-10	PG-XX-10
50	Denbidolo	9.1762	9.55	0.90	PG-XX-10	PG-XX-10	PG-XX-10	PG-XX-10
51	Welayta sodo	6.860	7.72	0.91	PG-XX-10	PG-XX-10	PG-XX-10	PG-XX-10

Sample Calculation

7-day consecutive temperature																			
2021	2022	2023	2024	2025	2026	2027	2028	2029	2030	2031	2032	2033	2034	2035	2036	2037	2038	2039	2040
30.01	28.63	30.80	27.89	27.49	28.45	32.35	28.71	30.88	28.58	27.79	28.63	31.16	27.73	31.27	30.66	29.98	28.78	31.64	22.79
30.61	28.57	31.04	27.75	29.98	28.70	31.96	29.25	31.01	28.20	28.84	29.55	30.52	29.55	31.60	31.34	29.94	29.34	31.95	22.70
29.64	28.82	31.23	27.88	29.03	28.91	31.89	29.19	30.97	28.65	29.49	29.91	30.69	30.46	31.37	31.56	30.28	29.20	31.61	21.85
30.16	28.23	30.96	27.22	29.50	28.49	31.73	29.55	31.09	29.76	29.83	30.05	31.11	30.89	31.71	31.11	30.17	29.50	31.14	21.58
30.30	27.61	30.94	27.40	30.63	28.81	31.94	29.68	31.57	29.20	30.02	30.16	31.24	30.94	31.78	30.89	32.01	29.60	30.86	19.99
29.13	29.56	30.94	27.38	31.03	28.87	31.92	29.62	29.15	29.25	30.59	30.78	31.91	29.67	30.80	31.58	30.44	29.73	30.51	22.18
29.42	29.45	31.84	27.14	28.86	28.83	30.54	29.58	29.72	29.24	31.18	30.79	31.52	29.36	30.30	31.52	29.76	29.90	30.61	22.78
Mean		**29.6**																	
Standard Dev. Calculation = (X-mean)2																			
2021	2022	2023	2024	2025	2026	2027	2028	2029	2030	2031	2032	2033	2034	2035	2036	2037	2038	2039	2040
0.154	0.977	1.395	2.968	4.506	1.355	7.490	0.821	1.591	1.074	3.341	0.964	2.398	3.535	2.754	1.101	0.136	0.694	4.121	46.537
0.999	1.099	2.039	3.483	0.130	0.844	5.482	0.132	1.944	2.008	0.607	0.004	0.827	0.004	3.938	2.986	0.104	0.077	5.443	47.803
0.001	0.623	2.606	3.008	0.345	0.491	5.200	0.184	1.848	0.928	0.015	0.086	1.151	0.719	3.065	3.769	0.444	0.172	3.992	60.261
0.299	1.921	1.819	5.737	0.013	1.265	4.496	0.005	2.178	0.022	0.046	0.189	2.239	1.618	4.383	2.230	0.310	0.013	2.318	64.476
0.466	4.015	1.745	4.882	1.042	0.651	5.399	0.004	3.827	0.170	0.165	0.300	2.650	1.758	4.708	1.634	5.752	0.000	1.545	92.678
0.236	0.003	1.766	4.973	2.008	0.558	5.310	0.000	0.212	0.136	0.947	1.364	5.285	0.003	1.407	3.868	0.683	0.012	0.804	55.210
0.037	0.028	4.972	6.121	0.563	0.613	0.859	0.001	0.012	0.141	2.439	1.382	3.649	0.063	0.466	3.641	0.021	0.081	0.984	46.750

sum (X-mean)2	**643.35**
Standard Dev.	**2.05**

Performance Grade determination max pavement Temperature

SHRP Model

$$Tpav, 20mm = (Tair - 0.00618Lat^2 + 0.2289Lat + 42.4)(0.9545) - 17.78 + z\,\sigma air$$

Variable	value	Reliability	z	PG	Recommended PG Value
$Tair$	29.61	50%	0	52.4	PG-58-10
Lat	9.01891	95%	2.055	56.662	PG-58-10
σair	2.05				

Performance grade determination Max pavement Temperature

LTPP Model

$$Tpav, h = 54.32 + 0.78Tair - 0.0025Lat^2 - 15.14\,log10(d + 25) + z\,(9 + 0.61\sigma^2 air)0.5$$

Variable	value	Reliability	z	PG	Recommended PG Value
$Tair$	29.61	50%	0	52.2	PG-58-10
Lat	9.01891	98%	2.055	59.2	PG-64-10
σair	2.05				

Performance grade determination Min Pavement Temperature

SHRP Model

$$Tpav, l = Tair + 0.051\,d - 0.000063\,d^2 - z\,\sigma\,air$$

Variable	value	Reliability	z	PG	Recommended PG Value
$Tair$	value	50%	0	3.3	PG-XX-10
Lat	9.01891	98%	2.06	2.2	PG-XX-10
σair	0.79				
1-day mean tem	2.31				

Performance grade determination Min Pavement Temperature

LTPP Model

$$Tpav, l = -1.56 + 0.72Tair - 0.004Lat^2 + 6.26\,log10(d + 25) - z\,(4.4 + 0.52\sigma^2 air)0.5$$

Variable	value	Reliability	z	PG	Recommended PG Value
$Tair$	value	50%	0	10.1	PG-XX-10
Lat	9.01891	98%	2.06	5.7	PG-XX-10
σair	0.55				

APPENDIX-C-Global Climate Model Temperature Simulation

INM-CM5-0, and CMCC-ESM2 model with SSP 2 4.5 Scenario.

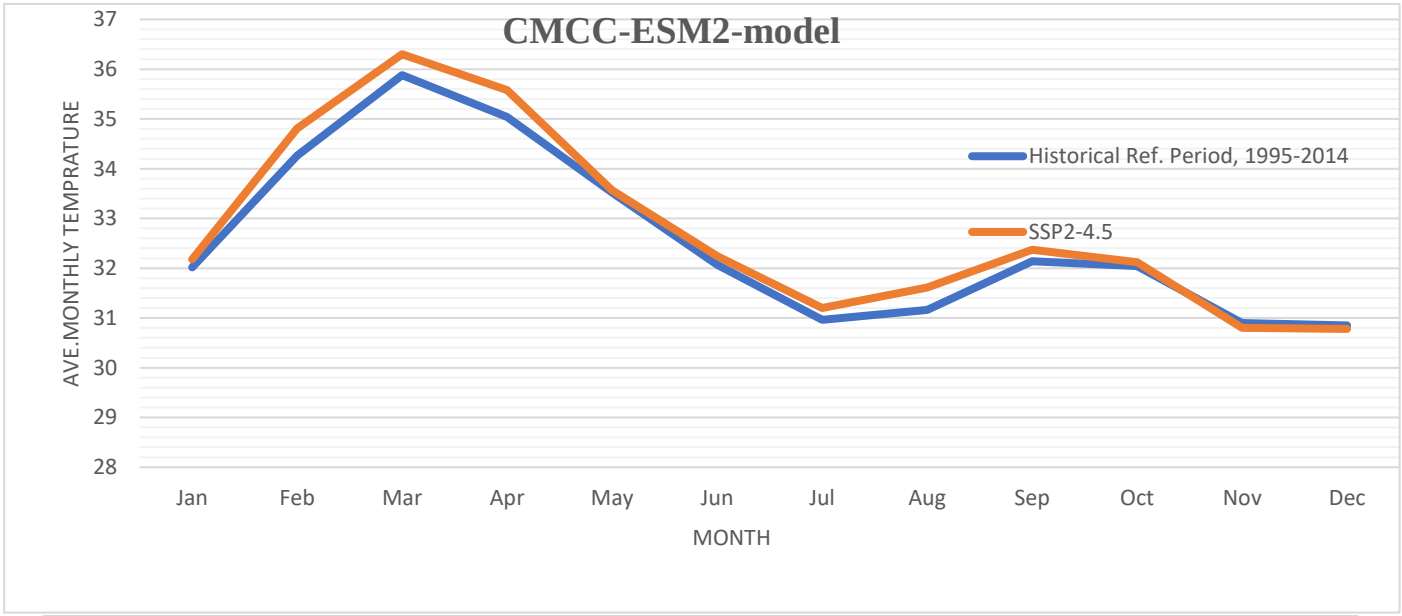

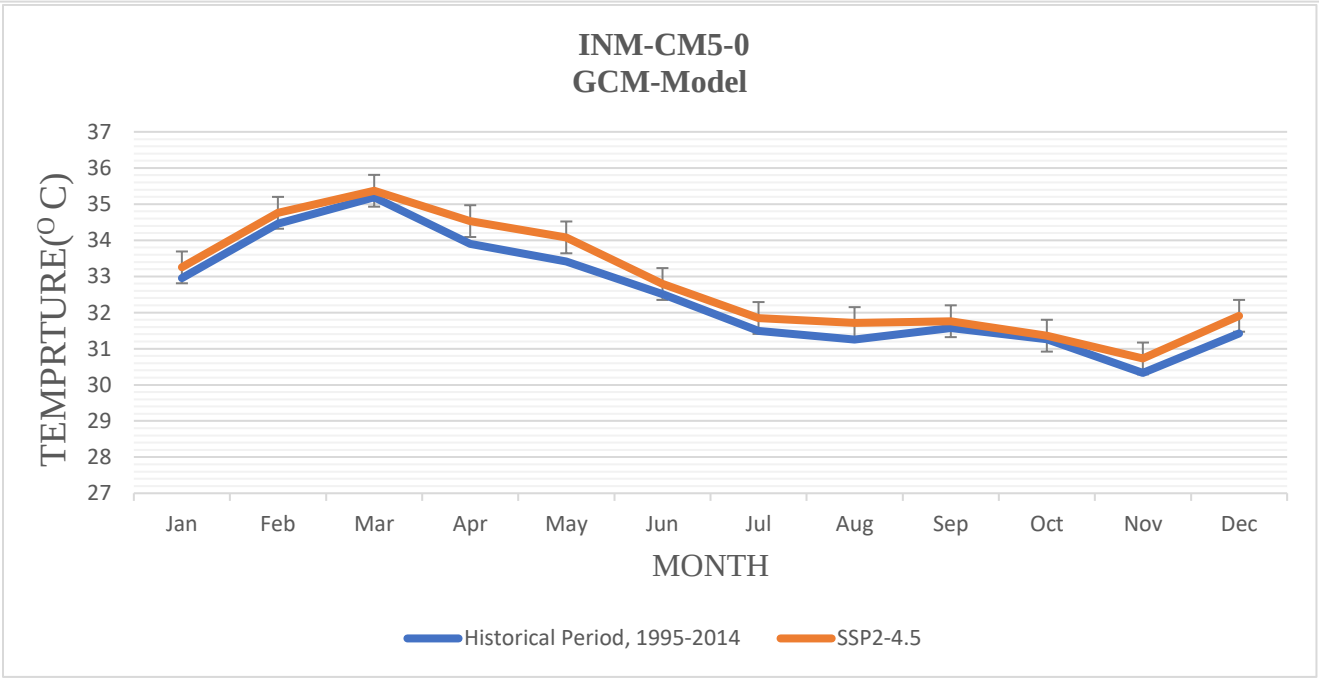

Distribution of Ethiopia temperature in future

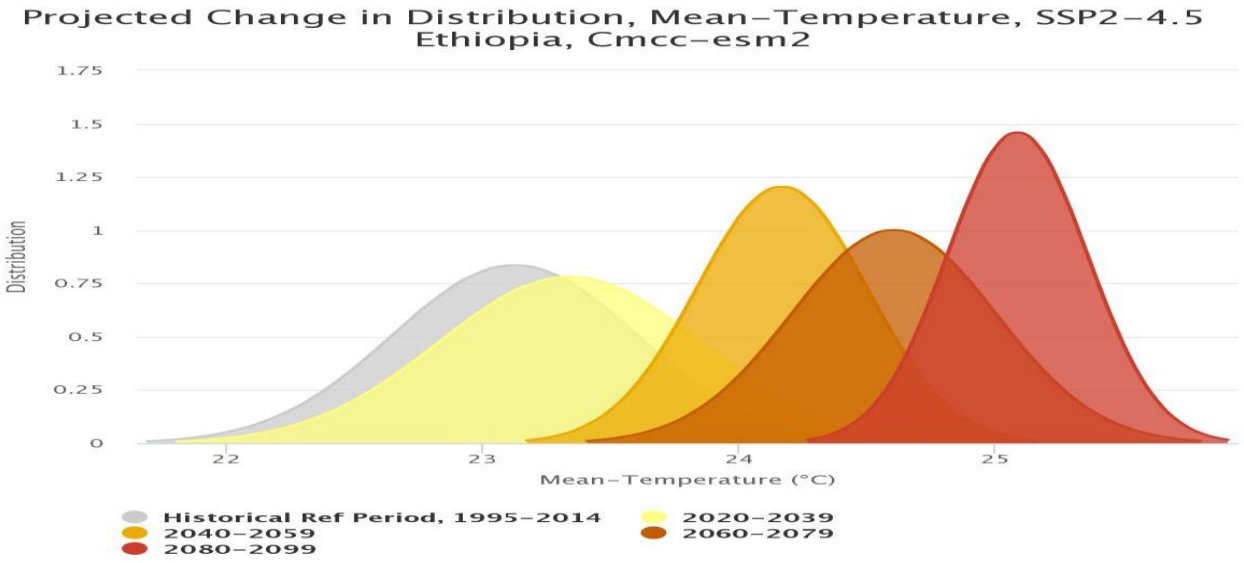

SSP2(4.5)

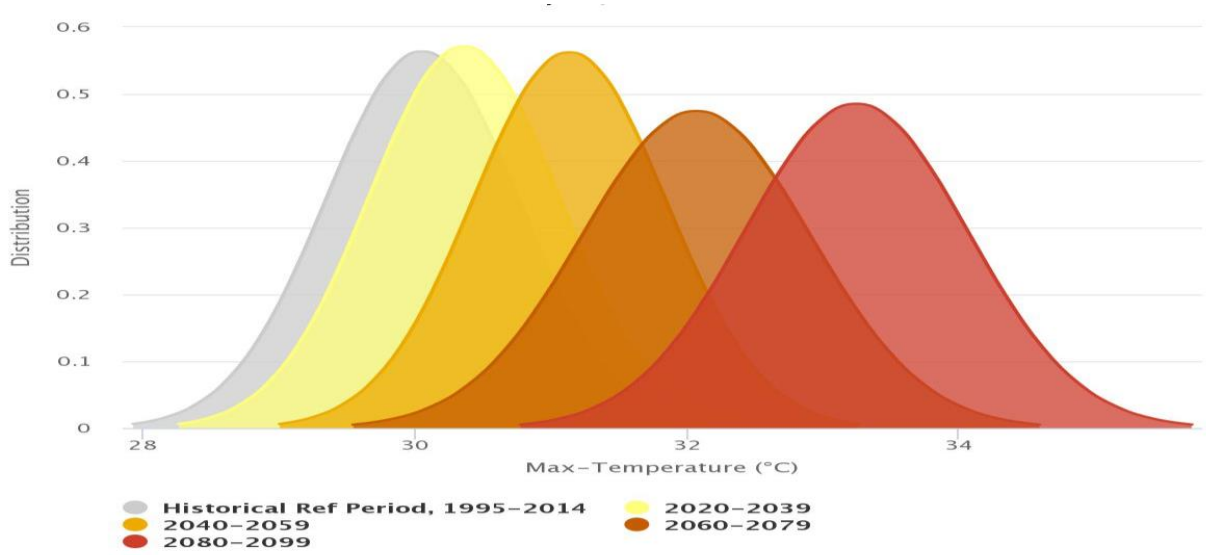

SSP 5(8.5)

APPENDIX-D- Temperature Correction

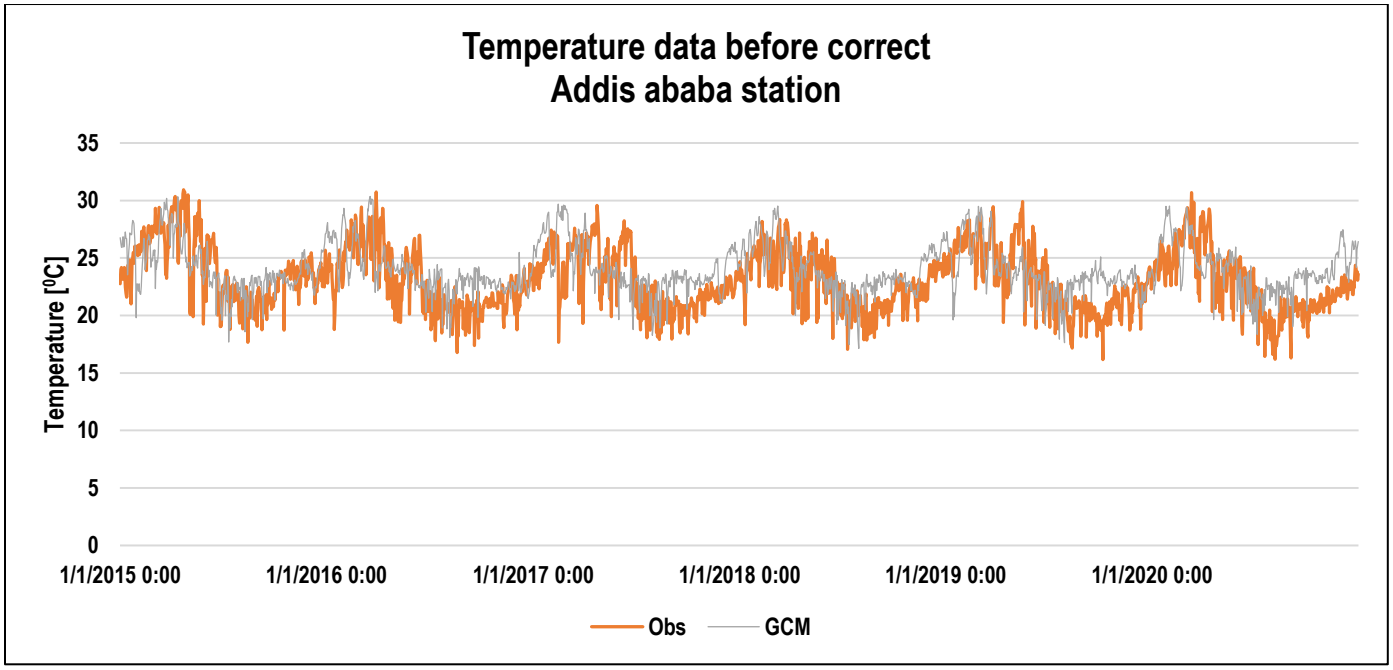

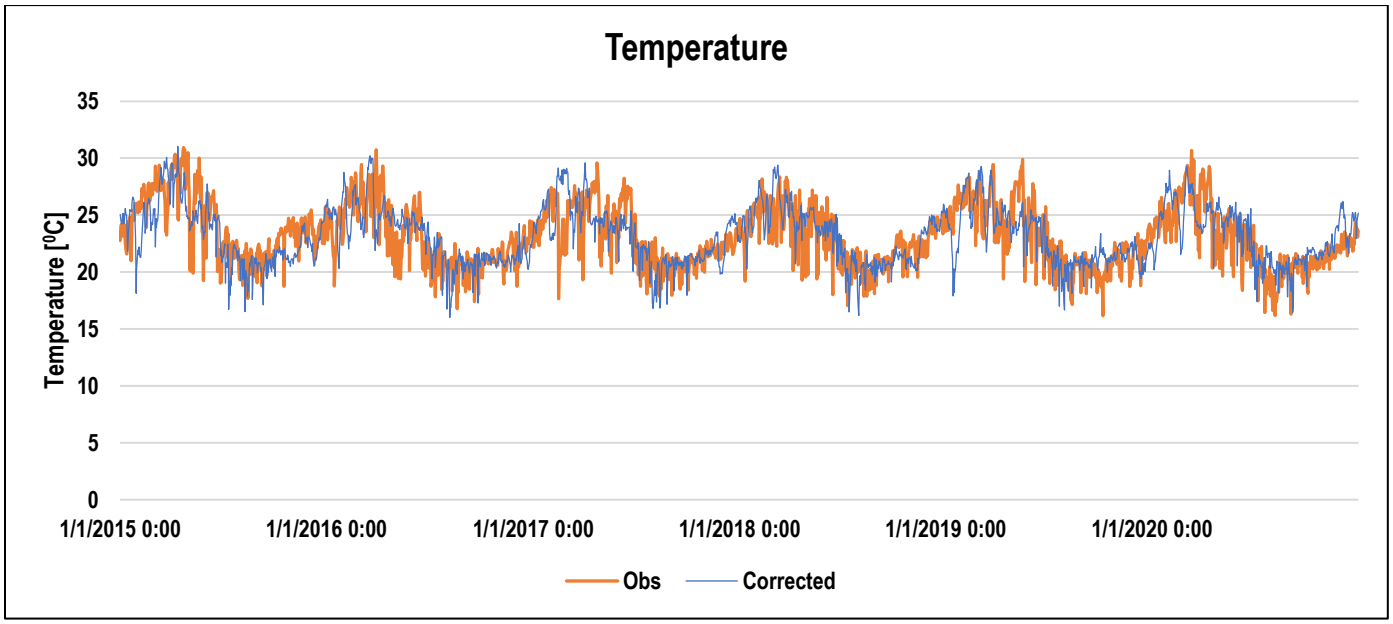

APPENDIX-E -Grade Change Station

Grade change SSP 2(4.5)													
S/N	Location	2020-2040				2040-2070				2070-2100			
		50%	98%	50%	98%	50%	98%	50%	98%	50%	98%	50%	98%
1	Addis Ababa				6				6				6
2	Assosa			6	6			6	6			6	6
3	Metema						6	6	6		6	6	6
4	Bahr Dar		6				6				6		
5	Debrebirhan												
6	Dire Dawa												
7	Jigiga		6				6				6		
8	Tipi												
9	Harar												
10	Gewane									6			
11	Dubti		6	6	6		6	6	6		6	6	6
12	Zeway		6				6				6		
13	Hosanna		6				6				6		
14	Lalibela				6	6		6	6	6		6	6
15	Weielu			6				6		6		6	
16	Elidar		6		6		6	6	6		6	6	6

17	Adigrat						6				6		
18	Adawa									6			
19	Alamata						6						
20	Arbaminch		6		6		6		6		6		6
21	Arsi												
22	Enjibara										6		
23	Bale			6									
24	Bench maji												
25	Borena		6				6				6		
26	Dangila									6			
27	Debre markos										6		
28	Debre tabor	6		6	6	6		6	6	6		6	6
29	Degehabour												
30	Harerge	6				6				6		6	6
31	Nekemte			6	6			6	6			6	6
32	Gode		6				6				6		
33	Gonder	6				6				6			
34	Gurage												
35	Hawassa			6	6			6	6			6	
36	Illubabor												
37	Jima												

38	Kefa		6										
39	Kemashi												
40	Kemisie												
41	Liben	6		6	6	6			6	6			6
42	Mekele		6				6				6		
43	Metekel					6				6			
44	Fitche												
45	Sekota		6				6				6		
46	Shinle	6				6				6	6		6
47	South omo												
48	Humera	6	6	6	6	6	6	6	6	6	6	6	6
49	Welwale										6		
50	Dembidolo				6				6				6
51	Welayta sodo	-	-	-	-	-	-	-	-	-	-	-	-

N.B == 6^{o} c

Grade change SSPS5 8.5													
S/N	Location	2020-2040				2040-2070				2070-2100			
		50%	98%	50%	98%	50%	98%	50%	98%	50%	98%	50%	98%
1	Addis Ababa	6		6	6	6		6	6	6	6	6	6
2	Assosa	6	6		6	6	6		6	6	6	6	6
3	Metema		6		6		6		6		6		6
4	Bahr Dar		6				6				6		
5	Debrebirhan										6		
6	Dire Dawa												
7	Jigiga		6			6	6				6		
8	Tipi												
9	Harar												
10	Gewane												
11	Dubti		6		6		6	6	6		6	6	6
12	Zeway		6				6			6	6		6
13	Hosanna		6				6				6		
14	Lalibela	6	6	6	6	6		6	6	6		6	6
15	Weielu	6		6	6					6			6
16	Elidar	6	6	6			6	6	6				
17	Adigrat	6	12	6	6		6				6		
18	Adawa					6				6			
19	Alamata	6	6	6		6	6	6		6	6	6	

20	Arbaminch				6				6				-6
21	Arsi	6		6	6				6	6		6	6
22	Enjibara						6				6		
23	Bale	6	6	6				6		6		6	
24	Bench maji	6	6	6									
25	Borena		6				6				6		
26	Dangila									6			
27	Debre markos		6				6				6		
28	Debre tabor	6	6	6	6	6		6	6	6		6	6
29	Degehabour	6		6	6		6				6		
30	East harerge	-6						6	6			6	6
31	Nekemte	6			6								
32	Gode						6				6		
33	Gonder		6				6				6		
34	Gurage	6	6	6	6				6				6
35	Hawassa		6	6				6				6	
36	Illubabor		6										
37	Jima		6				6				6		
38	Kefa												
39	Kemashi	6	6	6	6								
40	Kemisie												
41	Liben	6		6	6	6		6	6	6		6	6

42	Mekele		6				6			6	6		
43	Metekel					6				6			
44	Fitche	6		6	6					6		6	6
45	Sekota	6	12	6	6		6			6	6		
46	Shinle	6	6	-6	-6	6				6	6	6	6
47	South omo		6	-6	-6					6			6
48	Humera												
49	Welwale		6		6		6		6		6		6
50	Dembidolo	6	6	6		6			6	6			
51	Welayta sodo	6			6								

APPENDIX- F DSR -Result

80/100

Test information						
Sample type	80/100-agedl					
Plate diameter	25 mm					
Test Gap	1mm					
Test Frequency, rad/s	10					
Test Mode	10%					
Result						
Trial	Trial-1			Trial -2		
Test Temperature	51.97	57.97	64.03	52.03	57.95	64.02
Complex Modulus, G*, for 10 cycles (kPa to three significant figures	8713.70	3515.60	1369.50	8794.50	3791.50	1422.80
Phase angle, δ, for 10 cycles (nearest 0.1 degrees)	83.30	85.47	86.90	82.95	85.13	86.76
G*/(sinδ) (nearest 0.01 kPa)	8773.62	3526.62	1371.51	8861.50	3805.24	1425.08
Fail temperature	59.49			59.83		
Average	59.66					
PG-Grade	**58**					

Test information						
Sample type	80/100-orginal					
Plate diameter	25 mm					
Test Gap	1mm					
Test Frequency, rad/s	10					
Test Mode	12%					
Result						
Trial	Trial-1			Trial -2		
Test Temperature	51.82	57.97	63.95	51.91	58.05	63.94
Complex Modulus, G*, for 10 cycles (kPa to three significant figures	3731.80	2447.30	646.09	3748.90	2396.80	630.39
Phase angle, δ, for 10 cycles (nearest 0.1 degrees)	85.93	87.01	87.68	86.19	87.29	88.01
G*/(sinδ) (nearest 0.01 kPa)	3741.24	2449.27	646.62	3757.20	2398.36	630.77
Fail temperature	59.18			59.09		
Average	59.13					
PG-Grade	**58**					

60/70

Test information						
Sample type	60/70-orginal					
Plate diameter	25 mm					
Test Gap	1mm					
Test Frequency, rad/s	10					
Test Mode	12%					
Result						
Trial	Trial-1			Trial -2		
Test Temperature	57.92	64.09	70.15	58.14	64.04	70.01
Complex Modulus, G*, for 10 cycles (kPa to three significant figures	3957.40	1650.10	759.34	3912.40	1611.20	787.37
Phase angle, δ, for 10 cycles (nearest 0.1 degrees)	85.75	86.99	88.04	85.79	86.84	87.62
G*/(sinδ) (nearest 0.01 kPa)	3968.31	1652.38	759.78	3922.99	1613.65	788.05
Fail temperature	68.09			67.96		
Average	68.03					
PG-Grade	**64**					

40/50

Test information				
Sample type	40/50-orginal			
Plate diameter	25 mm			
Test Gap	1mm			
Test Frequency, rad/s	10			
Test Mode	12%			
Result				
Trial	Trial-1		Trial -2	
Test Temperature	64.00	69.93	63.96	69.91
Complex Modulus, G*, for 10 cycles (kPa to three significant figures	1900.50	884.62	1866.00	903.21
Phase angle, δ, for 10 cycles (nearest 0.1 degrees)	87.28	88.08	87.38	88.37
G*/(sinδ) (nearest 0.01 kPa)	1902.64	885.12	1867.95	903.58
Fail Temperature	69.26		69.32	
Average	69.29			
PG-Grade	**64**			

Test information						
Sample type	40/50-Aged					
Plate diameter	25 mm					
Test Gap	1mm					
Test Frequency, rad/s	10					
Test Mode	10%					
Result						
Trial	Trial-1			Trial -2		
Test Temperature	63.95	70.00	76.08	63.94	69.93	70.02
Complex Modulus, G*, for 10 cycles (kPa to three significant figures	5197.10	2273.10	998.22	5024.10	3488.00	2469.50
Phase angle, δ, for 10 cycles (nearest 0.1 degrees)	84.16	85.98	87.33	84.03	85.80	84.56
G*/(sinδ) (nearest 0.01 kPa)	5224.21	2278.71	999.30	5051.50	2476.15	3472.30
Fail temperature	71.74			71.58		
Average	71.66					
PG-Grade	**70**					